Warning of in-flight icing risk through fusion of satellite products, ground observations, and model forecasts

Von der

Fakultät für Mathematik und Physik

der

Gottfried Wilhelm Leibniz Universität Hannover

zur Erlangung des Grades

DOKTOR DER NATURWISSENSCHAFTEN

Dr. rer. nat.

genehmigte

Dissertation

von

Dipl.-Met. Jakob Tendel

geboren am 8. April 1979 in Berlin

2013

Referent: Prof. Dr. Thomas Hauf

Korreferent: Prof. Dr. Günther Groß

Tag der Promotion: 25.04.2013

Zusammenfassung

Ziel dieses Promotionsvorhabens ist die Weiterentwicklung des bestehenden ADWICE Systems zur Diagnose von unterkühltem Flüssigwasser in Wolken, ein Hauptauslöser von Vereisung an Luftfahrzeugen im Flug. Ein Hauptproblem der aktuellen Vereisungsdiagnose mit ADWICE, welche sich neben Beobachtungen auch auf Modelldaten stützt, ist der systematisch zu große Anteil des gesamten Diagnoseraums, in dem Vereisungsbedingungen diagnostiziert werden. Dieses klassische over-forecasting führt zwar zu einer hohen Erkennungsrate von positiven Vereisungsbeobachtungen, resultiert aber auch in einer ungenügenden Beschreibung vereisungs-freier Gebiete für darauf angewiesene Luftfahrzeuge und zu einer hohen Rate an Fehl-Warnungen für alle Nutzer.

Im Rahmen dieser Arbeit wurde ein Algorithmus zur Verwendung von Satellitendaten in der ADWICE Diagnose entwickelt und in einer ersten Ausbaustufe implementiert. Der Satelliten-Algorithmus trägt primär zur Reduktion des over-forecasting bei, indem vereisungsfreie Gebiete aus dem Diagnoseprodukt entfernt werden. Im Weiteren werden, wo unter den Gegebenheiten der Satelliten-Fernerkundung möglich, Gebiete mit Vereisungsbedingungen identifiziert und im Diagnoseprodukt eingefügt bzw. bestätigt. Die in dieser Dissertation vorgestellte Validierungs-Studie zeigt, dass wetterabhängig eine Reduktion des gesamten Vereisungsvolumens um bis zu 30% erzielt wird, wobei gleichzeitig die Detektion von Vereisungsbedingungen mittels Satellit die hohe Erkennungsrate aufrecht erhält oder gar verbessert. Dieser kombinierte Beitrag zu Volumenreduktion bei gleich hoher Erkennungsrate stellt eine beträchtliche Verbesserung der Diagnose dar und ist die primäre Errungenschaft dieser Arbeit.

Diese Dissertation diskutiert die grundsätzliche Motivation für die Entwicklung von fortschrittlichen Vereisungsdiagnose- und Vorhersagesystemen, geht speziell auf die Eigenschaften von ADWICE und ähnlicher Systeme ein und dokumentiert die erfolgreiche Weiterentwicklung von ADWICE durch Einbindung von Satellitendaten in die Diagnose von unterkühltem Wolken-Flüssigwasser.

Schlagworte:

    Flugzeug-Vereisung, Satelliten, unterkühltes Flüssigwasser

Abstract

The objective of this dissertation is the integration of satellite data into the existing ADWICE system for the diagnosis of supercooled liquid cloud water, which is the primary cause of in-flight icing on aircraft and a major aviation hazard. It has been shown that the current ADWICE algorithm systematically overestimates the proportion of total atmospheric volume that is covered by icing conditions. While this over-forecasting does lead to a high detection rate for aircraft icing encounters reported by pilots, it also results in an insufficient description of icing-free regions and a high incidence of false alarms for all users.

This thesis presents the development and implementation of an algorithm that integrates satellite-based cloud property retrieval products into the ADWICE icing diagnosis for the purpose of reducing over-forecasting through the removal of cloud free areas from the diagnosis product. A simultaneous satellite-based detection of additional icing areas serves to maintain or improve the correlation of the ADWICE icing diagnosis with icing pilot reports. A validation study presented in this thesis is able to demonstrate a reduction in overall icing volume by up to 30% while the satellite-based detection of icing conditions maintains a high diagnosis accuracy against positive icing reports, together resulting in a considerable increase in volume efficiency. This increase in volume efficiency of over 50%, depending on the circumstances, is the major achievement presented here.

This thesis presents the basic motivation for the creation and continuing development of advanced icing forecast and diagnosis systems, offers a detailed description of ADWICE and similar systems and documents the successful and beneficial integration of satellite data into the diagnosis of aircraft icing conditions caused by supercooled liquid water.

Keywords:

    aircraft icing, satellite, supercooled liquid water

Acknowledgements

I would like to take this opportunity to thank a number of people that have been of immeasurable assistance in this endeavour and who can be assured of my eternal gratitude. I want to thank my family, starting with my lovely wife and daughter as well as my mother, for patience, support and encouragement. I would like to especially thank my father for his active participation in proofreading and for his eye for detail in completing this challenging project.

My gratitude also belongs to my adviser and mentor Prof. Thomas Hauf, who gave me the opportunity to work on this interesting project and whose support as well as advice was invaluable.

I would also like to take this opportunity to thank Deutscher Wetterdienst (DWD) for their funding as well as active technical support for this and other projects, without which they would not have been possible in that form. I also want to thank my colleagues at the National Center for Atmospheric Research (NCAR) in Boulder, Colorado who were kind enough to host me as a visiting scientist for the core of this project's data gathering period.

Table of Contents

List of Figures

Abbreviations

ADWICE	Advanced Diagnosis and Warning system for aircraft ICing Environments German in-flight icing forecast and diagnosis system
AIRMET	Airman's Meteorological information
AMDAR	Aircraft Meteorological Data Relay
ATR	"Avion de Transport Regional", European manufacturer of aircraft
Cb	Cumulonimbus, anvil cloud
CFR	US Code of Federal Regulations
CIP	Current Icing Potential, US in-flight icing diagnosis system
COSMO	Consortium for Small-scale Modelling, European cooperative development community for regional weather modelling
CTT	Cloud Top Temperature; satellite-derived product
CTH	Cloud Top Height; satellite-derived product
DIA	Diagnostic Icing Algorithm, ADWICE diagnosis module
DIA-SAT	upgraded DIA, with satellite data
DIP	Diagnostic Icing Product, output of DIA
DLR	Deutsches Zentrum für Luft- und Raumfahrt
DWD	Deutscher Wetterdienst
FAA	(US) Federal Aviation Administration
FAR	FAA Federal Aviation Regulations
FIP	Forecast Icing Potential, US in-flight icing forecast system
FIR	Flight Information Region
FL	Flight Level
GAFOR	General Aviation Forecast
GAMET	General Aviation Meteorological information
GOES	"Geostationary Operational Environmental Satellite" US West and East.
IIDA	Integrated Icing Diagnostic Algorithm
IMuK	Institut für Meteorologie und Klimatologie, Leibniz Universität Hannover
IN	Ice-Nuclei

LM	Lokal-Modell, pre-cursor to COSMO regional weather model
LTM	Less than *Moderate* (icing)
LWC	Liquid Water Content; mass density of liquid water g/m^3
LWP	Liquid Water Path; column total of liquid water g/m^2
METAR	Meteorological Aerodrome Report
METEOSAT	"Meteorological satellite", European geostationary weather satellite
MOG	*Moderate* (icing) or greater
MSG	METEOSAT Second Generation
MVD	"Median Volume Diameter", diameter equivalent to the median volume of a drop size distribution, used as an approximation
MWO	Meteorological Watch Office
NCAR	National Center for Atmospheric Research, Boulder, CO
PIA	Prognostic Icing Algorithm, ADWICE forecast module
PIP	Prognostic Icing Product, output of PIA
PIREP	Pilot Report
RAP/RAL	Research Application Program/Laboratory , NCAR research unit
RUC	Rapid Update Cycle, US regional research weather model
SIGMA	System of Icing Geographic identification in Meteorology for Aviation, French rapid-update nowcasting of in-flight icing conditions
SIGMET	Significant Meteorological information
SIGWX	see SWC
SLD	Supercooled Large Droplet
SLW	Supercooled Liquid Water
SLWC	Super-cooled liquid water content (see LWC)
SWC	Significant Weather Chart
WMO	World Meteorological Organization
WRF	Weather Research and Forecast (model)

1. Introduction

This thesis documents the ADWICE II development project to integrate advanced satellite cloud property products into the ADWICE system for diagnosing and warning of aircraft in-flight icing. This development project was conducted at the Institute for Meteorology and Climatology (IMuK) of the Leibniz University Hannover, and at the National Center for Atmospheric Research (NCAR) in Boulder, Colorado, USA by the author.

In-flight icing occurs in conditions where liquid water droplets are present in the atmosphere at temperatures below freezing (supercooled liquid water) and freeze onto the aircraft on contact. This represents a significant hazard to safety of flight due to the detrimental impact of ice build-up on aircraft aerodynamics, control surfaces, sensors, or cockpit window visibility. The traditional and legally certified icing warnings are produced in a largely manual process by forecasters using ground-based observations and pilot reports of icing encounters to outline broad areas of increased icing potential.

The continuing trend of rapidly increasing air traffic volume, and the public's unwillingness to accept a proportionate increase in accidents and incidents, has driven a requirement for more exact and effective air traffic management that must explicitly take into account the distribution and intensity of aviation weather hazards to be successful at minimising weather-related delays while simultaneously increasing safety. The EU funded research project FLYSAFE developed critical processes and technology towards bringing weather data from the ground into the cockpit and into the flight planning and management process (Hauf et al. 2007). This work has informed many of the approaches and technology decisions made as part of the on-going research and development project SESAR. The US aviation community has also been active in developing systems to increase air traffic capacity, efficiency, and safety among other things by integrating next-generation weather forecast products into an intelligent flight planning and management strategy as part of the NGATS/NextGen project (Reynolds et al. 2012).

The general trend towards integrating advanced weather data into air traffic management received added impetus from some high profile crashes, such as the one at Roselawn, Indiana in 1994, which underlined the need for improved warnings of previously underestimated Supercooled Large Droplet (SLD) icing. This further motivated the creation and continuing development of a new generation of algorithm-based warning systems that go significantly beyond the traditional warning approaches. These so-called expert systems are highly specialised toward warnings of the specific phenomenon and base their analyses on a diverse collection of input data. Forecasts of future icing conditions are derived from automated processing and analysis of a number of atmospheric parameters

output by numerical weather prediction models, while a diagnosis of current icing conditions may include model data, ground observations, radar, and satellite data. Development of systems of this type is on-going at several institutions worldwide and an open exchange of ideas and experiences within an engaged scientific community is benefiting all participants. Aside from the ADWICE system in the focus of this project, the French SIGMA and US CIP/FIP system are also presented because of their many similarities.

The Advanced Diagnosis and Warning system for aircraft ICing Environments (ADWICE) is an expert system for in-flight icing and is developed and operated jointly by IMuK and Deutscher Wetterdienst (DWD). The operational ADWICE-DIA algorithm provides diagnoses of icing conditions over Europe by combining data from the COSMO-EU weather model with ground-based observations of precipitation type and radar reflectivity. The ADWICE II project encompassed the development and implementation of the next-generation DIA-SAT algorithm which integrates advanced satellite-based retrieval of cloud coverage and meteorological conditions at the cloud top into the icing diagnosis. The DIA-SAT algorithm represents a significant innovation over the previous generation algorithm by taking advantage of the large coverage area and high horizontal resolution of satellite observations to correct and also to augment ADWICE icing diagnosis output.

These achievements are demonstrated by a quantitative validation study using direct icing observations over the United States. The decision was made to perform this validation over the United States because the icing pilot reports (PIREPs), which are one of the primary data sources for icing validation, are more thoroughly and systematically collected over the US than in Europe. Performing this validation over the United States opened up the opportunity to compare the ADWICE-US icing product with the American FIP icing product. The validation and product inter-comparison was performed by the author personally during an extended stay as a visiting scientist at NCAR in Boulder.

Since the previous generation ADWICE algorithm was found to substantially overestimate the total atmospheric volume covered by icing conditions, one of the stated objectives for the new DIA-SAT algorithm was to correct this overestimation. The validation study presented in this thesis shows that DIA-SAT is able to reduce total icing volume in the diagnosis by approx. 30% while maintaining forecast accuracy as measured against direct observations of icing conditions.

The chapters of this document each represent one of the central themes of this multifaceted project. By documenting the progress of this project step by step, this thesis also

approximates a high level representation of the genesis of icing expert systems from the beginning. The diagram in Figure 1-1 below reflects the path from initial motivation for improved icing diagnosis to fully operational state-of-the-art expert systems and visualises the connection to the document structure.

Chapter 2 contains a summary of the aircraft in-flight icing problem and provides a review of relevant concepts in both aeronautical engineering and meteorology as an introduction for readers less familiar with the subject matter. Chapter 3 describes the current state of icing diagnosis and provides an outline of several approaches currently employed within the aircraft icing community as well as a description of the current ADWICE icing diagnosis algorithm and an introduction to state-of-the-art satellite-derived data products used in the ADWICE upgrade. Chapter 4 introduces the extended DIA-SAT diagnosis system by first describing the satellite-based reduction of over-diagnosed icing volume, the satellite-based detection of additional icing volume, and some details of the implementation into a running system. Chapter 4 closes with a validation study performed using US icing pilot reports, which documents the impact of satellite augmentation on the final diagnosis output. Chapter 5 provides a summary of the presented work, conclusions drawn from the findings, and an outlook to areas of promising future research and development.
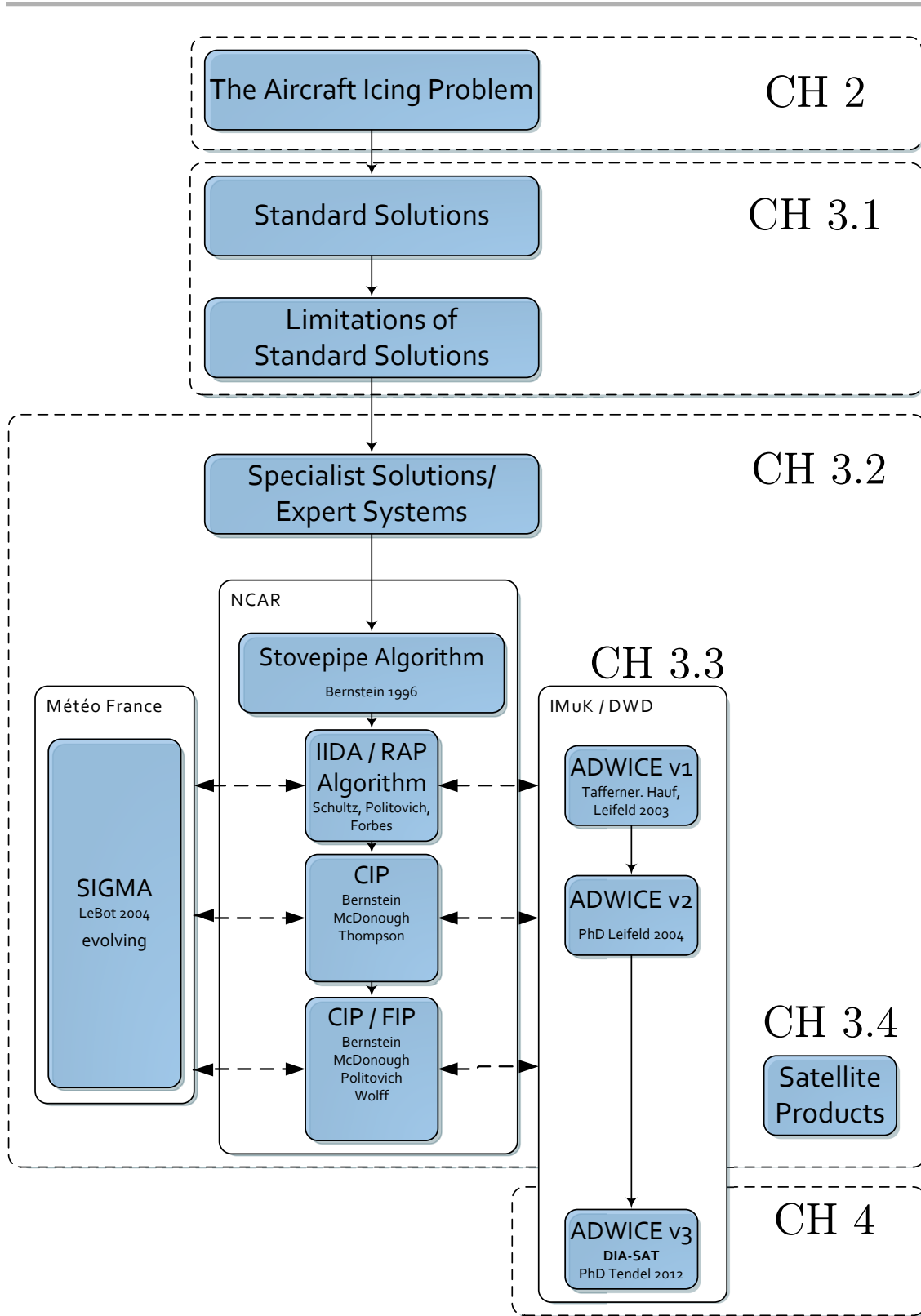
Figure 1-1:   Development path of icing warning systems, reflected in this document.

2.   The aircraft in-flight icing problem

In-flight icing is the result of atmospheric liquid water droplets at temperatures below freezing (supercooled) coming into contact with, and subsequently freezing onto, a passing aircraft. The amount of ice formed on the aircraft and the degree to which this affects the aircraft's flight safety is determined by a number of factors, some of which are meteorological and some of which are highly dependent upon the physical properties of a specific aircraft and its flight state.

The currently valid aircraft icing certification procedures have been in place essentially unchanged for several decades and only require certification for icing resulting from supercooled cloud droplets in a size range below 40µm (FAA 2012). This means they do not account for newer scientific insight gained about the unique icing threat posed by a certain kind of supercooled liquid water drops in the larger size range of drizzle drops (Politovich 1989). These Super-Cooled Large Droplets (SLD ; d > 40µm) contain a dramatically larger volume of water than cloud droplets and their greater mass causes them to behave differently in the disturbed aerodynamic environment around a passing aircraft. Both factors contribute to a large amount of super-cooled liquid water being deposited on an aircraft fuselage by relatively few droplets, potentially in areas not anticipated by aerodynamic modelling of smaller cloud droplets, which are the basis for icing certification rules. Scientific research and a significant rate of accidents and incidents involving SLD in recent decades, after the formulation of icing certification guidelines, has shown that meteorological conditions containing significant number concentrations of SLD occur sufficiently frequently to warrant a review of certification guidelines and to reinforce the requirement for more accurate aircraft icing diagnoses and forecasts.

2.1   Conventional icing

Ice accretion on an aircraft in flight occurs chiefly via contact between the aircraft and liquid water droplets in the atmosphere at a temperature below freezing. Such super-cooled liquid water (SLW) has the property of freezing on contact, which means that the parts of the aircraft facing the airstream (leading edges, cockpit, sensor tubes, and propellers) will experience the greatest ice build-up. Most clouds contain super-cooled liquid water, but under certain conditions enough SLW can be present to cause significant and potentially hazardous ice build-up on a passing aircraft.

2.1.1 Effect on aircraft

Accretion of ice on an aircraft in flight poses a safety threat via a number of mechanisms (CAA 2000). Ice on the wings is the primary threat because of its detrimental impact on smooth aerodynamic flow around the airfoil and consequent degradation of available lift. This increases the airspeed at which a wing will stall and thereby reduces the airspeed safety margin between stall speed and cruise speed (stall margin). Asymmetric ice build-up in particular may also cause one wing to stall at a higher airspeed than the other wing, initiating a sudden rolling manoeuver which may quickly lead to an unrecoverable flight state. Ice accretion on control surfaces may reduce their effectiveness through either mechanical or aerodynamic effects, reducing pilot control authority. Ice accretion on cockpit windows and sensor probes may significantly reduce a pilot's situational awareness by reducing outside visual references and rendering unreliable on-board sensors such as airspeed and attitude indicators, thereby impacting the pilot's ability to maintain stable flight. Icing related impairment of sensor probes may also impair the reliability of autopilot systems. Ice accretion on any part of the airframe can also increase drag by up to 80%. Propeller blades are an aerodynamic lifting surface very similar to aircraft wings and are therefore affected by icing in a similar fashion. Ice build-up on the leading edge of a propeller blade reduces aerodynamic effectiveness and therefore the propeller's ability to develop thrust. Although jet turbine engines are less vulnerable to icing directly on the rotating components due to the much higher rotating velocity and operating temperatures, ice build-up on the outside of the engine intake as well as on static structures within the engine may represent a hazard due to foreign object damage should a large enough piece of ice break loose and be ingested into the engine. Loss of thrust due to icing conditions is particularly serious if the aircraft is simultaneously experiencing both lift reduction and drag increase due to ice build-up on wings and fuselage, since each requires higher thrust to overcome. The weight gained due to icing is only a small fraction of total aircraft weight in any but the very smallest aircraft and is therefore an insignificant factor in most icing encounters.

Aerodynamic effects

The aerodynamics around an aircraft represents a complex and interlocking set of airflows around the various parts of the fuselage. Stable and safe flight is only possible when a smooth airflow is assured around the wings and control surfaces, and marginal amounts of ice contamination can already have very noticeable effects on aircraft performance and handling stability (Cooper et al. 1984).

An airfoil such as a wing has a precisely shaped cross-section that smoothly deflects the airflow in a way to induce a pressure difference between the top and bottom of the airfoil which results in a force acting perpendicular to the air stream. For a wing this resulting force is called lift and for a propeller thrust. The generation of sufficient pressure differential between upper and lower surface requires a smooth airflow that remains attached to the wing surface over as much of the airfoil area as possible, since any turbulence is associated with airflow separation and loss of lift.

Deviations from the optimal airflow can occur in situations where the aircraft encounters ambient turbulence, such as close to storm activity (convective turbulence, gravity waves), or through a mechanical obstruction such as a layer of ice changing the effective shape of aerodynamically active aircraft structures (airfoils) like wings, control surfaces or propellers.

Although a separation of the smooth airflow from the airfoil surface and a transition to turbulent flow always occurs at a certain point along the airfoil, one design goal is for this point to occur as far to the rear as possible. A large enough change in the shape of an airfoil's forward section will greatly degrade the smoothness of the airflow and cause the point of flow separation to move forward, resulting in a loss of lift. This is especially true for the sophisticated type of wing profile (super-critical profile) used on modern high performance passenger aircraft. If the loss of lift is large enough that the airfoil can no longer deliver the required amount, stable flight is no longer possible. This flow state is referred to as a stall.

Every aircraft has a certain safety margin designed into its configuration, but resilient handling qualities and aerodynamic efficiency are largely contradictory properties and must be balanced against each other. Stall margin refers to the airspeed difference in knots between current aircraft speed and the speed at which the wing stalls. A sufficiently high stall margin is also necessary to prevent external disturbances such as turbulence from creating local airflow conditions that would cause the wing to stall. Contamination of the wing through ice build-up raises the stall speed and consequently reduces the margin. Safe flight can no longer be guaranteed in the event of a disturbance to the aircraft aerodynamics that exceeds the safety margin. It is also possible for icing to impair the aerodynamic effectiveness of control surfaces such as ailerons or elevators and may even cause them to stall, reducing or eliminating control authority available to the pilot and potentially resulting in an uncontrollable departure from stable flight.

Mechanical effects

Some aircraft may be more vulnerable to ice reducing or blocking the freedom of movement of control surfaces, which in turn impacts the pilot's ability to control the aircraft (CAA 2000). Aircraft with control surfaces that are servo assisted, by hydraulic or other types of actuators, generally have enough control force to overcome any ice obstruction but small aircraft mostly do not have such systems. Since aerodynamic control surfaces are generally located at the trailing edge of wings and tail planes, clear icing formed through run-back in high liquid water content encounters is the main cause of significant mechanical obstruction of aircraft control surfaces. If sufficient amounts of super-cooled liquid water are able to reach the trailing edge before freezing, a solid and homogeneous layer of clear ice may form around and in between the moving parts of a control surface. Depending on the thickness of the ice layer and the amount of force a certain control surface is able to exert, the freedom of motion may be reduced or in extreme cases the control surface may be completely immobilised. Of particular concern are cases where control surfaces are mobilised while deflected, resulting in an aerodynamic force equivalent to a constant control input, and especially where control surfaces have been immobilised asymmetrically. Constant and even asymmetric control surface deflections are normally used for trimming an aircraft in stable flight but need to be constantly adjusted to suit the particular combination of attitude on airspeed. In cases where adjustment is no longer possible, any changes in airspeed and aircraft attitude (such as during a rapid descent to exit icing conditions) may cause immobilised control surfaces to exert an effective control input which destabilises the aircraft.

Instrument/cockpit effects

While ice build-up on cockpit windows and external sensors does not directly affect aircraft flight stability, it does impact the pilot's situational awareness which is necessary to fly the aircraft safely. Ice accretion on a cockpit window can quickly reduce a pilot's ability to clearly see the outside, potentially leading to a disorienting loss of visual reference as well as impairing the pilot's ability to assess icing on other parts of the aircraft. Critical aircraft instruments such as pitot tubes and angle of attack vanes are susceptible to icing if not properly heated. Accurate airspeed and attitude information is necessary for maintaining stable flight and is required for the correct operation of autopilot systems. Presented with inaccurate information about the aircraft flight state, a pilot or autopilot may be misled into taking a course of action that is improper or dangerous under the conditions. Loss of accurate airspeed information has been determined as a contributing factor to several icing related accidents. The most prominent case in recent times was Air France flight AF447 which crashed in the Atlantic Ocean in 2009, while attempting to penetrate a line of tropical thunderstorms (Tafferner, Hauf et al. 2003). Accident investigators were able to determine that the accident began with the autopilot system

deactivating after all airspeed sensors stopped reporting consistent readings. This was most likely due to blockage of the airspeed pitot probes with ice, cutting off the airflow required for proper operation. Given the high altitude of flight and the outside air temperature, it is almost certain that the probes were blocked by fully formed ice crystals as opposed to icing via supercooled liquid water. While the formation process may not be the same as conventional icing, high ice crystal mass concentration is also a significant hazard and is increasingly being recognized for its negative effects on sensors and engines of jet aircraft.

2.1.2 Icing types

The visual appearance of ice accretion on aircraft structures is described as either *Rime Icing*, *Clear Icing*, or *Mixed Icing*. Rime icing is formed by the classic riming process where small super-cooled liquid water droplets instantly freeze on contact with a suitable surface. The successive deposition of many layers of tiny frozen droplets traps a large amount of air and gives the icing layer a brittle low-density character similar to snow. Clear icing on the other hand is formed when larger amounts of super-cooled liquid water are simultaneously deposited on a surface, such as in an encounter with large diameter drops. If enough supercooled liquid water is present, the latent heat released during the freezing process can be sufficient to briefly delay the formation of solid ice crystals. During this brief period the high-speed airflow over the aircraft can cause significant amounts of liquid water to run back from the leading-edge along the aircraft surface before freezing. This process can lead to the formation of a smooth layer of liquid water which freezes uniformly and appears as a glassy, transparent layer of hard ice. Mixed icing has visual characteristics of rime icing as well as clear icing and occurs when conditions conducive to the formation of both types coincide.

2.1.3 Accretion rate

Accretion Rate, describes the rate at which the thickness of an icing layer increases per unit time and is usually expressed in inches per hour. Accretion rate is the rate of growth of the ice thickness along the local perpendicular (normal vector) at any given location on the aircraft surface. If the accretion rate is given without a specific location reference, it is assumed to refer to the maximum accretion rate experienced during a particular accretion event. In a winged aircraft this would typically occur along the leading edges of wings and tail surfaces. The definition of a single universal measure has so far remained elusive but the accretion rate is a useful measure for several aspects of icing intensity. At the same time, accretion rate and an icing intensity derived from it cannot practically be predicted by icing warning systems based on meteorological forecasts, since the accretion

rate is not exclusively determined by meteorological conditions but is also highly dependent upon the physical characteristics of the aircraft and its flight state. The interaction between these factors to determine the accretion rate is expressed in equation (2-1) (Jeck 1998). The accretion rate (rate of change of ice thickness D over time t, dD/dt) is expressed as the product of an empirical proportionality constant (A), the super-cooled liquid water content (SLWC), the collection efficiency (ß), and the true airspeed (TAS). This formula is valid for all cases where all or nearly all impinging super-cooled liquid water freezes instantly, along the wing leading edge during rime icing events or at the tips of growing ice horns when some runback occurs.

Accretion Rate:

$$dD/dt = (A)(SLWC)(ß)(TAS) \tag{2-1}$$

2.1.4 Collection efficiency (ß)

The collection efficiency (ß) from equation (2-1) above, defined as a weighting factor on the scale from 0.0 - 1.0, is a term that describes the fraction of all cloud droplets in the path of the aircraft that actually impact on the aircraft structure. The forward motion of an aircraft displaces significant amounts of air, which creates a pressure wave ahead of the aircraft analogous to a ship's bow wave. Water droplets suspended in air experience the displacement of the surrounding air as a force acting to displace them also, and to a greater or lesser degree will follow the airflow's streamlines around the aircraft structure.

The strength of the displacing force is related to the angle at which oncoming airflow is deflected by aircraft structures. This in turn is related to the thickness of the structure which can also be expressed as the radius of curvature at the leading-edge. Large blunt structures such as an aircraft nose divert airflow to a much greater degree than do thin structures such as wing and tail leading edges. As a rule, a thin structure has a higher collection efficiency than a thick structure. When considering wings, the angle of the airflow vector to the chord line of the airfoil (angle of attack/AOA) represents an additional dependency, since it modifies the airflow and results in a varying effective structure curvature radius for different AOA. The flow field and consequently the collection efficiency are also modified by the speed of the incident airflow (airspeed).

A water droplet's mass inertia (which is proportional to the third power of the radius, via the droplet volume) determines the degree to which it is pushed aside by the approaching aircraft. Small droplets closely follow streamlines and have a low probability of impacting the aircraft anywhere other than at stagnation points, whereas large droplets are dis-

placed much less and will therefore cross streamlines and impact aircraft structures with a higher probability and over a greater area around stagnation points. Strictly speaking, therefore, the collection efficiency should be considered separately for every drop size. However, in practice, the collection efficiency is expressed for the median volume diameter (MVD) representative of the drop size distribution in question (Finstad et al. 1988).

2.1.5 Interaction of parameters

The parameters in equation (2-1) combine in a linear fashion to determine the ice accretion rate. The factor (A) is a constant of proportionality required to resolve the relationship in equation (2-1) and its value is theoretically unique to each combination of the other three factors. However, numerical ice accretion simulations for a variety of aircraft types in a number of different environmental conditions and flight states have shown only a small variability in the values for (A) and suggest assuming a value of A=0.00116 (Jeck 1998).

The meteorological factors influencing accretion rate for instant-freezing cases are primarily the super-cooled liquid water content (SLWC) and also the drop size distribution which is represented in the value of (ß) as the MVD relative to which (ß) is specified.

The aircraft-specific physical parameters influencing the accretion rate, through their impact on the collection efficiency (ß), are the aircraft airframe dimensions, primarily the thickness and leading edge curvature of wings and tail surfaces, as well as the current configuration of wing high lift devices (flaps, slats) and landing gear.

Of the parameters that define the current flight state, the true airspeed (TAS) and the angle of attack (AOA) are two factors which directly influence the accretion rate. Both TAS and AOA play a role in determining the value for collection efficiency (ß), and the TAS also enters directly into equation (2-1).

The ice accretion rate, and thereby one measure for icing intensity, of a conventional icing encounter is determined by the meteorological conditions of the icing event, the physical properties of the aircraft and its current configuration, as well as the flight state (TAS, AOA). This assumes near instantaneous freezing (*Rime* or slightly *Mixed* icing) of cloud type droplets with a sufficiently Gaussian drop size distribution and an MVD of approximately 15µm, as is representative of an extended exposure to stratiform icing conditions. These assumptions represent past conventional wisdom about the general characteristics of cloud droplet icing and are still appropriate today for most icing encounters. However, these assumptions do fall short for a category of particularly hazardous icing conditions which has attracted increased attention over recent years and has motivated a re-examination of the scientific and regulatory status quo (Politovich 1996).

2.2 Unconventional icing

During the late 1980s and early 1990s awareness was growing of an unusual kind of icing phenomenon associated with extremely high accretion rates and large amounts of run back causing unusually large reductions in aircraft performance. This period was punctuated by two high-profile crashes of ATR commuter turboprop aircraft, one in Milan in 1987 and one in Roselawn, Indiana in 1994. Analysis (NTSB 1996) showed that these cases were associated with super-cooled drizzle drops which are much larger than the cloud droplets associated with typical icing events (Politovich 1989). These kinds of droplets are referred to as Super-Cooled Large Drops (SLD) and they are particularly hazardous because the nature of the icing that results from an SLD encounter is significantly different from and potentially much more severe than a conventional cloud icing encounter (Bragg 1996). Newer scientific data and closer attention to the details of routine icing encounters has demonstrated that SLD frequency of occurrence has previously been under-estimated. Unfortunately the icing envelopes proscribed in 14 CFR Part 25, Appendix C (FAA 2012; Jeck 2002,2003), which are used for designing and certifying aircraft for operations in known icing conditions, only cover the typical icing regime up to a mean effective drop diameter of 40µm. This means that aircraft operating today and into the foreseeable future are not designed or tested against operation under SLD conditions.
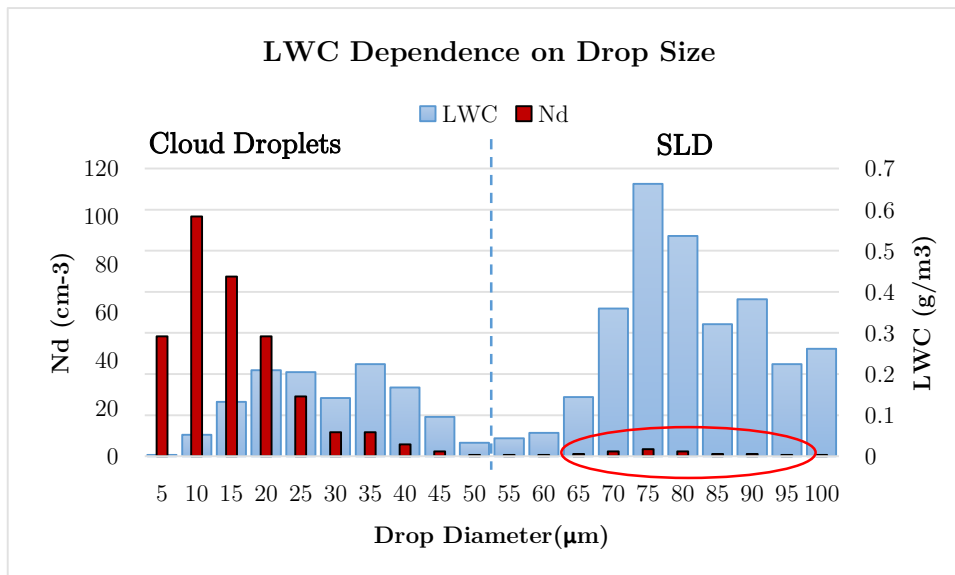
Figure 2-1: Drop size distribution (Nd, per cm³) and associated distribution of liquid water content (LWC, grams per m³). Highlighted: the great contribution to total LWC of numerically few larger drops.

Icing caused by SLD is so extremely hazardous primarily because of two factors. Firstly, droplets in the SLD size range above 40µm, because of their volume, require only a comparatively low number concentration to amass significant liquid water content (see Figure 2-1). Also, large and therefore heavy water droplets have a large mass inertia and are not easily swept aside by the airflow around an approaching aircraft and will impact the aircraft in numbers and in locations not anticipated by icing simulations and tests based on smaller droplet sizes. As a consequence, any aircraft structure has higher collection efficiency (see section 2.1.4) with respect to SLD, which further increases the LWC deposited on the aircraft. Since accretion rate is directly linked to liquid water content, this alone would represent a significant icing threat. However, the significant amount of LWC collected during an SLD encounter will generally also lead to thermodynamic conditions at the interface between the impinging water and the aircraft surface that prevent instantaneous freezing, allowing a large proportion of that water to run aft with the airflow along the aircraft skin. While freezing will eventually set in, this runback may extend a considerable distance from the leading-edge and may likely cause ice build-up outside of the area covered by de-icing equipment or may even reach and obstruct trailing-edge control surfaces.

Wider recognition of the significance of the previously underestimated SLD phenomenon has prompted a reassessment of long-standing regulations and procedures related to flight operations in icing conditions and has reinforced parallel efforts toward the establishment of requirements for updated aircraft icing certification (Cober and Isaac 2012).

2.3   Meteorological description of icing conditions

An understanding of the atmospheric processes that generate aircraft icing conditions plays an important part in the development of truly useful warning systems. The icing warning process involves defining atmospheric volumes where liquid droplet formation processes coincide with super-cooled temperatures and certain conditions necessary for those liquid droplets to persist at super-cooled temperatures. This section introduces a nomenclature with three drop size categories relevant to icing, reviews the formation process most common to each one, and discusses the additional atmospheric conditions necessary for the persistence of icing conditions. Finally, some of the differences between stratiform and convective icing conditions are discussed.

2.3.1 Drop size categories relevant to icing

There are three drop size categories commonly distinguished in the context of aircraft icing, although none of them are uniquely associated with super-cooled liquid water icing conditions and in fact are mostly found at temperatures above freezing. The categories in ascending order of droplet size are: *cloud droplets*, *drizzle drops*, and *raindrops*. Some of the differentiation between these categories derives from the formation process, since cloud droplets form through condensation and drizzle droplets through subsequent coalescence, while raindrops mostly form through melting of solid ice phase precipitation. Another differentiator is the precipitation property, absent for the fully suspended cloud droplets, light to moderate for drizzle, and strong for rain. Since each drop size category is separated by approx. one order of magnitude in drop diameter from the next, they also behave very differently in terms of the icing effects on an aircraft, as introduced in section 2.1.4.

Cloud droplets

Cloud droplets are the basic constituents of the liquid portion of clouds and are formed by the classic nucleation/condensation process, described in section 2.3.2. The drop size distribution within the cloud is determined by a range of factors such as aerosol number concentration, age of the cloud, and water vapour saturation levels. Cloud droplets can range in size from that of a moist aerosol particle (~1µm) all the way up to approaching the size of drizzle drops (> 40µm).

Drizzle (SLD)

Provided with sufficiently saturated conditions, cloud droplets grow through condensation into the size range of drizzle drops (40-500µm). Continued growth will come increasingly via collision coalescence since droplets in this size range begin to develop a downward velocity component relative to the surrounding air, colliding with smaller droplets that remain suspended. A proportion of liquid precipitation cases with droplets in the drizzle size range develop through the classic rain formation process of solid precipitation melting in a warmer air layer. However, within this document the term drizzle refers mostly to precipitation formed by collision coalescence. Droplets above 40µm at a temperature below freezing are also referred to as super-cooled large droplets (SLD). While the number concentration decreases with droplet diameter during coalescence growth, drizzle drops occurring in any appreciable number concentration will contain a significant proportion of a cloud's liquid water content due to the increase of droplet volume with the third power of the radius (see section 2.2).

Rain

Although more than one atmospheric process can result in the formation of liquid precipitation with drop sizes in the rain size range (500-2000µm), the classic rain formation process involves the melting of previously formed ice conglomerates (snow, graupel, etc.) falling into above-freezing air. Super-cooled rain, also known as freezing precipitation if it reaches the ground, is formed by raindrops falling into air with a temperature below zero. Flight through such conditions causes extreme instantaneous ice accretion and runback and must be avoided.

2.3.2 Cloud droplet formation and growth

The water content of the liquid and solid condensate particles that make up a cloud (water droplets and ice crystals) is derived from atmospheric water vapour. The conversion between gaseous, liquid, and solid phase is primarily driven by ambient temperature and local water vapour saturation. This section introduces the theoretical basis for cloud droplet formation and growth as it applies to the aircraft in-flight icing problem.

A cloud is a portion of the atmospheric volume which contains liquid and solid water condensate particles at a density sufficient to significantly alter the passage of light. While there are several categories of thin, nebulous, and even invisible (sub-visible) clouds, the clouds associated with aircraft icing are the typical tropospheric clouds of a dense and visually clearly delineated character, consisting to a large proportion of liquid water drops. Although the drop size distribution varies significantly between clouds and within a single cloud, the term cloud droplet in this context refers to the very smallest category of droplets which remain fully suspended in the air mass and move with it. Many attempts have been made to parameterise the drop size distribution in a useful way and one of the most frequently used approximations is that of (Marshall and Palmer 1948). It is most often used in the context of rain rate retrieval by precipitation radar, and is not always suitable for other applications.

The fundamental mechanism leading to the formation of cloud droplets is condensation of atmospheric water vapour from the gaseous to the liquid phase. Direct condensation of water vapour into a previously not existing water droplet is possible but atmospheric conditions cause naturally occurring condensation involving airborne particulate matter (aerosols). The parameters that guide this condensation process are the water vapour pressure near the vapour/liquid interface, its relationship to the saturation vapour pressure, and the modification of local saturation vapour pressure by the curvature of the droplet surface as well as by the chemical properties of the aerosol particle involved.

Attractive forces between water molecules in a body of liquid water act against a mole-
cule leaving the liquid phase and require a certain amount of energy to overcome. These
attractive forces are proportional to the volume of the body of water and for near spheri-
cal water droplets the volume is strongly correlated with the surface curvature. Therefore,
water molecules in droplets with a high surface curvature experience a lower retaining
force and more easily transition into the vapour phase. If ambient water vapour pressure
is low a net flux of water molecules out of the liquid leads to a decrease in droplet radius
which further accelerates the evaporation process and leads to an eventual disappearance
of the droplet. The ambient water vapour pressure required to maintain a balanced flux
of water molecules into and out of a water volume is called the saturation vapour pres-
sure and is dependent upon the curvature radius of the droplet. The ratio of saturation
vapour pressure over a curved surface (radius r) to that over a planar surface (radius ∞)
is expressed in the KELVIN equation (2-2) (Rogers and Yao 1989).

$$\frac{e_s(r)}{e_s(\infty)} = e^{\frac{2\sigma}{rR\rho T}} \tag{2-2}$$

This ratio depends upon the surface tension of the liquid (σ), the water vapour gas con-
stant (R) and the liquid's density (ρ) at the temperature (T). For small droplets with
r→0 the saturation vapour pressure rapidly approaches infinity, resulting in a constant
under-saturation of the water vapour near the droplet surface, which in turn exposes the
droplet to total evaporation. In order to persist and grow under the limited naturally
occurring levels of water vapour pressure, droplets require a certain minimum droplet
radius to reach and exceed saturation over the curved surface. This condition is satisfied
when water vapour condenses on the surface of certain aerosol particles that have the
required minimum radius.

Aerosol particles such as salt, dust, or soot particles that are able to serve as a condensa-
tion substrate are called cloud condensation nuclei (CCN). CCN type and concentration
varies greatly, with natural and man-made nano-scale dust and soot dominating over land
at number concentrations up to $10^5/cm^3$ whereas clean high-altitude or maritime air
masses may contain as few as $10^3/cm^3$. Additionally, CCN in maritime air masses are
typically dominated by phytoplankton-produced sulphate droplets as well as sea salt
crystals formed from evaporating spray droplets. While the average CCN size is around
0.1μm, sea salt crystals are often significantly larger at up to 20μm. While salt crystals of
this size are particularly effective cloud condensation nuclei since they exceed the critical
curvature radius at comparatively low levels of supersaturation, they are also present in
much lower number concentrations than other CCN. Cloud growth in clean maritime air
dominated by salt crystals therefore characteristically results in clouds made up of rela-

tively few but large cloud droplets. Maritime clouds of this type are therefore of particular relevance to aircraft icing because the combination of large average droplet size and high liquid water content can quickly lead to high levels of ice accretion.

Many types of CCN contain salts and are partially or entirely water-soluble. Salt ions dissolved in the water of a cloud droplet introduce an additional attractive force acting upon water molecules in the liquid that reduces the flux out of the liquid and into the gas phase which in turn reduces the necessary flux from gas to liquid required for equilibrium. This solute effect therefore reduces the saturation vapour pressure over the surface of such a solution in accordance with RAOULT's law.

The KÖHLER equation (2-3) describes the ratio of the saturation vapour pressure over a curved surface to that over a planar surface under the combined influence of curvature and solute effects.

$$\frac{e_s(r)}{e_s(\infty)} = \left[1 - \frac{b}{r^3}\right] e^{a/r} \tag{2-3}$$

Several parameters within this equation have been combined into the auxiliary factors a and b which are defined as follows:

$$a = \frac{2\sigma}{\rho R T} \approx \frac{3.3 \times 10^{-7}}{T} \ [m]$$

$$b = \frac{3 i m_v M}{4 \pi \rho m_s} \approx \frac{4.3 \times 10^{-6} i M}{m_s} \ [m^3]$$

σ	:	Droplet surface tension
ρ	:	Droplet density
R	:	Water vapour gas constant
T	:	Temperature
i	:	Van't Hoff factor
m_v	:	Molar mass of water
M	:	Solute mass
m_s	:	Molar mass of solute

A simplified KÖHLER equation may be formulated for sufficiently large radii and written as in equation (2-4) (Rogers and Yao 1989)

$$\frac{e_s(r)}{e_s(\infty)} = 1 + \frac{a}{r} - \frac{b}{r^3}$$ (2-4)

This formulation of the KÖHLER equation more clearly states the contributions by the curvature and solute effects in terms two and three on the right-hand side respectively. The KÖHLER equation can also be visualised graphically in the KÖHLER curve (Figure 2-2) which plots the dependency of droplet radius on ambient (super) saturation and allows the easy visual identification of the critical radius for a droplet with a particular solute mass at which it requires the greatest degree of local supersaturation to continue growing. The dashed line represents a pure water droplet solely under the influence of the curvature effect, illustrating the hyperbolic increase of required supersaturation with decreasing radius. The critical radius (*) describes the point on a droplet's growth curve at which the curvature effect begins to rapidly weaken, allowing further droplet growth through condensation at lower and lower degrees of supersaturation.
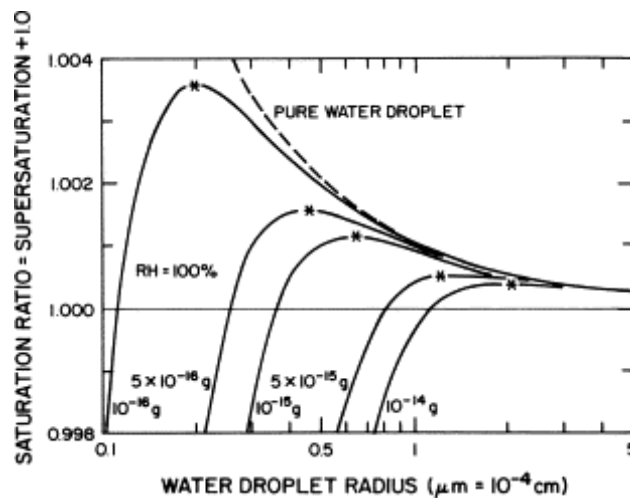
Figure 2-2:   KÖHLER curves for droplets with different solute mass. Critical radius
marked with (*). RH=relative humidity (Heymsfield 2003).

2.3.3 Drizzle drop formation and growth

While droplet growth up to radii of around 10µm occurs almost exclusively via condensation, further growth increasingly occurs via collision coalescence as a result of one of several meteorological processes (Rasmussen et al. 2002). Although drizzle drops are conventionally defined as having a diameter greater than 40µm, the droplet collision coalescence growth process that primarily forms them begins at much smaller sizes. Since

droplets above 10µm begin to fall and reach significant vertical velocity relative to smaller droplets, collisions between larger and smaller droplets become more frequent. The collision efficiency coefficient of a large (>10µm) falling droplet is largest for collisions with droplets approximately half its size, since smaller droplets are more readily pushed aside by the bow wave of an approaching large droplet, and droplets closer in size to the collecting droplet will have similar vertical velocity and therefore lower probability of collision.
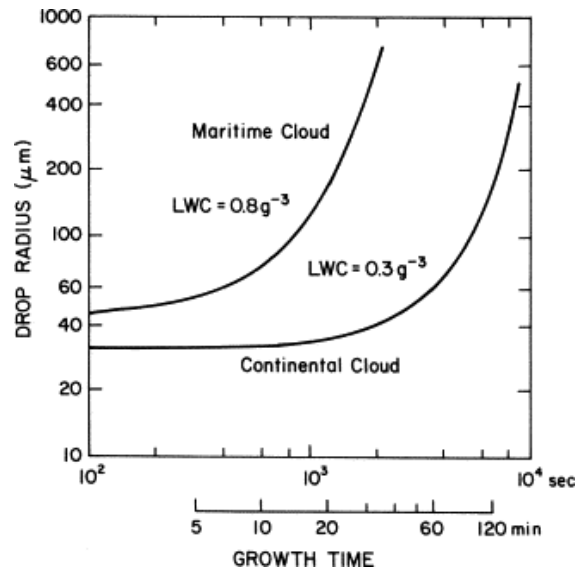
Figure 2-3:   Growth of droplet radius r over time, in maritime and continental clouds
(Heymsfield 2003).

Collision between two water droplets does not guarantee complete coagulation since there are several external factors such as aerodynamic and electrostatic effects as well as the collision angle modifying the collision/coagulation ratio. Although this ratio lies somewhere below 1.0, collision coalescence does significantly accelerate cloud droplet growth. This is clearly visible in Figure 2-3, which describes droplet growth over time separately for a maritime cloud and a continental cloud. Upon reaching a size range of 50-100 µm, droplet growth rapidly increases. Since the maritime cloud has a larger droplet diameter to begin with, the tipping point of coalescence growth is reached sooner than in the continental cloud.

Although it is often referred to as the "warm rain" process, collision coalescence can and does occur among super-cooled liquid cloud droplets wherever conditions allow them to persist. Super-cooled drizzle may also be formed by non-super-cooled drizzle precipitating into a sub-freezing air mass that contains too few active ice nuclei for effective and rapid glaciation.

One important mechanism for the depletion of SLWC besides freezing is evaporation of droplets falling into sub saturated air. A droplet's mass evaporation rate $\partial m/\partial t$ is dependent upon factors such as the droplet surface area, determined by the radius, as well as the local degree of sub saturation, again influenced by the radius via the curvature effect. Because of the highly non-linear relationship between diameter and volume, droplets at the lower end of the drizzle drop size spectrum must be considered small within the context of precipitation. These kinds of drizzle droplets are particularly vulnerable to evaporation effects and will be rapidly depleted at relative humidity values below 90%. The greatest majority of drizzle drops formed by collision coalescence evaporate somewhere between cloud base and the ground. The distance below cloud base at which precipitating drizzle droplets persist is governed by the product of vertical velocity and time-to-total-evaporation which is in turn determined by a combination of layer depth and intensity of sub saturation in the air mass below cloud base.

2.3.4 Raindrop formation and growth

Droplets with a diameter significantly above 500µm belong in the category of rain drops which are limited by aerodynamic shear forces to a maximum diameter around 2000µm. Coalescence growth to rain drop diameters happens in a minority of rain cases and only in intense tropical convection is it the primary rain formation mechanism. The term rain here signifies liquid precipitation formed through the classic rain formation process via melting of ice phase precipitation.
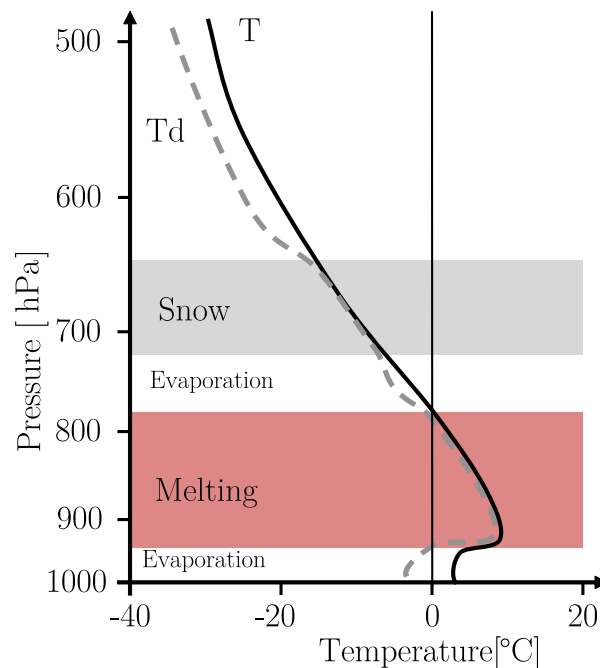
Figure 2-4:   Synthetic sounding of classic rain formation conditions, potential evaporation
              layers. Temperature (T) and dewpoint (Td).

The classic rain formation process requires the formation of ice phase precipitation above a layer of air with a temperature sufficiently above freezing to fully melt the precipitating ice particles, producing liquid precipitation droplets corresponding to the ice water content of the original particle. This formation process requires several atmospheric layers with specific properties, as arranged along the vertical axis in Figure 2-4. This sketch illustrates the elevated cloud at 700 hPa which is precipitating snow which will fully melt to form rain drops upon entering the above freezing layer of air below 800 hPa. This example already includes an additional factor in the form of the possible existence of layers of lower relative humidity between cloud and melting layer as well as near the ground. Although the saturation vapour pressure above an ice surface is lower than above liquid water surface at sub-freezing temperatures, and evaporation is therefore lower for ice particles and for liquid particles at the same ambient saturation, snowflakes are not spherical and have a very high surface area for their mass when compared to raindrops. Evaporation therefore has a strong contribution to the depletion of precipitating snowflakes in sufficiently sub saturated air. Dry air near ground level yet underneath a precipitating cloud may be found in situations such as an advancing warm front where a moist, precipitating air mass arrives first at altitude and time elapses before surface advection along with moisture introduced by precipitation is able to create saturated conditions near ground level.
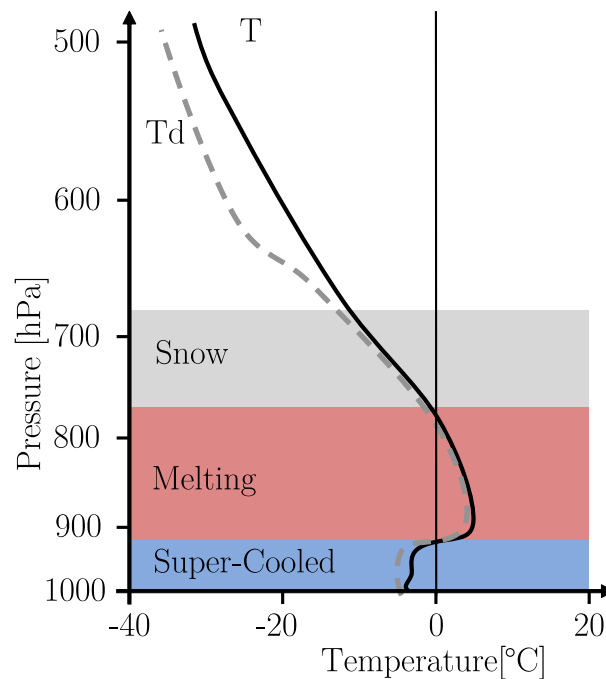
Figure 2-5:   Synthetic sounding of freezing rain. Temperature (T) and dewpoint (Td).

The formation of supercooled rain requires rain falling into a layer of air with temperatures below 0°C below the melting layer (Bernstein et al. 2000). A simple example of this is shown in Figure 2-5. The warm melting layer between approx. 800 hPa and 900 hPa is warm and deep enough to fully melt snow and sufficiently saturated to prevent significant evaporation of the resulting raindrops. Any raindrops falling into the cold air near the surface will be rapidly super-cooled and, assuming the absence of active ice nuclei, will reach the ground as freezing precipitation. Freezing precipitation poses a number of hazards to human activity besides aviation and regularly causes casualties and damage in road and pedestrian accidents as well as power outages in regions where powerlines may collapse under the increased weight of ice accretion.
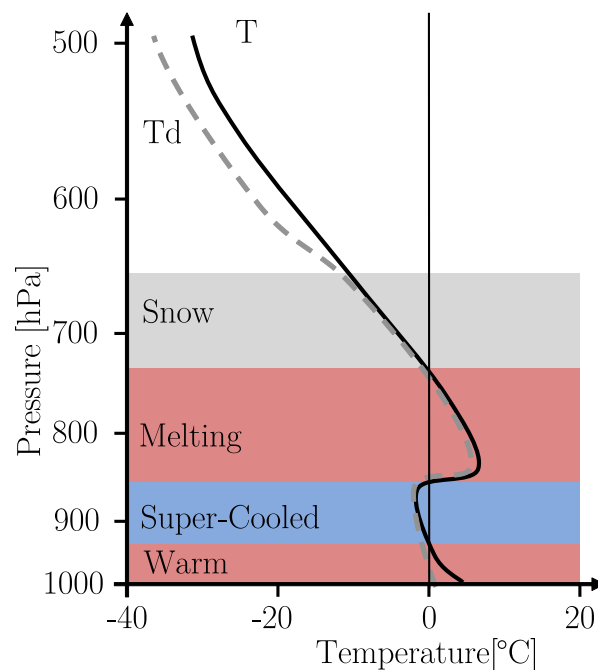
Figure 2-6:   Synthetic sounding of elevated freezing rain. Temperature(T) and dewpoint(Td).

A special case of supercooled rain occurs when an additional warm air layer at ground level is introduced to the situation described in the previous scenario. In this scenario (Figure 2-6) supercooled rain forms as in the previous scenario but does not reach the surface as freezing rain. After passing from the super-cooled air into the warm surface air, rain drops are warmed to above 0°C and return to being non-freezing when they reach the ground. Since the rain is not super-cooled when it reaches ground level, many of the hazardous effects normally associated with the freezing rain are avoided. However, any activities taking place within the height range of the supercooled air mass will be affected by freezing rain. This potentially includes structures that are tall and/or situated on high ground such as telecommunications towers or wind turbines. Conditions like these occurring close to an airport pose a particular hazard to aircraft landing and taking off. Since

ground operations at the airport are likely to be unimpeded, a larger number of take-offs and landings will be taking place compared to a conventional freezing rain situation, and aircraft will be at their most vulnerable flying low and slow just before landing or just after take-off.

An edge case of freezing rain occurs when a warm melting layer is insufficient to fully melt the precipitating snow. Partially melted snowflakes will rapidly refreeze upon entering a super-cooled cloud layer, since the ice crystal content remaining within each particle represents an active ice nucleus. Partial melting and refreezing converts falling snow into ice pellets, which may be observed at ground level as a common intermediate precipitation type between snow and rain during a warm front transit.

2.3.5 Supercooled liquid cloud water

The portion of cloud water content that exists at subfreezing temperatures in liquid form is referred to as super-cooled liquid cloud water (SLW). The fact that liquid water can exist at temperatures below 0°C (the supposed freezing point) is due to the physics of the freezing process. As with the condensation process, homogenous and heterogeneous freezing are differentiated. At temperatures between 0°C and -40°C, the freezing process generally requires the presence of some crystalline material to organise liquid water molecules into the nucleus of a crystal lattice. This process is called heterogeneous nucleation and once this has taken place, ice crystal growth within the liquid phase proceeds as normal. Homogenous freezing occurs spontaneously within pure water at -40°C. Super-cooled liquid water exists in a meta-stable state that is only possible where heterogeneous freezing cannot occur. This represents a local minimum in the energy potential curve of water in its liquid state, while the activation of freezing allows the water molecules to organise in the energetically more optimal crystalline configuration.
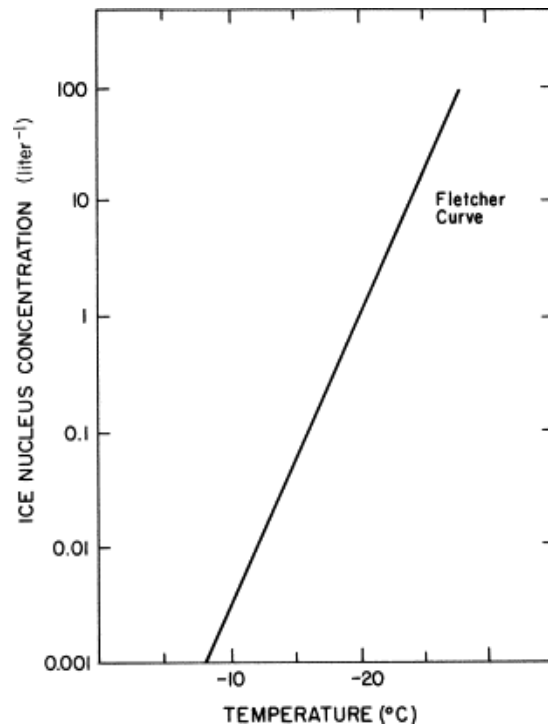
Figure 2-7: FLETCHER curve, global average of active ice nucleus concentrations versus temperature (Heymsfield 2003).

The crystalline particles that are able to initiate heterogeneous freezing are referred to as ice nuclei (IN) and they can be found among the crystalline fraction of common aerosol. The efficiency of an IN particle is inversely correlated with the temperature and requires the temperature to be below a certain threshold value for the IN to be active. This activation temperature varies with the type of IN particle but significant numbers of active IN are generally only found at temperatures below $-10°C$ and in number concentrations several orders of magnitude lower than those of CCN. The temperature dependence of IN activation is visualised in the FLETCHER curve as seen in Figure 2-7 above.

The overall low number of active IN in the temperature range from $0°C$ to $-10/-15°C$ allows the persistence of liquid water at significantly super-cooled temperatures. Most clouds above the homogenous freezing temperature contain of liquid water but the conditions that lead to a significant threat of aircraft in-flight icing consist of significant amounts of super-cooled liquid water with sufficient horizontal extent to sustain ice accretion for some time. These conditions occur most frequently at temperatures above $-10°C$, because of the temperature-dependent IN activation. Mixed phase conditions, where SLWC as well as ice crystals are present, expose the metastable quality of the supercooled liquid water state and will lead to rapid depletion of the liquid water content. Any contact between super-cooled liquid water drops and ice particles will initiate riming of the SLW on the ice crystal surface. Indirect mass conversion from the liquid to the ice

phase occurs via the vapour phase through the BERGERON-FINDEISEN process, where the difference in saturation vapour pressure over ice and liquid surfaces at super-cooled temperatures results in a net evaporation of liquid water droplets and a net growth of ice crystals through vapour deposition. Together, these effects result in efficient depletion of super-cooled liquid water droplets in the presence of ice crystals.

It is therefore essential to an accurate assessment of icing conditions to take into account as best as possible the distribution of IN and ice crystals acting as SLWC sinks in determining where the macro-physical potential for icing results in actual SLWC persisting long enough to be significant.

2.3.6 Stratiform, convective, and orographic icing

The micro-physical cloud formation and growth processes leading to supercooled liquid water content outlined above are influenced by the weather situation in the wider vicinity (Bernstein et al. 2007; Bernstein and LeBot 2009). This macro-physical state of the atmosphere is categorised at a high level according to the dynamic process responsible for the lifting of moist air which in turn is the primary source of water vapour for condensation in cloud formation and growth. Three broad types of lifting are generally distinguished, namely *frontal*, *convective*, and *orographic*. In an idealised case each is associated with a characteristic family of resulting cloud types, namely *stratus*, *cumulus*, and *orographic* clouds, respectively. Under naturally occurring conditions combinations of these processes are often active in any given area and this can result in a number of hybrid cloud types developing.

Stratiform or *stratus* clouds are formed by moderate wide area uplifting of moist air above the condensation level. Stratiform clouds exist in an atmospheric layer usually bounded by the local condensation level at the bottom and a moderate capping inversion at the top and frequently occur as multiple vertically stacked layers of varying layer depth, while the lifting responsible for the formation of stratus clouds is most often provided by dynamic features of the atmosphere such as warm fronts. The vertical velocity component generated by this type of lifting is typically on the order of 10cm/s, is able to support cloud and drizzle formation and growth via condensation and collision coalescence but is insufficient to support the direct formation of large raindrops. Formation of large drop rain, usually in *nimbostratus* clouds, occurs according to the classic rain formation process involving ice phase precipitation. Typical stratus clouds have a median volume diameter (MVD) of approximately 15μm (Jeck 2002). The maximum liquid water content of the stratus cloud is found to be correlated with the vertical as well as the horizontal extent of the cloud volume. Entrainment of sub saturated air at the sides as well as the top of a cloud reduces the peripheral LWC through evaporation and the greater

the horizontal extent of a stratiform cloud the greater the undisturbed internal volume and condensate mass. Assuming adequate vertical mixing, LWC increases linearly from the cloud base to a peak near the cloud top from where it diminishes due to entrainment evaporation (Pruppacher and Klett 1997). The area near the cloud top also has a higher probability of SLD formation through a combination of constant vertical advection of growing cloud droplets together with radiative cooling of the cloud top. Icing conditions in stratus clouds are characterised by mostly light to moderate icing intensity outside of the rare SLD cases. However, the potentially very large horizontal extent of stratus cloud formations put aircraft cruising or holding within the icing altitude range at risk of considerable ice accretion due to the extended duration of the exposure.

Convective or *cumulus* clouds are discreet convective cells or multi-cell clusters, each organised around an updraught core, and are formed when bubbles of warm moist air, energised by solar irradiation of the surface, rise beyond the cumulus condensation level (CCL). The subsequent development of the convective cloud is strongly dependent upon the instability and humidity of the atmospheric column, as may be expressed by the Convective Available Potential Energy (CAPE), and whether the rising air parcel has enough energy to reach the level of free convection (LFC) (Pruppacher and Klett 1997). Situations where convection does not reach the LFC result in shallow cumulus or stratocumulus with low precipitation potential, although SLD are not infrequently found in shallow maritime convection.

If convection does reach the LFC then free convection is initiated and will result in towering cumulus (*cu congestus*, *cumulonimbus*) reaching all the way up to the equilibrium layer and possibly even overshooting it. Tropical storm clusters and cyclones are among the deepest naturally occurring convection while some of the most intense single-cell convection occurs in severe super cell thunderstorms. CAPE is one of the main controlling parameters for the intensity of free convection and is instrumental in determining the intensity and extent of the updraught core as well as ancillary dynamic structures (downdraughts, anvil, overshooting). The updraught intensity may be measured in m/s and is in turn the limiting factor on the maximum hydrometeor size kept in suspension, with the maximum particle size occurring towards the top of the updraught core.

The total LWC is dependent on numerous environmental factors, chiefly CAPE and low-level water vapour inflow, but the LWC maximum is also concentrated around the updraught. Deep convection may rapidly transport considerable amounts of liquid condensates to high altitudes with corresponding low temperatures. The relative lack of activated ice nuclei within the updraught core enables supercooled liquid water to persist down to the homogeneous freezing temperature of $-40°C$ (Rosenfeld and Woodley 2000). Depending on the intensity of the convection, icing conditions encountered in convective

clouds are characterised by transient but high to extreme ice accretion rates (Jeck 2002) at altitudes not achieved by other SLWC formation mechanisms. Coupled with the inevitable strong turbulence and high likelihood of significant amounts of hail, flight through the core of deep convection is extremely hazardous.

Orographic clouds form as a consequence of forced lifting of moist air mass flowing over terrain. In its purest form this appears as a capping cloud directly over a ridge or mountain, although lenticular lee wave and rotor clouds are also observed at some distance (Pruppacher and Klett 1997). In the idealised mountain case the upslope flow of the air mass is analogous to frontal lifting and generates a cloud similar to a stratus cloud in certain respects. The portion of the cloud upstream from the terrain obstacle is characterised by a well-defined cloud base along the condensation level and a cloud top gradually rising towards a maximum height near the peak terrain elevation. Liquid water content increases from the point furthest upstream to a point near the peak elevation, where the maximum vertical forcing of air mass is taking place. The area behind the peak elevation is characterised by descending airflow which results in rapid evaporation of cloud droplets due to adiabatic compression and warming (see Figure 2-8 below).

In contrast to stratus clouds, the orographic cloud does not move with the surrounding air mass but represents a quasi-stationary volume with a constant flow of air and condensate passing through. New condensate is constantly forming on the upstream side, is part of the visible cloud while being transported through it, and is advected to the leeward side of the terrain to evaporate in the warming air (Borys et al. 2000). Cloud and drizzle droplet growth is limited by the same saturation and vertical velocity parameters as in a stratus cloud, but is further limited by the time taken by an air parcel to transit through the cloud volume. Particle size and LWC maxima and the resulting icing conditions may approximate those of convective clouds with similar vertical acceleration, although averages over the entire cloud volume are more like those of stratiform clouds. The potentially considerable horizontal velocity component through the cloud volume can under certain circumstances result in the horizontal advection of significant amounts of large hydrometeors out of the cloud volume and downstream. Given appropriate air temperature this has the potential for resulting in super-cooled precipitation occurring next to and not under a visible cloud, which represents an additional situational awareness challenge for pilots.
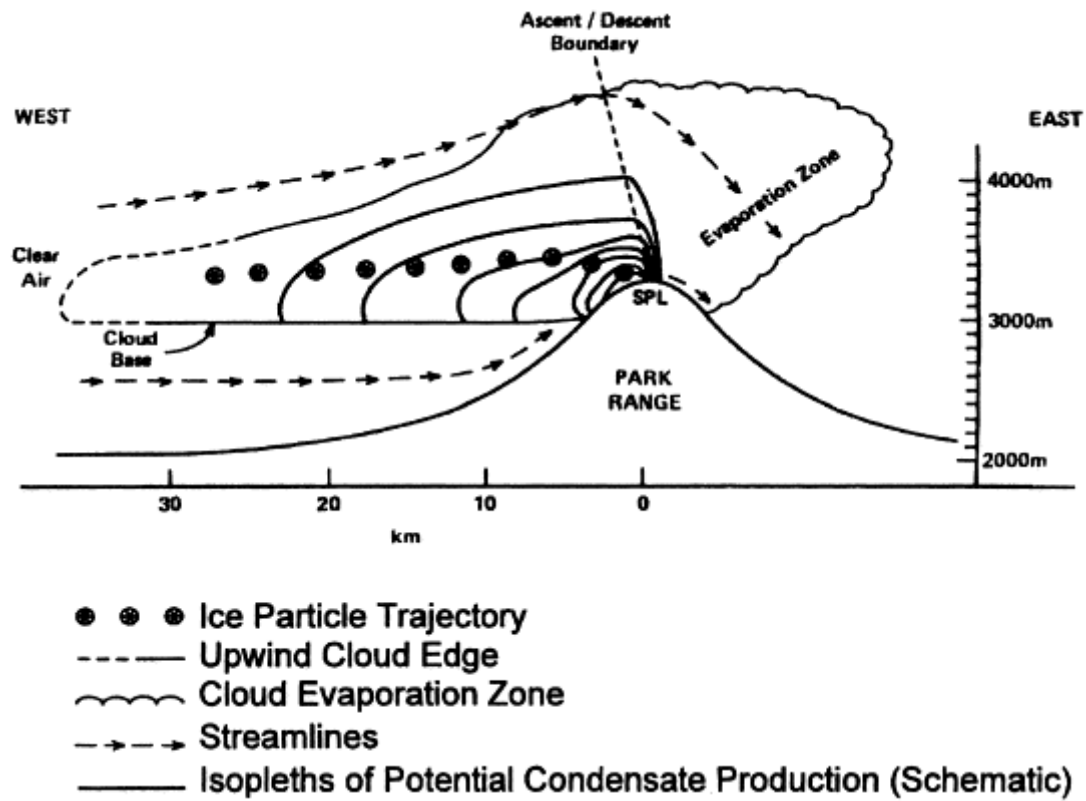
Figure 2-8: Schematic of orographic cloud formation ([Borys et al. 2000](#)).

3.   State of the art in icing diagnosis

Reliable and sufficiently accurate descriptions of weather hazards to aviation are required for effective and above all safe and cost efficient flight planning. Although aircraft manufacturers have adopted several technical precautions against icing risk, such as wing heating or mechanical de-icing boots, hazard avoidance is still a necessary part of flight safety. The science and technology supporting in-flight icing warnings has evolved and needs to continue doing so as new methods and data sources become available. This chapter provides a brief history of icing warning, introduces some common concepts of diagnosing weather hazards, and presents the current state of the art in icing diagnosis systems.

The aircraft icing phenomenon has historically been difficult to forecast accurately, so efforts were focused on establishing the best possible diagnosis of current conditions. Since icing conditions are also difficult to detect remotely, these icing diagnoses were based on pilot reports of icing encounters. This was sufficient to identify general areas and air masses with a higher icing potential and provided some benefits to aviators in terms of increased awareness. This broad-stroke approach is still in evidence today as the officially certified icing warning products highlight mesoscale areas of increased icing risk that are then treated as valid for up to six hours. These products are called SIGMET (SIGnificant METeorological advisory) and AIRMET (AIRman's METeorological advisory). More on these in section 3.1.3: "SIGMET/AIRMET".

The aviation community requires warnings for flight planning on different timescales. Strategic planning for long-haul flights requires information several hours in advance in order to calculate the most efficient flight path while maintaining safety. There is also a requirement for weather hazard warnings on a shorter tactical timescale, for example to calculate how many aircraft can land safely within the next half hour before an approaching thunderstorm will cause runway closure. Information about the precise location and vertical extent of weather hazards on the shortest timescale, called nowcast, is needed for example when navigating in the vicinity of thunderstorms or around airports. Icing has generally been treated as a tactical problem, requiring reactive mitigating actions if and when encountered.

While it is still primarily a safety of flight issue and icing forecasts are mainly used for early warning of aircrew for increased situational awareness, efforts at implementing "weather-smart" flight planning and management are increasingly recognising icing as contributing to weather related airspace capacity constraints that must be considered when guiding traffic flow patterns.

The icing certification level of an aircraft/crew/operator depends upon the ice protection equipment on the aircraft and certain required aircrew qualifications. The clearance level has a major impact on the individual icing warning requirements and strongly differentiates between two groups with and without clearance to operate in known icing conditions. Icing protected operators have clearance for and a certain tolerance of operating icing conditions and will fly in known or suspected icing conditions, of intensity within their tolerance, if routing efficiency requires it. These customers want to know where icing can occur and how severe it will be. Non-equipped flights, and therefore without clearance for icing conditions, are also often under visual flight rules (VFR) conditions and must maintain a safe distance from weather at all times. These customers need a high confidence in ice-free conditions, and have no need for icing intensity information.

Following realization and acceptance by air transport stakeholders that non-traditional icing conditions (SLD) represent a real and regularly occurring hazard to aircraft operations (e.g. FAA 1997), steps were undertaken to increase aviation safety in the light of this. A number of measures were adopted by national and international governing bodies of civilian aviation to achieve this goal, including definition of a new requirement for improved icing warning products with higher spatial and temporal resolution. SIGMET/AIRMET would continue to be the officially certified solution, but new icing products based on direct observations and Numerical Weather Prediction (NWP) would provide valuable information as a supplement. This new generation of algorithms use model data to derive the atmospheric state in three dimensions with high resolution and gapless coverage. Combined with actual observations, this overcomes the greatest inadequacies of the standard warning products. Examples of this new generation of systems are the Current Icing Potential (CIP) icing diagnosis algorithm developed at NCAR in the US, the SIGMA icing nowcasting system by Météo France, and also the ADWICE system presented here.

3.1   Standard solutions to icing diagnosis

Standard solutions for icing warning for each defined Flight/Upper Airspace Region (FIR/UIR) are a legally mandated deliverable for the meteorological watch office (MWO) responsible for each individual region, as defined in the ICAO Convention on International Civil Aviation, also known as the Chicago Convention. The responsibilities of an MWO are defined in Annex 3: Meteorological Service for International Air Navigation in its current 16th edition (ICAO 2007). Annex 3 also specifies the responsibilities of the World Area Forecast System (WAFS) whose individual centres are required to produce comprehensive wide area forecasts of significant aviation weather in a Significant Weather Chart for high and medium altitudes four times a day. See Figure 3-1 for an example.
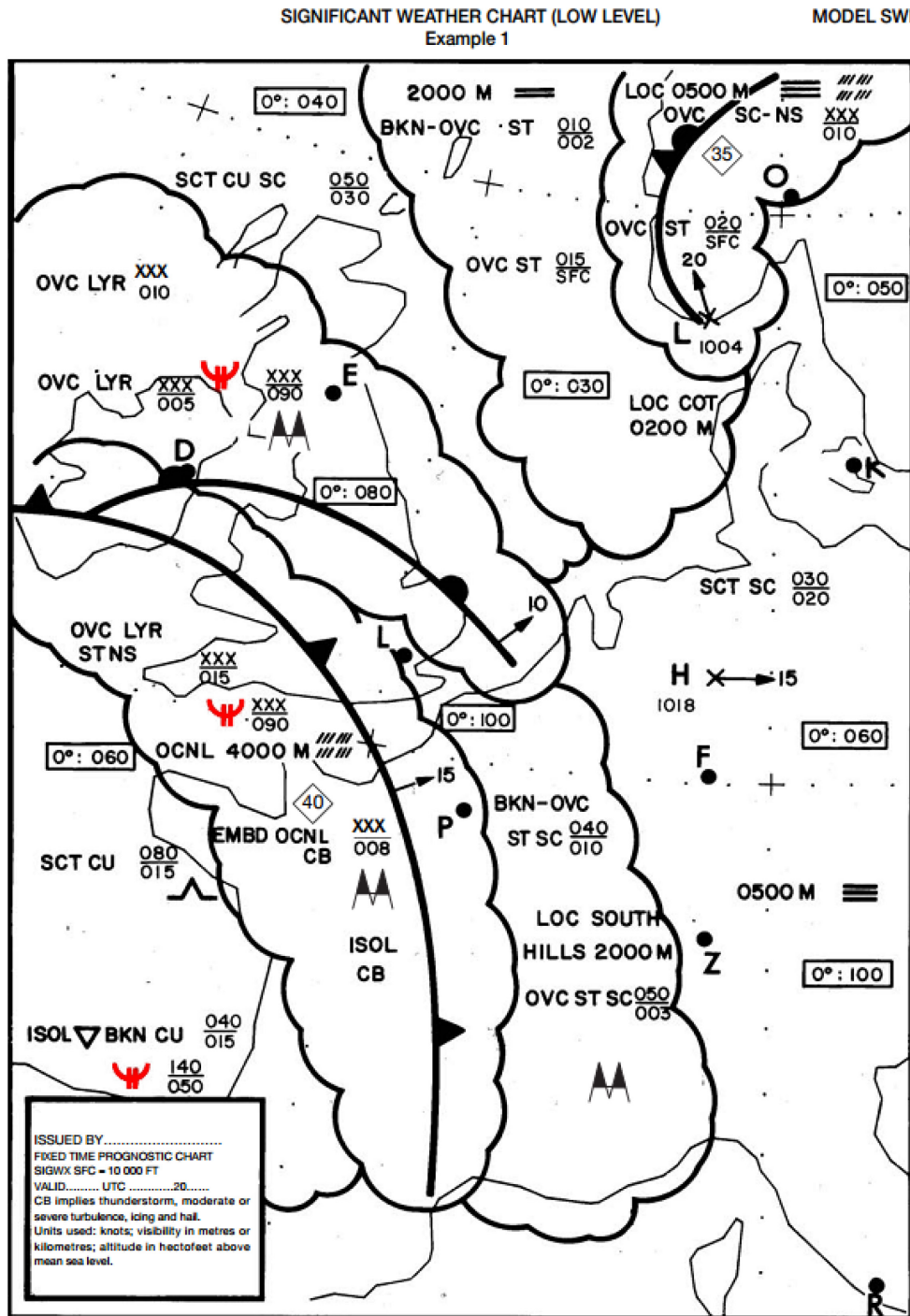
Figure 3-1: Significant Weather Chart (Low Level), with icing warnings highlighted (red) (ICAO 2007).

Each MWO is responsible for a number of aviation weather services related to the creation, collection, and dissemination of weather observations and warnings. There are two principal forecast and warning products of significance for in-flight icing, SIGMET and AIRMET. SIGMETs are warnings of an aviation weather hazard within a particular UIR above FL100, while AIRMETs are warnings of significant aviation weather below FL 100. Both SIGMETs and AIRMETs may be prepared in a textual telegram style (see section 3.1.3) but issuance of a graphic chart in the style of the SIGWX is also encouraged.

The certified warning products are traditional methods with significant shortcomings in the context of today's increasingly integrated and demanding air traffic system. Until very recently, the diagnosis of icing conditions was not automated but was a largely manual process performed by skilled aviation weather forecasters. Using all available observation sources (e.g. pilot reports, ground-based observations) and experience with icing weather situations, the forecaster would produce an estimate of icing coverage and altitude for large and conservatively outlined areas corresponding to weather systems containing suspected icing conditions. These warnings are disseminated as SIGMET/AIRMET in a textual telegram style, as well as on charts depicting the area of coverage. This warning is then valid for 4-6 hours, when an updated assessment is issued. The underlying assumption is that icing conditions are persistent enough to support this rather long validity range.

3.1.1 Pilot reports (PIREPs)

The first weather hazard early warning system for aviators consisted of reports about weather hazard encounters by other pilots. In a time before on-board weather radar, pilots often had to rely on reports by other pilots further ahead on the same route as the sole source of information about weather hazards ahead and there was increasing incentive to systematically request, collect and disseminate PIREPs. Even today, when most large aircraft are equipped with on-board weather radar and there are several ground, air, and space-based remote sensing systems, some aviation weather hazards remain difficult to detect at a distance. In its current form the PIREP system still plays an important role in making pilots aware of potentially harmful weather phenomena in their surroundings. It also represents an important source of direct observation data that can be used to verify remote sensing and forecasting approaches.

The method for submitting pilot reports has changed little over time and is mostly via voice communication over radio. While there is a basic agreed-to standard formula for the way PIREPs are encoded, there is still a certain amount of interpretation required. PIREP location is often reported as a range and bearing from a certain reference point

("25nm south-west of Chicago"), or on a line between two points of reference (Detroit - Buffalo). There are again historical reasons for this due to the fact that for most of aviation history, navigation was accomplished relative to such known reference points and not by absolute geographic coordinates. It was only with the advent of computerised satellite navigation systems that aircrew had easy access to precise location information, but the relaying of such coordinates via voice radio remains impractical. PIREP altitude reporting on the other hand is generally reliable as this is a parameter available to the aircrew as a precise measurement, and can be easily relayed via voice communications as a simple flight level statement.

Another difficulty in the evaluation process is the fact that PIREP reporting time and location is not necessarily equivalent to the time and location of the actual weather hazard encounter, and not all PIREPs explicitly report the observation time. A proportion of PIREPs are submitted with a significant time delay after the actual observation was made, since during the weather hazard encounter the aircrew was probably preoccupied with operating the aircraft. It is difficult to establish retrospectively whether the pilot report's associated timestamp refers to the actual time and place of the encounter or if it represents the time and location of the report submission.

For modern numerical evaluation methods and for comparisons with gridded forecast models, PIREPs need to be associated with a specific grid point. This necessitates a conversion step, most often via first determining precise geographic coordinates of the PIREP location. Although powerful parsing algorithms have been developed that enable an automatic conversion of the great majority of submitted PIREPs, certain assumptions that must be made for such a step may introduce additional error in the PIREP location. As with any observation, the reported type and especially the severity of the weather hazard is down to the pilots' subjective impression. This is influenced by a range of factors such as pilot workload, visibility (day/night), and even the type of aircraft involved. While technical equipment may be able to provide a more objective assessment of intensity, instrument-based icing severity detection is not straightforward and also depends on a number of outside factors.

Key to this is also the organisational issue of the lack of a scientifically meaningful, standardised, and universally accepted parameters for icing severity. Efforts to relate icing severity to one single measurable, forecastable atmospheric parameter have so far failed (Jeck 1998), since the actual icing severity experienced by one specific aircraft during one specific icing episode depends on many factors (see Chapter 2: The aircraft in-flight icing problem). Also, pilot reports are naturally biased strongly towards observation of an actual event, as opposed to the absence of such. Negative PIREPs are admissible and are also regularly reported, but mostly near the boundary to a previously reported

weather hazard. As a result of the lower reporting incentive, negative PIREPs are rarer than positive PIREPs by about an order of magnitude. Taking into account these cumulative error sources in the chain of PIREP reporting, it is important to assure a sufficiently large sample size when comparing PIREPs to other observations or forecasts in order to increase the confidence in the observation to an acceptable level. When using pilot reports as "truth" data for analysis and forecast validation, the unsystematic and highly biased distribution creates some difficulty for compiling robust statistics of forecast accuracy and necessitates the exclusion of some otherwise common statistical measures (Brown and Young 2000).

Efforts are underway to move PIREP reporting away from unreliable and inconvenient voice communication channels into digital data-links. Such PIREPs reported via a cockpit software interface are referred to as AIREPs (aircraft report). Aircraft equipped for AIREP reporting are still rare. An advantage of AIREPs is that they contain precise location information from the aircraft navigation system. Additionally, a fully automated data-link of aircraft on-board sensors via the systems AMDAR (ACARS) and TAMDAR (Murray et al. 2004) is also increasingly widespread. These developments result in much improved data quality and quantity, benefiting diagnosis as well as validation efforts.

3.1.2 Ground based observations

As demonstrated in earlier studies (Bernstein et al. 1997), there is a strong correlation in certain cases between ground weather phenomena and icing conditions aloft. Careful interpretation of ground weather reports such as SYNOP/METAR permit some inferences to be drawn as to the in-cloud conditions, thereby enabling the detection of some icing conditions purely on the basis of weather observations from the ground. Earlier applications of this approach (e.g. the *stovepipe algorithm*, (Bernstein 1996)) focused largely on the differentiation between SLD and non-SLD icing conditions through the analysis of precipitation type reported at ground level. With the high density of human-staffed SYNOP and METAR weather reporting stations in central Europe capable of reporting significant weather several times a day, it was feasible to implement in ADWICE a more nuanced analysis of reported weather to support the diagnosis of icing conditions. The known formation process for certain types of precipitation observed at ground level requires certain atmospheric conditions along the precipitation path and this allows some conclusions to be drawn about the presence or absence of certain icing conditions. For example, the observation of snowfall at ground level is a strong contra-indicator for the presence of supercooled liquid water between ground level and the snow's formation layer, since super-cooled liquid water does not persist in the presence of ice crystals because of

direct and indirect scavenging, through riming and BERGERON-FINDEISEN conversion respectively. Conversely, the observation of freezing precipitation is a direct proof of supercooled liquid water and therefore icing conditions, requiring no further interpretation beyond the question of vertical extent.

The phenomena observable from the ground that are most useful for the diagnosis of icing conditions aloft are certain types of precipitation at the surface. Freezing precipitation such as freezing rain or freezing drizzle is the most direct indicator for icing conditions aloft as it itself already consists of supercooled liquid water. Therefore icing conditions prevail between the surface and the layer where this precipitation formed (within the cloud layer above), or the top of the supercooled air mass, whichever is lower. Freezing precipitation is one of the most extreme forms of icing conditions and therefore ground observations can be a valuable data point in locating this rare but very hazardous phenomenon. Other forms of precipitation such as ice pellets indicate the existence of supercooled liquid water above, albeit less reliably. Convection is generally relevant to air operations as it poses multiple hazards to aircraft. Ground and radar observations of convective activity contribute significantly to weather hazard awareness, as does the ground-based observation of runway visible range and cloud ceiling height.

The precise observation of precipitation type at the surface relies on the presence of a human observer at the station. While METAR observation stations at airfields may routinely have human observers, SYNOP stations, especially in Europe, are increasingly automated and lack the capability to precisely distinguish precipitation type. This reduces the number of stations available for making icing-relevant ground observations. Weather radar is also a valuable source of remote sensing data that may help to confirm the identification of certain types of icing conditions. Weather radars operate at a wavelength selected to provide optimal detection of precipitation and because of that they are well-suited to identify areas of convective activity where icing conditions can be inferred. This information about the location of convective precipitation can be used to support a diagnosis of convective icing.

3.1.3 SIGMET/AIRMET

Aviation weather forecasts and advisories are currently published in a variety of formats, tailored to their respective user group. While some are targeted specifically at general aviation customers (GAMET/GAFOR), two others are more generally used by all types of operators when assessing icing risk. These products are the SIGMET and AIRMET. They are defined in ICAO Annex 3 Chapter 7 (ICAO 2007) and are officially certified

channels for dissemination of significant icing risk warnings. Each Flight Information Region (FIR) has a responsible Meteorological Watch Office (MWO) that is mandated to provide regular SIGMET/AIRMET updates.

A SIGMET is issued when the responsible MWO has determined a sufficient likelihood of a severe occurrence of one of a number of aviation-relevant weather phenomena such as thunderstorms, turbulence, icing or volcanic ash. SIGMETs are issued for a defined geographic region, either a Flight Information Region (FIR) or Upper Flight Information Region (UIR). These are airspace volumes precisely defined under ICAO regulations and partition controlled airspace, frequently along national borders. FIRs encompass lower altitudes and UIR cover higher altitudes generally used by passenger flights at cruise altitude. Some FIRs encompass national airspace of several smaller countries, while some larger countries have more than one FIR to cover their airspace. Because they encompass the UIR and the other products are only valid up to a certain altitude (often FL100, approx. 10 000ft), SIGMETS are the primary source of certified icing warnings for operations at cruise altitude. SIGMETS are generally valid for four hours, but can be withdrawn earlier or may be renewed as necessary.

An example of a SIGMET in telegram form is presented in Figure 3-2. It warns of icing over the Milan flight FIR in northern Italy on June 25, 2012 at 1026 UTC. The first line contains the MWO identifier (WS=SIGMET, IY=Italy) followed by the FIR/UIR tag (31=FIR), the reporting station's ICAO code (LIIB=Rome), and finally the time stamp (25=day-of-month, 1026=time in UTC). The second line begins with the ICAO code for the control centre in charge of the FIR in question (LIMM=Milan) followed by the SIGMET keyword and a unique count value (01). The line closes with a validity time range (beginning/until) of the same time stamp format and ends with a hyphen after a repeat of the control centre ID to positively terminate the line. The third and fourth lines contain the actual weather information and read like this: "Milan FIR has a *Severe* icing observation, reported via AIREP, on the 25th at 0609 by a medium-size aircraft between flight level 170 and 190, 25 nautical miles northeast of Bolzano (LIPB). Weather is stationary, no change expected during validity period".

```
WSIY31 LIIB 251026
LIMM SIGMET 01 VALID 251031/251431 LIMM-
MILANO FIR SEV ICE OBS AIREP 250609 MED ACFT BTN FL 170/190 25NM NE
OF LIPB STNR NC=
```

Figure 3-2:   Example SIGMET telegram text (aviationweather.gov).

AIRMETs are encoded in a slightly different format from SIGMET, but carry a similar type of information. The difference lies mainly in the fact that AIRMETs are a supplement to the lower altitude general aviation products (GAxxx) and therefore are not only for severe events, but are issued for moderate events to account for smaller aircraft. There are three AIRMET types (sierra, tango, zulu), that concern different weather hazards. Icing is reported in the ZULU AIRMET, which transmits icing warnings and freezing level height for FIR subsections and has a valid time of six hours.

For several decades SIGMET and AIRMET have formed the basis of aviation weather hazard warning. They have proven useful and reliable for highlighting regions of increased hazard potential where pilots need to focus greater attention on weather events to assure safety of flight. However, as air traffic density is continually increasing, weather hazards have become a constraint on airspace capacity and new approaches are needed for more efficient route finding while maintaining safety. In this evolving context, where advanced concepts in air traffic management require much more precise and timely weather information to maximise air traffic efficiency, SIGMET and AIRMET are proving increasingly inadequate. They cover very large areas to describe sometimes quite localised weather events. This results in large volumes of unaffected airspace being unnecessarily associated with a weather hazard warning, even when taking into account a weather hazard's potential increase in effective area through translation during the validity time period. This inclusive definition of SIGMET and AIRMET represented the conservative choice in the past, but is coming under increasing pressure from air traffic stakeholders that demand higher precision and temporal resolution. Specifically, a high value is being put on the ability to identify hazard free areas with high confidence and on reduced over-forecasting.

3.2   Augmentation with model data

Requirements for advanced icing diagnosis systems emerging in the 1990s ([FAA 1997](#)) specified a higher spatial and temporal resolution than SIGMET/AIRMET can provide. Ground observations are not uniformly distributed across the land mass and are unavailable over the oceans, so a new means for icing diagnosis had to be developed. By the late 1990s, developments in numerical weather prediction (NWP) had progressed sufficiently to make model-based icing diagnosis feasible. While the global NWP models provided coarse horizontal resolution, regional models were adequate in terms of their grid resolution and in terms of the accuracy with which they predicted many relevant atmospheric parameters.

However, due to the complexity and inherent instability of the processes that lead to the formation of icing conditions, and the fact that some parameters (such as ice nuclei) that influence these processes are not modelled in operational NWP systems, a process of indirect icing retrieval from model output had to be developed. Algorithms in this category are called "Expert Systems", because they are specialists in the detection of very specific weather phenomena and have been adapted to produce output most relevant to their specific target audience.

Such systems have now been in development for some time and are being made available by several national weather services to flight planners and general aviators through a variety of outlets such as aviation weather websites or integrated self-briefing software systems. These icing diagnosis and forecast products have been shown to provide icing awareness information at a much higher resolution, allowing the improved pinpointing of hazard areas as well as the identification of low risk or risk free areas with high confidence. In addition to the distribution of icing potential and an estimate of icing severity, a diagnosis of likely meteorological icing type is performed. This enables a classification of icing via the expected droplet size category, namely: cloud droplets ($<$40µm), stratiform SLD (40-500µm), convective SLD (40-500µm), and freezing rain ($>$500µm).

3.2.1 New forecast products as advisory supplement

Even though the advantages of a more granular icing forecast have largely been realized and are benefiting aviators today, icing expert systems have still not been certified as fully independent icing forecasts on the same legal standing as SIGMET or AIRMET. Therefore icing expert systems are currently classed as "advisory supplements" to the classic icing products.

There are several different approaches to deriving icing conditions from weather model output and some of the possible conceptual differences will be illustrated by contrasting the working principle behind ADWICE and that of the US Forecast Icing Product (FIP) and French SIGMA systems. These systems are designed to derive an estimate of icing potential from the output of their respective NWP models and the final output is actually very similar in terms of the meteorological meaning as well as the final presentation for the customer. There is, however, a significant difference in the basic working principle used to arrive at that output.

3.2.2 The Current/Forecast Icing Product CIP/FIP

The aircraft icing research facility at NCAR, responsible for the development of icing warning systems on behalf of the US National Weather Service (NWS) and the Federal Aviation Administration (FAA), has developed two related and complementary systems for the diagnosis and forecasting of in-flight icing conditions. Called the *Current* and *Forecast Icing Product* (CIP / FIP) (Bernstein et al. 2005; McDonough et al. 2003), they are applied to the model-based and observation-based diagnosis of current icing conditions and the fully model-based forecast of future icing conditions, respectively. Both warning systems have been thoroughly investigated to document the advances over earlier warning approaches, to demonstrate suitability and reliability for future expanded use in operational settings (Chapman et al. 2004; Madine et al. 2008).

The CIP diagnosis algorithm uses ground observations (METAR, radar, lightning detection), pilot reports (PIREPs) of icing encounters, satellite spectral channel radiances as well as model data to derive a three-dimensional icing potential product (Chapman et al. 2004). Until recently the model used was the RUC-Rapid Update Cycle regional model, but FIP and CIP have since been converted to use the WRF-RR model. Both CIP and FIP share the basic ingredients-based approach of identifying areas with icing potential through the cumulative contribution of input parameters to overall icing potential and probability. The weighted contribution of each ingredient is defined via interest maps to generate a total interest field for in-flight icing potential.

The forecast product FIP operates fully in this way, deriving icing potential from model forecast fields such as temperature, humidity, total water content and some derived properties. The diagnosis system CIP modifies the model-based diagnosis by integrating direct observations where available. CIP currently uses spectral channel radiance products from the GOES geostationary satellite imager and employs some windowing and channel differencing techniques to derive information about the cloud top properties such as temperature and particle phase. CIP is notable for taking advantage of the numerous icing PIREPs available over the US to inform the icing diagnosis and development work is underway to improve the way in which PIREPs and other point observation are embedded and smoothed into the gridded analysis fields.

3.2.3 Rapid update nowcasting system SIGMA

The French national weather service Météo France has an icing warning system with a few unique features. The SIGMA system (LeBot 2004) is different from the other two systems presented here in that it is configured as a rapid update regional nowcasting system featuring a 15min update cycle instead of the more usual hourly forecast/diagnosis.

The SIGMA domain covers France and its immediate surroundings with a basic in-flight icing nowcast and supports nested areas of higher quality diagnosis through advanced radar sensing and physics simulations around airports. SIGMA in-flight icing nowcasts are based mainly on model output of temperature and humidity from the ALADIN regional model. These are subsequently modified by the application of satellite-derived cloud top temperature and the distribution of precipitation as derived from weather radar. The satellite product is used for detecting cloud-free and therefore icing-free areas as well as identifying clouds whose tops are in the temperature range most likely to support icing conditions, in accordance with the "warm tops" approach. The nested high-quality nowcast zone currently established around Paris can take advantage of the presence of advanced 3D radar which produces a three-dimensional radar reflectivity composite and a melting layer product. Advanced microphysics simulations produced by the AROME model are intended to improve the estimation of super-cooled liquid water persistence and therefore icing threat within the vicinity of the airport's terminal manoeuvring area.

3.2.4 ADWICE model-based icing diagnosis

The Advanced Diagnosis and Warning System for Aircraft ICing Environments (ADWICE) is the German regional in-flight icing diagnosis and forecasting expert system. Development was begun at DLR (Tafferner, Hauf et al. 2003) and is now shared between the University of Hannover and the German Weather Service (DWD) (Leifeld 2004; 2007), which also performs routine operation of the system. The ADWICE module responsible for generating icing diagnoses from NWP model data is called the ADWICE – Prognostic Icing Algorithm (PIA) and its purpose is to derive a three-dimensional field of icing potential from the most recent model run for any given diagnosis time, several hours in advance. The prognostic PIA algorithm is closely related to the ADWICE diagnostic DIA algorithm which determines the current icing situation using ground observations augmented with weather radar and model fields. The diagnostic algorithm DIA that forms the basis of the major development work described in this thesis is discussed in more detail in the following section 3.3

3.2.4.1 The COSMO model

In the beginning of ADWICE development in the late 1990s the choice was made to base the ADWICE Prognostic Icing Algorithm on the LM (*Lokalmodell*) regional weather model (Doms, Schättler 2002) then in development at Deutscher Wetterdienst (DWD). While only a regional model covering the central European landmasses, the LM provided a combination of spatial resolution (7 km), vertical resolution (35 layers), and a useful selection of forecast atmospheric parameters that allowed an estimation of icing conditions based on physical principles.

The year 2005 saw the introduction of a comprehensively extended model version. While maintaining the basic architecture of the LM model and its 7 km grid spacing, this new version would cover a much greater area from Iceland to North Africa while also increasing the number of vertical layers from 35 to 40 (see Figure 3-3). The second change would mainly benefit low altitude layer density for improved simulation of boundary layer processes.

LME development was subsequently placed under the administration of a cooperative organization called the 'Consortium for Small scale Modelling' (COSMO) that has coordinated development work across member organizations and helped the newly renamed COSMO model evolve significantly over the project lifetime (Schulz and Schättler 2011). The COSMO-EU name refers to a specific configuration of this model operated by DWD as a regional model covering the above mentioned domain. A second model configuration called the COSMO-DE (formerly LMK, for "*Lokalmodell – Kürzestfrist*") covers Germany and its immediate surroundings with a 2.8 km model resolution, and adds explicit convection simulation. That system, however, is not used for ADWICE at this time.
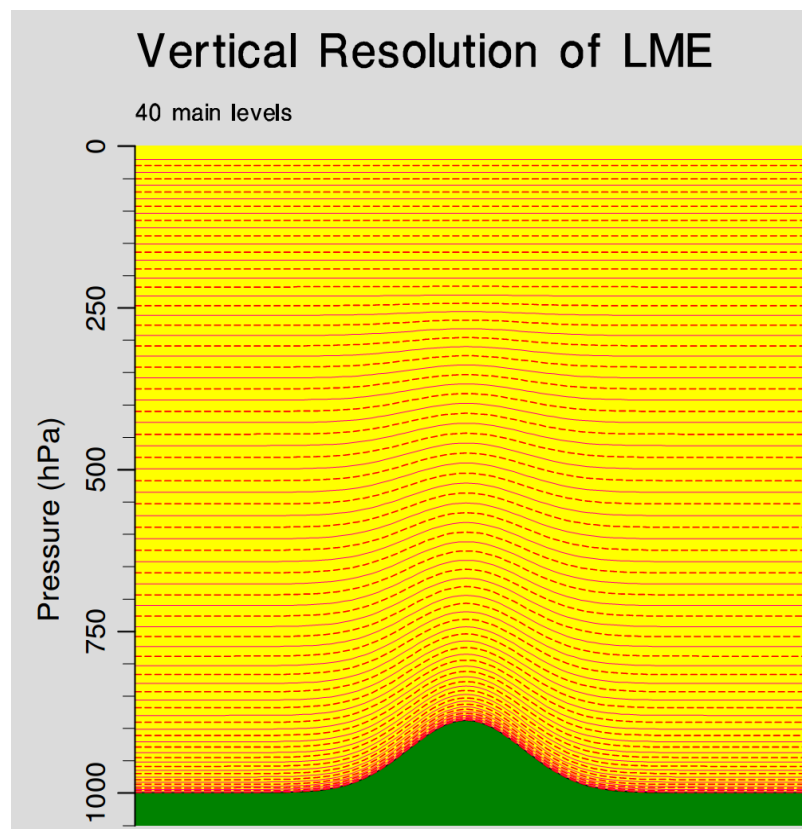
Figure 3-3:   Schematic of LME/COSMO-EU vertical model structure with vertically
              dampened terrain following model layers. ©Deutscher Wetterdienst

As currently implemented, the ADWICE PIA uses several model output parameters that provide information about potential icing conditions. These include three-dimensional fields of temperature, pressure, specific humidity (QV), and specific cloud liquid water content (QC). In addition to this the model provides upper and lower boundaries of convective activity per column as derived from the model's convection parameterisation.

Temperature

Temperature information plays a very important role in icing diagnosis, as the phenomenon occurs in a very characteristic temperature range. Current NWP models with their advanced dynamics and thermodynamics modules provide very satisfactory forecasts of air temperature distribution, which makes these forecasts fields a reliable quantity.

Pressure

Air pressure is an important parameter in many processes that involve vapour saturation and thereby influences a large number of the phase change processes that are central to the icing phenomenon. Air pressure forecasts out of the model also deliver realistic values and distributions and can therefore be seen as sufficiently reliable.

Specific humidity (QV)

The (mass) specific humidity is referred to by the symbol QV and represents the mass of water vapour per unit mass of dry air [kg/kg]. The specific humidity is a measure of the absolute water vapour content of air, but with knowledge of temperature and pressure it can be converted to the relative humidity parameter which describes the degree of saturation of the air mass. Since the conversion processes between the vapour phase of water and condensates as a whole are robustly implemented in models, at least in terms of the overall vapour-condensate conversion rates, the specific humidity field of the model output is also quite reliable.

Specific cloud liquid water (QC)

The specific cloud liquid water (QC) is analogous to the specific humidity (QV) in that it is a mass-specific parameter that describes the content of liquid water per unit mass of air. As mentioned in the description of QV, the large-scale conversion rates between water vapour and condensates are understood and quite well implemented in the model. However, the precise condensation/sublimation/evaporation/coagulation processes between different condensate classes (e.g. cloud droplets, ice crystals, snow, rain), as represented in the model's bulk microphysics scheme, are difficult to describe precisely as these are unstable or metastable conditions that depend on many environmental factors at very small spatial and temporal timescales, many of which are not implemented in current models (e.g. aerosols, ice nuclei).

Aside from the fundamental difficulties of modelling highly unstable conversion processes between the phase states of water, especially in mixed phase conditions at temperatures below 0°, there are also several more practical limitations on using the direct model output of cloud liquid water content for icing diagnosis. One of the main operational priorities for the model operators and developers is the prediction of realistic precipitation rates at ground level, since a majority of the direct and indirect customer base of model forecast information are concerned with surface weather conditions. This target audience includes the agricultural community, power companies, traffic and road safety stakeholders, and many more. Since surface precipitation rates are such a priority in the model development, the cloud microphysics scheme has been optimised for that application, with a lesser focus on accurately describing the distribution of the different condensate classes at altitude. Investigations by (Herbort 2005; Roloff 2012) have demonstrated in detail the tendency in the model microphysics to convert most of the condensate mass to snow at any temperature below 0°, thereby reducing the amount of forecast liquid cloud water to unrealistically low levels.

Parameterised convection

The COSMO-EU model with 7 km grid resolution does not explicitly resolve convective cells, and uses the TIEDTKE convection parameterisation scheme to provide lower and upper bounds to convective activity for each model column. This information is used in the ADWICE PIA to determine the vertical extent of convective icing potential.

3.2.4.2   ADWICE prognostic icing algorithm

The approach used by ADWICE to derive icing conditions from model output is based on the detection of four icing scenarios using several criteria that define conditions for separate common and characteristic icing situations (Tafferner, Hauf et al. 2003). Two of the scenarios are based on the analysis of vertical profiles of temperature, pressure, and humidity for every column in the model's 3D forecast field. The third scenario is based on the model's parameterization of convection while the fourth scenario is defined by a more general combination of temperature and humidity.

Scenario *General*

This scenario is intended to capture several different formation mechanisms for icing conditions that do not include SLD icing and cannot otherwise be derived more explicitly from model output. This includes multilayer icing situations with one of the previous icing scenarios assigned at lower altitudes. Also, icing can form under conditions that are not associated with characteristic features in vertical profiles and can therefore not be detected by such an analysis, but must rather be derived from general environmental conditions simulated in the model. The icing scenario *General* is therefore defined by a combination of criteria for temperature and humidity along a sliding scale. The admissible temperature range is from $-20°C$ to $0°C$ and the RH threshold is a function of the temperature and varies from 63% (at $-20°C$) to 82% (at $0°C$). This loose definition increases the overestimation of icing conditions and leads to the output product covering a substantial area with icing warnings.

Scenario *Freezing*

This scenario represents icing conditions caused by supercooled liquid precipitation, which can arrive at ground level in the form of freezing rain or drizzle. This phenomenon is caused by precipitation falling into a warm melting layer at altitude which lies above a sub-freezing air mass (see Figure 3-4). If the combination of the melting layer's vertical extent and temperature delta above freezing is sufficient to fully melt ice particles during their transit time, fully liquid precipitation drops will enter the subfreezing air mass below and continue falling as supercooled liquid precipitation. In the absence of ice crystals that could act as ice nuclei, the drops will remain super-cooled as long as the surrounding air is at temperatures below freezing. Should the sub-freezing air mass extend all the way to the ground, there is a high likelihood of freezing precipitation. Due to the fact that precipitation droplets are far larger than cloud droplets, freezing precipitation forms an extreme case of icing conditions and represents a major hazard to any aircraft. Consequently any areas where scenario *Freezing* is detected are automatically assigned the highest icing severity category.
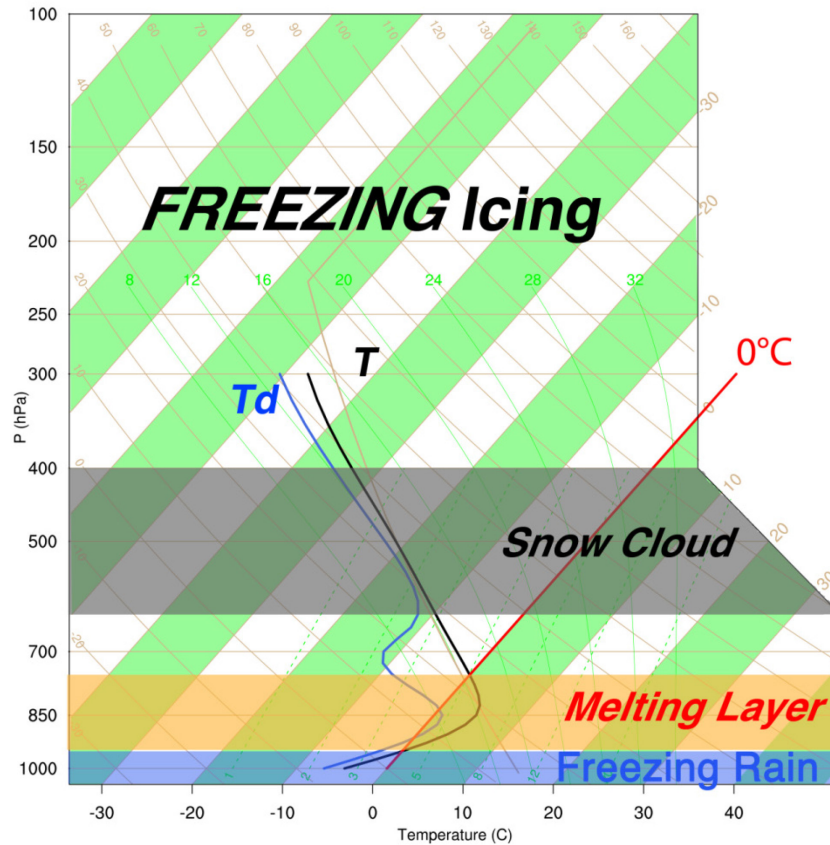
Figure 3-4: Icing scenario *Freezing* in a Skew-T sounding. Adapted from ([Leifeld 2004](#)).

Scenario *Freezing* is one of the two scenarios that the ADWICE model diagnosis detects via analysis of vertical profiles. The algorithm works from ground level upwards and analyses the values of temperature, relative humidity (RH), and the geometric height. A vertical sounding or equivalent model profile exhibits characteristic features that are used to diagnose freezing precipitation conditions. Existence and vertical location of these features are used to describe four characteristic zones that must all meet certain criteria for a positive diagnosis of freezing conditions. At first, the algorithm steps up the vertical temperature profile layer by layer to determine the point at which temperatures drop below freezing, if this is not already the case at ground level. From that point upwards the algorithm looks for temperatures to rise above freezing again, which indicates the presence of warm air above a sub-freezing layer, and describes the lower boundary of the warm nose melting layer. Stepping further up the temperature profile, the upper boundary of the warm nose is established. Since precipitation is required to fall into the warm nose in order to result in freezing precipitation below, a precipitating cloud must exist above the warm nose. In order for these conditions to be diagnosed, the algorithm looks for an air mass at relative humidity equal to or greater than 80%, with a thickness of at least 3000m. The final condition is that the cloud base may not be more than 3000m above the warm nose, to account for sublimation depletion of falling snow. If these condi-

tions are met then it is assumed that 100% liquid precipitation will be falling out of the warm nose melting layer, and the scenario *Freezing* is assigned to any layers with a temperature between 0°C and −20°C below the warm nose.

Scenario *Convective*

Convective activity represents a serious hazard to aviation, and pilots attempt to avoid flying near it where ever possible. The most noticeable effect on aircraft from convection is through turbulence, ranging in intensity from mildly uncomfortable to catastrophically destructive. However, as described in section 2.3.6, icing conditions exist in and around most types of stronger convective activity. This is due to the rapid lifting and resulting adiabatic cooling of moist air masses, which leads to the formation of large amounts of liquid water through condensation. This rapid transport to a great height coupled with a low ratio of ice nuclei to liquid water mass, even in mixed phase conditions, leads to the persistence of supercooled liquid water within convection at temperatures down to the homogeneous nucleation temperature of −40°C. Convection therefore represents extreme icing conditions both in terms of the large amount of liquid water that may be formed in the updraught, as well as the unusually low temperature at which it may be encountered.

Since the COSMO model's horizontal resolution (7 km) is not fine enough to resolve conventional convection, it provides an upper and lower boundary for convective activity on every grid point. This is derived from the model's internal parameterisation of convective activity which in turn is based on the mass flux scheme by (Tiedtke 1989). Where none of the two preceding icing scenarios has been detected and the geometric thickness, the depth, of convection is larger than 3000m, a potential for convective icing is assigned to all grid points with a temperature between −40°C and 0°C. The criterion for the minimum depth of a convective layer was introduced to assign convective icing conditions only to stronger convection while excluding areas of weak shallow convection, which do not represent a significant icing hazard to aviation.

Scenario *Stratiform*

This icing scenario is also based on an analysis of the vertical profile of temperature and humidity but is designed to detect icing conditions created by collision coalescence growth of supercooled cloud droplets in a stratus type cloud below a temperature inversion (see Figure 3-5). If the vertical profile exhibits a temperature inversion at temperatures below freezing that is associated with a sufficiently strong humidity gradient from saturated conditions below the inversion to drier conditions above, then the area below the inversion that is saturated and at temperatures below freezing (super-cooled cloud) is assigned icing potential.
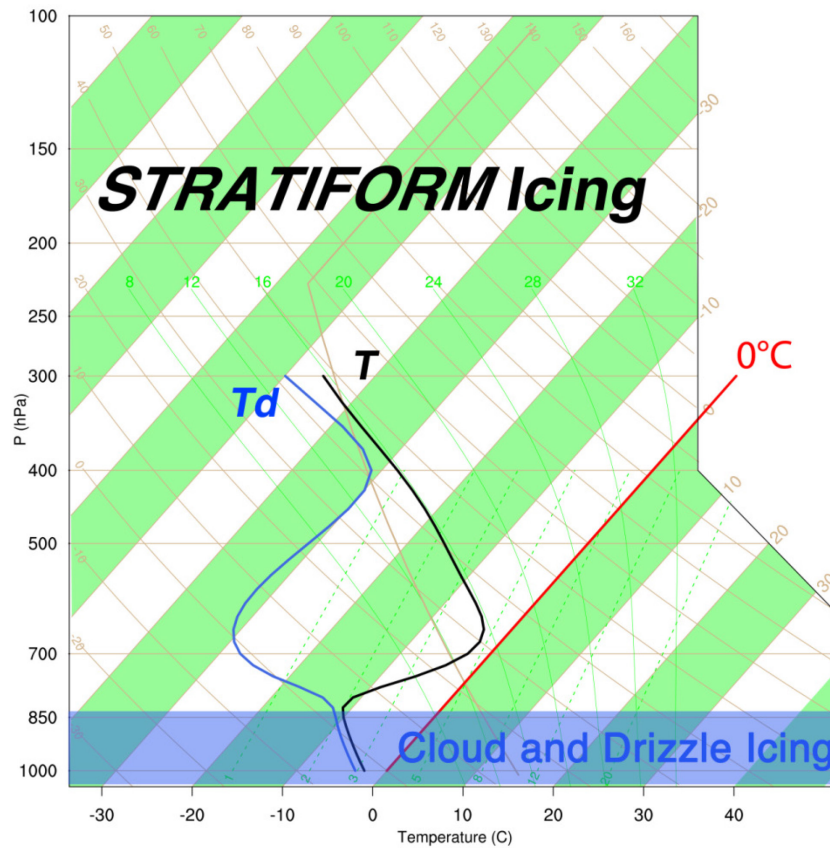
Figure 3-5:   Icing scenario *Stratiform* in a Skew-T sounding. Adapted from (Leifeld 2004).

The scenario *Stratiform* is the second scenario that is diagnosed by analysis of the vertical profiles of temperature, relative humidity (RH), and geometric height. Similar to the scenario *Freezing*, the first step is the detection of layer temperatures between −20°C and 0°C, to establish the lower boundary of icing potential. Within this sub-freezing air mass, the algorithm then searches for a characteristic relative humidity gradient that is stronger than −2.5% RH per 100m. This kind of humidity gradient is seen as denoting the top of a stratiform cloud layer. The assumption is that such a stratiform cloud layer at temperatures below zero will contain a significant amount of super-cooled liquid water, unless ice nuclei are somehow introduced from outside. Therefore the final criterion is that there may not be a precipitating cloud too close above this stratiform cloud layer. The conditions for establishing the existence of a precipitating cloud correspond to those in the scenario *Freezing* in that the algorithm searches for an air mass of relative humidity equal to or greater than 80% with a vertical extent of 3000m or more that is at most 3000m above the stratiform cloud layer top. Should such a precipitating cloud layer be detected, it is assumed that snow falling into the super-cooled liquid stratiform cloud will lead to rapid scavenging and glaciation, therefore quickly removing the icing threat. If a precipi-

tating cloud is not detected, any layers below the characteristic RH gradient with a relative humidity greater or equal to 85% and temperature between -12°C and 0°C are assigned the icing scenario *Stratiform*.

Icing severity

Following the detection of icing scenarios, ADWICE calculates an icing severity value for each area that has been assigned an icing scenario. The icing severity calculation makes use of several atmospheric parameters directly or indirectly taken from the model output.

Super-saturation with regard to ice

One of the additions in the ADWICE V2 update by ([Leifeld 2004; 2007](#)) was the implementation into the icing severity calculation of the atmospheric super-saturation with regard to the ice phase. It was noted that verification studies of relative humidity from soundings had indicated a correlation between this parameter and icing conditions reported by aircraft. This empirically established correlation remained valid when applied to model simulations and is able to provide a beneficial contribution to the overall determination of icing intensity distribution. A saturation of greater than 100% over an ice surface at temperatures well below freezing is interpreted in ([Leifeld 2004](#)) as implying a thermodynamically unstable state with the bulk of water molecules existing in the metastable liquid phase. This assumption is based on the fact that any significant ice water content would initiate BERGERON-FINDEISEN conversion and rapid depletion of supersaturation.

The icing intensity algorithm detects layers of supersaturation with regard to ice (filtering single layers to achieve a more robust result) and then separately calculates the degree of super-saturation within that layer as well as the geometric layer depth. Both parameters are then converted by fuzzy logic membership functions into weighted factors contributing to the final determination of icing intensity.

Liquid water content derived by parcel method

The original LM model did not forecast liquid cloud water explicitly. However, the supercooled liquid water content is an important factor in determining the ice accretion rate and thereby the icing severity during an aircraft icing encounter. The icing intensity calculation does not explicitly solve an equation for accretion rate, but rather defines icing intensity as being proportionate to liquid water content with the proportionality constants varying slightly for different types of icing conditions. At the time ADWICE was created, the best available option was to implement an estimate of condensate mass derived via the parcel method, in which all air parcels above cloud base in a vertical column are assumed to be saturated and are then theoretically lifted by one vertical layer. In a

saturated air parcel subjected to adiabatic cooling during lifting, the water vapour in excess of saturation is assumed to condense into liquid cloud droplets. In practice, the difference in water mixing ratio (specific humidity QV) between two model layers is then taken as the liquid water content.

A number of the assumptions and simplifications involved in this approach are inappropriate when applied in such a general fashion. Estimating liquid water content through the parcel method is only applicable when dealing with near adiabatic convective conditions.

Liquid water content from model QC field

More recent versions of the COSMO-EU model contain a sophisticated microphysics scheme that generates condensates of four classes (cloud water, cloud ice, rain, snow) and governs the conversion rates among these classes and between condensates and water vapour. The liquid water content is now a forecast variable for each model grid point and was therefore subsequently integrated into the icing intensity algorithm as a weighted contributing factor.

However, full reliance on the QC field is not yet possible since, as mentioned previously, (Herbort 2005; Roloff 2012) have shown a tendency in the microphysics scheme to suppress super-cooled liquid water content in favour of snow. While the structures in the QC field are qualitatively consistent with the structures in other simulated fields, the extent and total mass of liquid water are well below the value is expected based upon climatology is and a direct measurements. The deficit in achieving realistic mass ratios between condensates classes may be viewed in the context of an on-going emphasis in the model development community to achieve realistic precipitation rates at the surface. While the direct model output of the parameter specific cloud water content (QC) can currently only make a small contribution to the calculation of icing severity, efforts are underway to better understand the microphysics scheme in terms of relative condensate masses and hopefully find an optimised solution that is able to derive a more realistic distribution of liquid water content for use in icing diagnosis.

Depth of convection derived from model convection parameterisation

The only information about the strength of convection that is supplied by a non-convection-permitting model such as COSMO-EU is the upper and lower boundary of convection as derived from the convection parameterisation. The layer depth of convection is converted into a weighting factor via another membership function.

Combined icing intensity

These factors are combined to a factor Ftotal for *Convective* and *Stratiform/General* cases separately via two different weighting functions. Areas with scenario *Freezing* are automatically assigned the maximum icing intensity. The factor Ftotal is a scalar value on a range from 0 to 1. Thresholds are then applied to this scale to assign the icing severity categories *Light*, *Moderate*, or *Severe*. Currently there is no implemented feedback mechanism from the icing intensity calculation back to the icing scenario calculation. This leads to a problematic situation where certain areas may be diagnosed with an icing scenario but where the icing intensity calculation results in very low or even non-existent Ftotal values.

Currently such areas are not filtered and will remain assigned with their icing scenario and an icing category of *Light*. The satellite-assisted icing diagnosis algorithm DIA-SAT developed in this study implements the option of applying a lower icing intensity threshold to the diagnosis product, which can be set to remove these extremely light icing areas. The effect of this on forecast accuracy with and without the additional application of satellite data is the subject of on-going research.

3.3   ADWICE Diagnostic Icing Algorithm

The Diagnostic Icing Algorithm, or ADWICE-DIA, is the part of ADWICE that is designed to establish the current icing situation using the model-based icing diagnosis product together with ground-based weather observations and weather radar scans.

An icing diagnosis is an analysis of the current general weather situation achieved by analysing and bringing together several disparate sources of information. Unevenly distributed and highly local ground observations deliver a different insight into on-going weather processes than radar reflectivity products or satellite cloud top retrievals. Often, these different observations do not even confirm or contradict each other, but rather add nuances to the larger picture. As such, a diagnosis can only be a best effort approximation of actual conditions, its accuracy depending heavily upon the coverage and confidence level of its input observations as well as the system or forecaster's skill at correctly inferring the on-going weather processes from them. The challenge in developing an icing diagnosis system is implementing in automated program logic the skill and experience of a human forecaster. ADWICE is the result of decades of collective experience in the icing and aviation community published in the literature, as formalised in the Diagnostic Icing Algorithm.

The diagnostic icing algorithm DIA is closely related to the model-based diagnosis algorithm which is called prognostic icing algorithm PIA presented in the previous section. Both are based around the concept of icing scenarios that describe four different circumstances for the formation of icing conditions. The differences between PIA and DIA lie in the data sources and criteria applied to identify these icing scenarios. Since the diagnostic system has access to ground observations, many opportunities exist to identify or exclude certain icing scenarios based upon the observed precipitation type. In many cases this removes the need to rely upon features in vertical profiles of humidity parameters from the model to estimate precipitation type.

3.3.1 Data points used for icing diagnosis

Primary sources of information are ground observations (from SYNOP and METAR reports) of significant weather that can be a strong indicator of icing conditions aloft. Weather radar data is used to support the diagnosis of precipitation conditions that are routinely associated with icing. The gaps that exist in the coverage of ground observation data, either where stations are too far apart or where there are no stations at all (e.g. at sea), are filled with model based icing information taken from the most recent Prognostic Icing Product.

Ground observations

The direct observations currently used in ADWICE are ground-based SYNOP and METAR reports of icing relevant weather phenomena as well as information about height of the cloud base and cloud cover, as introduced in section 3.1.2. ADWICE represents an attempt to extract the maximum amount of icing relevant information from ground observations. Compared to earlier approaches that focused mainly on SLD conditions and associated ground weather phenomena, ADWICE addresses a larger range of icing conditions and their associated weather effects that may be derived from ground observations by careful analysis.

Present Weather

Icing diagnosis from ground observations relies upon the fact that weather phenomena visible at ground level contain a lot of information about cloud physics processes occurring above. Previous research (Bernstein et al. 1997) has shown a significant correlation between certain weather effects visible from ground level and the formation of icing conditions in cloud layers. The knowledge about these correlations is leveraged in ADWICE to the greatest extent possible for the determination of icing scenarios that describe discrete icing formation processes.

Cloud base height (ceiling)

The cloud base height as observed from the ground may be used as a convenient lower boundary for diagnosed icing conditions in situations where no freezing precipitation is occurring. The observed cloud base height is also used to correct the lower boundary of model based icing fields where applicable.

Weather radar

Weather radars are designed to detect areas of significant precipitation and are therefore tuned to wavelengths in the S and C bands that are best reflected by common particle sizes of rain and snow. A composite reflectivity product from a Europe-wide weather radar network is used to support the diagnosis of precipitating weather systems and their associated icing risk. This product, interpolated to the ADWICE grid, assigns a single value of radar reflectivity in dBZ to each grid point within the area of coverage. Experience has shown that the presence of a strong radar echo contraindicates drizzle formation via the warm rain process, as drizzle droplets are too small to generate a strong radar echo. On the other hand, the presence of a strong radar echo is able to support the diagnosis of certain other icing formation processes such as freezing rain through the melting of snow or due to convection. A radar reflectivity of 19dBZ is currently used in ADWICE as the threshold between light and strong reflectivity.

Model-based icing product

The prognostic icing product PIP is the output of the model-based icing algorithm presented in detail in [section 3.2.4](). It is a fully model-based diagnosis of icing conditions that is generated by applying the icing algorithm to the model forecast fields for the current diagnosis time. It provides a value for the icing scenario for every model grid point and is used to fill in areas of the Diagnostic Icing Product where no observations are available. Additionally, for cases where the ground observation-based diagnosis algorithm provides inconclusive results, the PIP is adopted after a plausibility check that corrects instances where the PIP value is contraindicated by ground observations.

3.3.2 Determining icing scenario in the Diagnostic Algorithm

The Diagnostic Icing Algorithm (DIA) implements a scenario based approach, similar to that of the prognostic icing algorithm. The main difference between the two is that the diagnostic icing algorithm begins icing scenario classification with an analysis of ground observations and attempts to confirm this choice from subsequent analysis of vertical profiles of atmospheric parameters from model simulations. This is in contrast to the PIA, which bases the scenario identification directly upon an analysis of characteristic

structures in the vertical profiles. As discussed previously in <u>section 3.1.2</u>, several weather phenomena that are readily observable from ground level exhibit a strong correlation with icing conditions above.

Ice pellets, reported as significant weather with the code number 79, form when liquid precipitation that has been super-cooled or only partially melted during its fall freezes before reaching ground level. Prior research, for example by (<u>Bernstein et al. 2000</u>), has shown ice pellets to be an excellent indicator of SLD conditions above. Conversely, there are certain types of observable weather that strongly contra-indicate some or all types of icing conditions. An example is observed snowfall, which permits the conclusion that there is negligible supercooled liquid water content between ground level and the snow's formation layer, since the introduction of any appreciable amount of ice crystal mass into a layer of supercooled liquid water would lead to its rapid depletion through riming or glaciation.

Diagnosis scenarios

Scenario Freezing

The definition of what constitutes freezing precipitation and the mechanisms by which it is formed are identical in the Diagnostic Icing Algorithm compared to the Prognostic Icing Algorithm, but the process by which this type of scenario is identified is different. The Diagnostic Icing Algorithm, since it has ground observations available, will begin the diagnostic process by searching for model grid points that are associated with ground observations of a type that are correlated with freezing precipitation through a warm nose melting layer.

The ground observation does not have to include freezing precipitation explicitly. There are many cases where supercooled liquid precipitation can be present at altitude but may change this state through one of several processes before it reaches the ground, such as warming to above freezing temperatures in a warm air mass near the ground, or freezing to ice pellets before reaching ground. Therefore, a whole range of precipitation types from the rain and shower class, along with ice pellets or strong radar echoes without observed snow, are seen as indicating possible icing conditions compatible with the *Freezing* scenario. However, if freezing rain is reported, the layer closest to the ground can be assigned scenario *Freezing* without further checks.

If a valid indicator for scenario freezing is found in the observation data, the algorithm will attempt to confirm this initial assessment by analysing the vertical profile to identify the features characteristic of the freezing rain process. This involves stepping up the vertical temperature profile to establish the boundaries of sub-freezing air layers and to

identify a possible warm nose melting layer. In a departure from the process as implemented in the Prognostic Icing Algorithm, the Diagnostic Algorithm does not need to search for a precipitating cloud above the warm nose melting layer, since the ground observations already provided evidence of precipitation that has gone through a melting process. If the DIA can identify such a warm nose melting layer, all sub-freezing layers below the bottom of the warm nose (at the 0°C line) will be assigned the icing scenario *Freezing*. The DIA differentiates between points where the icing scenarios of the forecast and Diagnosis agree ("confirmation"), points where forecast and Diagnosis have different icing scenarios and the diagnosis corrects the forecast ("change"), and points where the diagnosis determines an icing scenario where the forecast had none ("set").

If the DIA is not able to find a warm nose signature in the temperature profile of the column in question, it will at first attempt to find such a signature at neighbouring grid points up to a distance of five in all directions. This can correct for a possible phase error in the model forecasts compared to actual conditions.

If this neighbourhood search is also not successful, and a warm nose signature cannot be found anywhere in the vicinity, the assumption is that the precipitation in question formed through a different process not involving a melting layer. This is quite possible since the visual differentiation between rain and drizzle can at times be difficult and may lead to an incorrect identification of freezing rain conditions, which would indicate a warm nose type melting process, as opposed to freezing drizzle conditions, which imply stratiform warm rain formation via coagulation. This possibility is accounted for in the PIA by attempting a confirmation for grid points with reported freezing rain under the *Stratiform* scenario.

There is always the possibility that further layers with icing conditions may exist above the primary icing area being investigated. Any additional layers with temperatures between 0°C and −20°C and a relative humidity above 80% are assigned the icing scenario *General* (either "confirmed", "changed", or "set").

Scenario Stratiform

The scenario *Stratiform* describes a cloud layer of low to medium altitude (usually less than 1000m) and moderate thickness (2000m at most) that is assumed to consist of liquid cloud droplets. This type of stratus cloud is formed by weak uplifting such as along a warm front or upstream of orography. Cloud droplets are generated by condensation on CCN and grow via collision coalescence processes, potentially allowing a drizzle precipitation process to begin. This is the essence of the non-classic precipitation forming process also known as "warm rain", which stands in contrast to the classic rain formation process of solid precipitation (e.g. snow) melting during its fall to form large raindrops.

The precipitation types generated by warm liquid stratiform clouds fall generally into the drizzle category, be it warm, freezing, frozen (ice pellets) or only visible at distance. Even visible precipitation not reaching the ground as well as fog or haze conditions may be observed below stratus clouds containing icing conditions. Therefore the diagnosis of stratiform icing conditions begins with the observation of such conditions at ground level. Especially strong evidence of icing conditions in the cloud above is provided if freezing drizzle is reported or if there are unconfirmed freezing rain observations from the previous analysis of scenario *Freezing*. If such freezing drizzle conditions are observed, the lowest column layer will automatically be set to *Stratiform* icing without extra confirmation.

Lacking a sharply delineated melting layer, the characteristic signature in the vertical layer associated with stratiform clouds is a strong decrease in relative humidity at the cloud top, coupled with a temperature inversion. Since only low and relatively warm stratus clouds can reasonably be assumed to contain the largely ice free supercooled liquid water icing conditions, a limit is imposed on the height of the cloud base and the depth of the cloud layer acceptable for confirmation of *Stratiform* icing. If the height of cloud base is supplied by ground observation, it is used to calculate the icing volume. If the cloud base is not observed then a height of 400m has been established as a reasonable estimate. The cloud layer itself must not be deeper than 2000m and the temperature at cloud top must not be below -12°C. If a cloud top cannot be identified from the relative humidity profile, a cloud top of 1000m above established cloud base is assumed. Any layers below the cloud top with temperatures between 0°C and -12°C and a relative humidity greater than 85% are assumed to be part of the cloud and are assigned the icing scenario *Stratiform* (either "confirmed", "changed", or "set"). A check for a cloud higher up that might snow into the stratus cloud, as performed in the Prognostic Icing Algorithm, is omitted as observed drizzle precipitation could not form in such a case.

The confirmation of *Stratiform* icing through vertical profile analysis also has the flexibility to search a small area around the original grid point if a relevant stratus cloud top signature is not immediately found. The scenario *Stratiform* also accounts for the possibility that further layers with icing conditions may exist above the primary icing area being investigated. Again, any additional layers with temperatures between 0°C and -20°C and a relative humidity above 80% are assigned the icing scenario *General* (either "confirmed", "changed", or "set").

Scenario *Convective*

Any convection of sufficient strength, as evidenced by its vertical extent or depth, is a serious hazard to aviation for a number of reasons. Aside from violent turbulence or the chance for large hail encounters, any moderate or greater convective updraught will contain a significant amount of super-cooled liquid water in the SLD size range. Therefore convective systems are a serious icing hazard in their own right. Ranging in size from fair weather *cumuli* on the order of 100m to mesoscale convective systems (MCS) of hundreds of kilometres horizontal extent and over 10,000m depth, convective weather systems are also associated with a wide range of liquid and solid precipitation types. Almost all of these, however, are found in the area immediately downwind of individual updraughts and usually combine a high intensity with a short duration, often accompanied by lightning. This type of precipitation event is generally called a shower.

Ground observations associated with convective icing are therefore of the shower precipitation type. Since showers are such a dynamic weather event that is relatively short lived as well as moving rapidly, the likelihood of a ground observation station experiencing a shower at the precise synoptic observation time is very low. Therefore shower observations during the past hour, which are also recorded, are included in the list of acceptable indicators for convective icing conditions. In addition to this, if the reported low cloud type is *cumulonimbus*, this is also seen as a sufficient indicator for convective icing potential.

The COSMO-EU model does not provide explicit resolution of convective cells, but rather provides lower and upper bounds of convective activity via the Tiedtke parameterisation scheme (Tiedtke 1989). No vertical profile analysis is performed for the confirmation of convective icing conditions, but rather the depth of convection is calculated from the provided lower and upper boundaries. To exclude shallow convection with a negligible icing threat to aviation, a convective layer depth of at least 3000m is required for convective icing to be successfully confirmed. All layers with in this convective zone that have a temperature between 0°C and −40°C are assigned the icing scenario *Convective.*

The scenario *Convective* also permits secondary layers of icing to exist above the established top of convection. As with the previous two icing scenarios, any additional layers with temperatures between 0°C and −20°C and a relative humidity above 80% are assigned the icing scenario *General* (either "confirmed", "changed", or "set").

Remaining indeterminate icing areas

While the criteria established for the previous three explicit icing scenarios enables the PIA to reliably detect areas that are characteristic of each, experience shows that non-standard or otherwise indeterminate areas of icing will not be detected. Also, there will likely be areas where some of the observation information will contradict the forecast icing product in ways other than establishing a new or different icing scenario. Therefore the PIA contains a number of steps after the scenario detection presented in the previous subsections, which are designed to detect less well-defined icing conditions as well as using available observation information to reduce the icing area in the diagnosis product in comparison to the model product.

The purpose of this element in the DIA is to make a definitive decision about any grid points for which the model product has determined icing scenario *Stratiform* that the diagnosis algorithm was not able to confirm or change. The chosen approach is to look for certain characteristic observations that can be seen as contradicting the character of stratiform icing conditions with collision coalescence droplet growth and drizzle formation. Specifically that means that observed precipitation of type rain, snow, shower, or thunderstorm are seen as contra-indicating stratiform icing conditions. The same is true if a scenario of type *Convective* has already been confirmed at some point within that column, or if the radar reflectivity is greater than 19dBz. If any of these three criteria are true then all previously unprocessed grid points with scenario *Stratiform* are reclassified as *General* icing. If none of these three conditions are true then the initial assessment of *Stratiform* icing is marked as confirmed.

Any gridpoints with scenario freezing assigned by the model-based algorithm, that could not be independently verified or corrected in the initial diagnosis, are checked against potentially contradictory weather observations. As a first step if any non-freezing precipitation is reported, icing at the lowest layer is set to *None*. Furthermore if the weather observations are not of the type drizzle, rain, or ice pellets or if the reported radar reflectivity is zero, then any grid points with icing scenario freezing are reassigned to icing scenario *General*. Any grid points with initially assigned scenario freezing that are not associated with one of these contra-indicators are marked as confirmed *Freezing*.

Since any grid points with observed precipitation or other weather phenomena that are associated with convective activity would already have been detected by the initial diagnosis algorithm, the plausibility check for unconfirmed scenario convective is restricted to a temperature range. Any grid points with scenario *Convective* that lie in a temperature range between 0°C and −20°C are confirmed as *Convective*, all others set to none.

A further analysis is performed to detect grid points with significant cloud cover (greater than 4/8) and the right temperature and humidity conditions that have not been assigned any icing due to the lack of ground observations and/or appropriate model results. Under the condition that a grid point is associated with an observed cloud cover of greater than 4/8, no forecast or diagnosed icing scenario within the whole column, and that nowhere above cloud base in layers with relative humidity above 80% does the temperature leave the range 0°C and −20°C, all layers above observed cloud base with relative humidity above 80% and temperature in the icing range are assigned scenario *General*.

Previous research has shown (Bernstein et al. 1997) that there is a strong positive correlation between a cloud's horizontal extent and its potential for icing. It is generally valid to assume that cloud coverage of 4/8 or lower is a reliable indicator of sub-critical or even negligible icing conditions. Any grid points with associated cloud cover of 4/8 or less are therefore assumed to have insignificant icing threat and are set to *No Icing*. The observed height of the cloud base can be used to correct the lower boundary of model diagnosis icing volume. Provided that no freezing precipitation has been detected, any icing layers below the observed cloud base are set to *No Icing*.

3.3.3 The final Diagnostic Icing Product

The Diagnostic Icing Product represents the sum total of the evaluations presented in the previous subsections. The inclusion of direct observation and remote sensing data in the icing diagnosis process allows for a much refined description of icing conditions wherever this observation data is available. It is intended for the diagnosis to begin with a study of actual conditions and to let this inform further confirmation activities. It is therefore quite possible for the diagnosis product to differ noticeably from the model product, if locally observed conditions indicate a different icing formation process than that inferred from model results.

The DIP consists of a set of output fields that are equivalent to those produced by the prognostic product PIP. For most diagnosis users the focus will be on the icing intensity product, which is calculated by the same method used in the PIP and also presented in terms of severity categorized into *Light*, *Moderate*, and *Severe*. Of less interest to operational users, but rather more for scientific and analysis applications, is the scenario product which forms the basis of the icing diagnosis and describes the identified icing formation mechanisms, as discussed the preceding sections. These two products are produced in two versions each, differing in the vertical coordinate. One set is the original product generated grid-point for grid-point on the native terrain-following model vertical layers. The other set is converted to present the icing information on a number of common flight levels (1FL is 100ft at US standard atmosphere conditions).

Performing icing diagnosis by the method described above provides a number of benefits over purely model-based approaches. Provided the source is sufficiently reliable, any kind of direct observation of weather represents valuable additional information and can be treated as input data of a higher order than any model processing can provide. Basing an icing diagnosis on data points from a combination of different observations, augmented with model data where necessary and appropriate, uses the strengths of each data source to the maximum advantage and results in a representation of the current icing picture that is not only built upon sophisticated weather modelling but is also firmly rooted in reality. In addition to this, the observation data provides a valuable real-time perspective as compared to model data that may be a few hours old at a time of validity.

Despite the many upsides that a fusion of ground observations and model data brings to the icing diagnosis, it also introduces several complications. Chief among these is the uneven distribution of ground observations of type SYNOP/METAR. While central Europe has the densest and most active network of ground observation stations anywhere in the world, slightly more remote areas already exhibit gaps between the coverage of adjacent stations. The implemented area of influence of 70km around each station is it itself somewhat arbitrary and not appropriate for every weather situation. Assuming horizontal homogeneity on this scale for dense stratus clouds may be acceptable, doing so for certain other weather situations may not be. If one weather station reports conditions that are not aligned with those from surrounding stations, and this leads the diagnosis algorithm to determine a significantly different icing situation, this difference will apply to the whole area of influence around the weather station and will therefore cause a large patch within the diagnosed icing field that sharply contrasts with its surroundings.

This effect can be seen along the front edge of an advancing front that is well represented in the model based product in terms of its structure, but may contain a small phase error. Assuming that the real front advances at a slightly slower rate than the modelled front, ground observations along the modelled front's leading edge will report cloud free or low cloud coverage, which will be represented in the diagnosis product as an area of *No Icing* around the respective stations. Areas between stations are filled in with the model product displaying the faster advancing front. In the final diagnosis product, this then appears as a zone of frontal icing with conspicuous circular holes. This effect also occurs in situations where a relatively small opening in cloud cover is reported at the ground as low cloud cover and then represented in the icing output as a large cloud free area that does not correspond to reality. The reverse effect naturally also occurs with ground observations of icing conditions which may be restricted to the immediate vicinity of the station, resulting in excessively large areas of icing being diagnosed.

3.4 Satellite cloud top products

With the advent of next-generation geo-stationary weather satellites, advanced cloud property retrieval products have become available at a sufficient spatial and temporal resolution to permit operational employment in weather hazard diagnosis. The METEOSAT second-generation (MSG) satellites provide high quality imaging spectrometer data for cloud property retrieval covering the whole visible Earth disc around 0° longitude and extending far enough north to include all but the north-eastern corner of the ADWICE model domain. The greatest advantage of such satellite coverage is the near complete coverage of the entire model domain with a uniform set of high-quality direct observations of cloud properties, with a spatial resolution similar to that of the model grid. A number of satellite cloud property products may be used in combination to determine the distribution of likely icing conditions near the cloud top. The following products are available operationally and with sufficient reliability to provide value for icing diagnosis.

3.4.1 Cloud type (cloud mask)

The cloud type product (CT) provides a granular classification of each satellite image pixel in terms of the cloud cover detected there. Cloud free pixels are identified separately for over-land and over-water. Cloudy pixels are classified in terms of height category from very low to high, with a separate category for partially cloudy pixels. In future versions of the product, a differentiation between stratiform and convective clouds is planned. Pixels clearly identified as cloud free are categorised as to whether they are over land or over water. Distinguishing clouds from a frozen surface (snow over land, ice over water) is particularly difficult and associated with greater uncertainty due to the similarity in radiative properties of bright ground cover and a cloud with the same surface temperature. Pixels where this distinction could not be performed with sufficient confidence are highlighted separately. Additional quality assurance fields are included that provide information about the perceived quality of the retrieval process at each pixel that permit an assessment of the accuracy and trustworthiness of the data product.

3.4.2 Cloud phase

The cloud phase product (CPhs) is produced as part of the cloud type retrieval algorithm and provides a per-pixel retrieval of the effective water phase at cloud top. This is important to identify clouds that have not begun to glaciate and could potentially support existence of supercooled liquid water. Thick clouds with frozen tops can be assumed to have negligible icing risk within the glaciated layer and can even remove icing risk from a

lower layer by precipitating ice crystals which scavenge the supercooled water (see section 2.3.5). Under some circumstances a partially glaciated cloud might sustain icing conditions. However, this is generally limited to deep convection with showers or thunderstorms that produces enough liquid water through condensation to locally overwhelm the available active ice nuclei.

3.4.3 Cloud top temperature

The cloud top temperature (CTT) is derived via the brightness temperature of the cloud top. For dense compact cloud layers this temperature corresponds well to the actual temperature near the cloud top. However, thin semi-transparent layers of cloud at higher altitudes and hence colder temperatures may affect the thermal signature attributed to the dense visible clouds below and may negatively affect the accuracy of the retrieved cloud top temperature. The CTT retrieval algorithm attempts to correct for this effect and highlights areas of potentially higher CTT error.

3.4.4 Cloud top height

Cloud Top Height (CTH) is derived by matching measured CTT to the closest temperature value from a vertical profile produced by a forward simulation of the vertical temperature profile across the satellite field of view. Since the model relates temperature to geometric height, the height of the detected cloud top can thereby be inferred. Some Quality Assurance (QA) processing is applied to account for data reliability and possible inversion artefacts that may require disambiguation between multiple locations along the vertical profile.

3.4.5 Liquid water path

The liquid water path (LWP) is defined as the amount of liquid water in the entire atmospheric column above a unit area on the ground and is commonly expressed in g/m^2. LWP is derived from satellite imaging spectrometer readings by an indirect retrieval process that matches radiance values at the cloud top from several spectral channels of the satellite instrument to a set of precomputed data that correlates channel radiances to LWP. This approach has been shown to be moderately successful so far. Absolute derived values show a fluctuating mean error, which indicates additional external factors influencing LWP that are not included in the retrieval algorithm. However, the gradients are reasonably representative of actual conditions and are therefore useful in identifying local maxima of LWP (Haggerty 2005). Since icing intensity correlates well (but not exclusively) to the local supercooled liquid water content, these LWP gradients can be used to identify local maxima in icing potential.

4. ADWICE diagnosis including satellite data

The primary objective for the development and implementation of the DIA-SAT satellite augmented icing diagnosis algorithm was the leveraging of advanced cloud top property data products derived from geostationary weather satellite measurements to reduce the excessive amount of atmospheric volume assigned with an icing risk by the baseline ADWICE diagnosis algorithm. A new generation of satellite sensors and constant development of advanced retrieval methods has allowed the application of satellite data to a growing list of aviation weather hazard diagnosis problems (Mecikalski et al. 2007).

Incorrect non-warnings (misses) of icing conditions are seen as more harmful than false alarms, so ADWICE is configured conservatively to prioritise minimum misses over false alarms. Therefore some over-diagnosis/over-forecasting is to be expected, but a reduction of overall diagnosed icing volume was nonetheless necessary to more accurately describe areas actually free of icing conditions, since many small General Aviation aircraft need to keep a safe distance from any weather hazard. The reduction of excessive icing volume to more closely approximate the actual distribution of icing conditions serves the related goals of improving customers' experience of overall diagnosis accuracy and specifically improving guidance for users focused on icing free areas. The key to achieving a real improvement in icing diagnosis quality lay in maintaining a high forecast accuracy against positive icing observations while substantially reducing the overall atmospheric volume of diagnosed icing, and the addition of satellite data with their unique capabilities played a crucial role in making that possible.

Satellite data can be applied in several different ways to improve the diagnosis of aircraft in-flight icing conditions (Minnis et al. 2004a). A reduction in icing volume can be achieved by taking advantage of information contained in satellite cloud products about cloud-free (and therefore icing-free) parts of the atmosphere, as well as through the definition of criteria such as a warm cloud top temperature that indicate a sufficiently low probability of icing conditions within the cloud layer. Satellite-based detection of areas with increased icing potential was also developed and implemented and correlates well with icing pilot reports (PIREPs). In addition to detecting new areas of increased icing potential and increasing the detection rate against positive icing observations, this new capability can also be employed to protect areas of known high icing potential from any measures aimed at icing volume reduction.

A high rate of detection for icing PIREPs, combined with a large reduction in total atmospheric volume diagnosed with icing, results in a dramatic improvement in the volume efficiency VolEff of the diagnosis. Although the PIREPs of no-icing observations are un-

systematic and biased toward areas with icing conditions, and the arithmetically calculated False Alarm Rate is therefore less reliable, it is nonetheless reasonable to assume that an improvement in the designation of icing-free atmospheric volume will have a positive impact on the overall incidence of false alarm events, reported or unreported.

This chapter begins with an outline of the satellite-based measures implemented to reduce over-diagnosis of icing volume, followed by a description of the implemented satellite-based icing detection and an overall description of the DIA-SAT algorithm. Finally, the results of a validation campaign conducted over the United States using local icing PIREPs and satellite products are presented with an example case.

4.1   Reduction of over-diagnosis

Reduction is the process of removing incorrectly identified icing conditions from parts of the model grid where satellite data positively indicates no-icing conditions. Reduction is performed with high confidence for cases where satellite cloud retrieval shows no or low coverage with icing relevant cloud types. The cloud mask derived from METEOSAT cloud products is sufficiently reliable for clouds in the size and temperature range relevant for icing, and can therefore be applied with a high degree of confidence. Cloud coverage for very low/warm clouds (close to surface temperature), such as low stratus or fog, or extremely high thin ice clouds (sub-visible cirrus), may be misidentified at a higher rate, but apart from rare supercooled fog events they are not relevant for the formation of icing conditions. A second opportunity for reduction exists wherever the model-based algorithm has over-estimated the cloud-top and has assigned icing potential to a portion of the atmospheric column that lies above the cloud top as measured from the satellite. A final step of reduction is possible wherever low liquid water clouds are detected with a cloud top temperature warmer than the icing threshold temperature. Such a cloud will generally contain negligible amounts of super-cooled liquid water, as a cloud with a cloud top temperature above freezing is not expected to contain significantly supercooled air mass further down.

4.1.1 Cloud mask
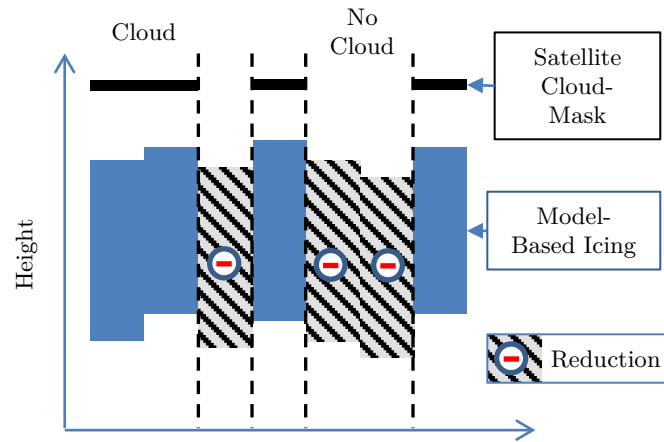
Figure 4-1: Reduction of entire column icing by application of a satellite-derived cloud mask. Cloud-free areas are marked no-icing.

While conditions capable of sustaining supercooled liquid water content (sub-freezing temperature, high relative humidity, and absence of ice nuclei) may exist outside of visible cloud, actual cases of extra-cloud SLWC are determined by advection from the place of formation. While a certain amount of lateral advection of precipitation scale droplets may occur around convective or orographic events, icing conditions outside of clouds are generally restricted to the volume below the cloud. It is therefore generally valid to assume that cloud free areas on the order of a model grid box (7km x 7km) are also free of icing (Figure 4-1). The types of dense and cold clouds that produce icing conditions can be reliably identified from satellite imagery, which lends a high degree of confidence to the determination of icing free conditions via a cloud mask (Thompson et al. 1997).

4.1.2 Cloud top height
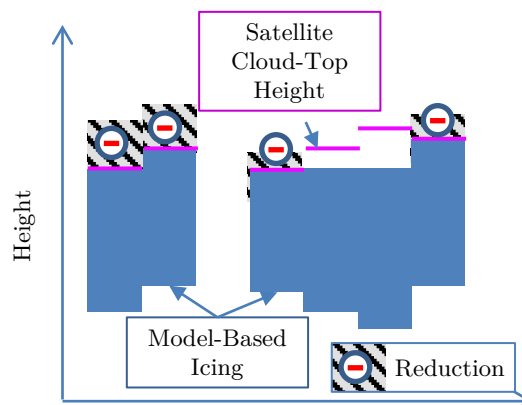
Figure 4-2: Reduction of icing above cloud top.

Similar to removing diagnosed icing potential from the entire column where the satellite detects cloud-free conditions, it is also possible to remove icing from the part of the atmospheric column that lies above the cloud top as determined from the satellite cloud-top height (CTH) product (see Figure 4-2). CTH is indirectly derived from the cloud top temperature determined from the radiative brightness temperature value which is matched to a simulated vertical temperature profile to determine geometric height. Therefore, there is a certain amount of simulation error associated with this parameter. While (Haggerty et al. 2005) showed that frequent presence of thin sub visible cirrus causes the satellite derived cloud top height to overestimate actual cloud top height as reported by research flights, the average overestimate in a cloud top height by model simulations is even greater. Since ADWICE currently only indirectly determines cloud top height via the model's relative humidity or convection parameterization, there are frequent discrepancies between the derived upper icing boundary and the satellite CTH. An application of the CTH product to the reduction of diagnosed icing can provide a valuable reduction in mis-diagnosed icing at higher altitudes.

4.1.3 Cloud top temperature

Most clouds contain some supercooled liquid water in small amounts which do not present a significant hazard to aviation. Therefore, any additional data sources that may help in identifying non-hazardous cloud formations can provide a real benefit in reducing incorrect icing warnings. Under certain circumstances, satellite products can provide an indication of the presence of icing conditions in a cloud. Conversely, satellite products can also under certain conditions support conclusions about the absence of icing in a specific cloud. A cloud top temperature above freezing is seen as a reliable indicator of the absence of icing conditions within that cloud and any icing diagnosed within that column may be removed.

Idealised stratus

Consider an idealised fully liquid stratiform cloud of the type discussed in section 2.3.6, with sufficiently large horizontal extent, a well-defined capping inversion layer and sufficient internal mixing. Such a cloud would exhibit a liquid water content (g/m^3) vertical profile that gradually increases with height from the cloud base up to a LWC maximum at about 80% of cloud thickness followed by a more rapid decrease towards the cloud top. The LWC maximum is caused by weak lifting inherent in stratiform cloud formation transporting cloud droplets upwards, increasing their vertical velocity delta with respect to larger drops. This increases the collision probability and further accelerates coalescence growth of large droplets in the upper part of the cloud. Radiative cooling of the cloud top also contributes to accelerating condensation processes in the upper cloud. Because of the

LWC maximum and the higher number concentration of larger drops, the greatest in-flight icing risk is generally found slightly below the very cloud top. The decrease of liquid water content towards the very top of the cloud is caused by entrainment of dry air from above causing evaporation.

Significance of cloud top temperature

A major indicator for the likelihood of significant supercooled liquid water within such a stratus cloud is the temperature at the cloud top. Because the stratus cloud in question is assumed to be well mixed and capped by an inversion layer, no strong discontinuities in the temperature gradient are expected within the cloud. Further, assuming a temperature increase from the cloud top to the cloud bottom with the moist adiabatic lapse rate, the cloud top will be the coldest part of the cloud. Therefore, a cloud with a cloud top temperature above 0°C is assumed to contain no layers with subfreezing temperatures and therefore no supercooled liquid water content. Experience has also shown that clouds with a cloud top temperature below −20°C have a considerably increased likelihood of containing or gaining ice crystal content sufficient to rapidly deplete existing supercooled liquid water, thereby eliminating the in-flight icing threat.

Identification of non-hazardous clouds

The combination of satellite-based cloud top temperature and cloud phase retrieval enables the detection of most un-obscured supercooled liquid cloud tops throughout the satellite field of view. For the reasonably common single layer case, cloud top temperature, phase and liquid water path retrieval can highlight areas of likely negligible supercooled liquid water content where clouds do not meet the criteria for icing conditions. The difficulty lies in identifying areas where the cloud top belongs to single layer clouds that support the above assumptions. In multilayer cases the cloud top products apply only to the uppermost layer and allow no assumptions about lower cloud layers. Since the identification of multilayer clouds based purely on satellite products is currently insufficiently accurate, the reduction of icing volume based solely on cloud top temperature is restricted in this implementation to the clear case of satellite-measured cloud top temperature above freezing.

4.2 Satellite-based icing detection

Going beyond reduction, satellite cloud products can also be used to confirm an existing icing diagnosis and may help to locate areas of icing potential that have not been identified through ground observations or model-based analysis (Ellrod and Bailey 2007). This can be applied where ground observations are inconclusive or where ground observations are not available at all for large areas. This is also particularly relevant for detecting vari-

ous hazardous weather conditions such as strong convective storms over the oceans where
no weather radar is available (Donovan et al. 2008). Since the ground observations pro-
vide information mainly about icing-relevant processes in the lowest cloud layer, the
perspective on cloud top conditions provided by the satellite may even be complementary
to ground observations. This can be particularly useful in confirming or correcting the
upper boundary of icing layers. Complete reliance on model-based vertical profiles not
supported by ground observations is seen as less reliable and icing diagnosis in such cases
can benefit from the input of satellite direct observation data.
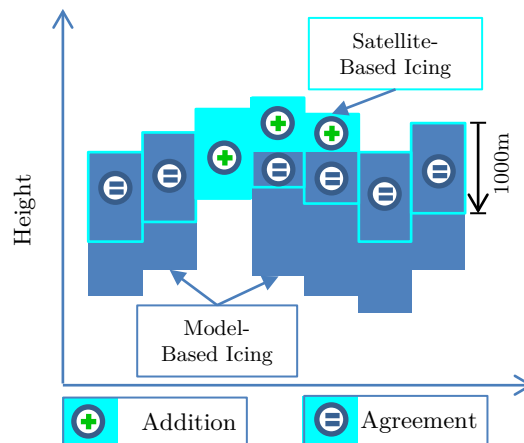
Figure 4-3:   Addition of icing from satellite data.Icing conditions are detected at cloud top and
an assumption is made about vertical extent.

A combination of the previously introduced cloud properties retrieved from satellite ob-
servations can be used to identify areas of high icing potential. Since icing conditions
often form near the top of clouds, particularly in the common stratiform or stratocumu-
lus cases, satellite products are ideally suited to provide additional data. The currently
implemented icing detection algorithm identifies cloud cover from the cloud mask, search-
es for liquid-water cloud tops and selects those that are below freezing (Figure 4-3). An
additional useful indicator of significant icing potential is the satellite-derived liquid wa-
ter path (column total liquid water). Although the absolute values from this product are
still somewhat unreliable, the gradients of LWP are qualitatively accurate and are al-
ready useful for identifying areas of increased LWC in clouds. This means that local
maxima of liquid water path for supercooled liquid cloud tops have been found to corre-
late with in situ measurements of liquid water content (Haggerty et al. 2005;
Smith et al. 2003). Combined with the derived super-cooled liquid water field, clouds
with significant super-cooled liquid water content near the cloud top can be identified.
Since no depth information about SLWC volumes can be derived from these satellite
products, a layer depth for satellite-derived icing must be estimated. For similar indeter-
minate cases, ADWICE already assumes a layer thickness of 1000m, which is in line with

accepted practice. Wherever the satellite diagnosis has detected icing potential, all model layers within 1000m below satellite-derived cloud-top height having a temperature below freezing are assigned the icing scenario *General* which corresponds to cloud-droplet icing without precipitation. Any pre-existing icing values from another part of the algorithm that fall within the 1000m range remain unchanged.

Satellite products are not available at all times because of the day/night cycle, and other external factors such as cirrus cloud cover which may degrade data quality, so that the challenge lies in maximising the benefit from using satellite data while minimising the introduction of additional error. This is accomplished by implementing logic in the diagnosis algorithm that adaptively chooses on a per-gridpoint basis which data inputs are viable and reliable for inclusion into the icing diagnosis, based on local conditions and satellite data quality information.

4.3   Integrating satellite data into ADWICE

Icing diagnosis as implemented in ADWICE brings together three very distinct data sources, namely gridded model data, wide area remote sensing data from radar and satellite, and point observations from manned ground stations. These must all be carefully brought together to produce a final diagnosis output (Bernstein et al. 2006). An important aspect of designing the diagnosis algorithm is defining an order of precedence for the diverse input data. In ADWICE, surface observations are treated as the most direct and reliable data sources, followed by remote sensing retrieval (radar, satellite), followed by model data. A model-based icing diagnosis is used as a first guess in the ADWICE diagnosis algorithm. Satellite and radar products interpolated to match the model grid can be used to confirm or to amend the model forecast on a grid point by grid point basis. Ground observations will overrule the other sources, but are restricted to a small circle of influence around the station. However, the use of satellite data is itself subject to some limitations as to where they may be employed.

Obstruction of view

Icing-relevant liquid water clouds, because of the atmosphere's temperature gradient, are mostly low to mid-altitude clouds. However, there are many weather patterns where other higher altitude cloud layers may simultaneously obscure a satellite's view of the lower icing clouds. The proportion of icing relevant liquid clouds that are obscured from satellite view by high ice clouds varies greatly with the current activity of organised cirrus-producing convective systems or jet streams within the field of view. Multilayer cloud conditions with translucent upper layers cause mixing of radiative properties and spectral features from several layers, thereby also introducing errors into the retrieval of cloud top

properties ([Smith et al. 2012]). The cloud type product (CT) provides a useful stratification of identified clouds by height and also explicitly labels areas with partial cloud cover as well as cloud free and indeterminate areas. The quality assurance (QA) routines of the satellite retrieval algorithm also provide useful information about quality of the input and confidence in the product's accuracy. This set of information is used in the icing diagnosis to determine areas where the satellite products can be used for icing diagnosis and where they should not be used.

Solar angle restrictions on satellite products

The retrieval algorithms for some products such as CTT rely solely on spectral channels in the thermal infrared and these products are therefore available by day and by night. However, others also require data from channels that lie in the visible solar bands, meaning these products are only available for daytime. As a consequence some products such as LWP have been implemented with separate algorithms for daytime and night-time retrieval, and may exhibit different characteristics for each mode. The shadow area between earth's daytime and night-time hemispheres (the "terminator"), is a particularly challenging environment because radiative conditions within a vertical column vary between night and day, degrading usefulness of solar channel information while also resulting in a rapidly changing thermal background signal which complicates infrared channel retrieval. The quality assurance data supplied with the cloud type product contain channel availability information that allows an assessment of retrieval reliability ([NWC-SAF 2012]). The transition from day to night algorithm modes is often visible in animations of satellite cloud products as a line-shaped boundary translating across the field of view. The visual characteristics and texture of the data field on either side of this boundary are often different enough to be readily visible. It is the responsibility of the icing diagnosis algorithm to take into account areas where the satellite products are degraded or contain unreliable information.

4.4   Algorithm implementation

The intent of this development is to leverage the advantages that satellite remote sensing can bring to icing diagnosis, while building upon the established strengths of the existing ADWICE system. A deep review of the diagnosis algorithm was performed, taking advantage of numerous opportunities to improve efficiency and modularise the code. This overhaul has enabled the inclusion of satellite-derived information into the core of the algorithm and the increased modularity has opened the door for easier inclusion of further data sources in future. A positive side-effect of these activities was the reduction in the number of lines of code to about one third of the original number, aiding readability and maintainability for future development work.

The resulting diagnosis algorithm is configured in a way that produces the same output as the previous version if satellite data are not available, but performs the described reduction and addition steps whenever they are. The overall amount of reduction and addition is highly dependent upon the current weather situation and the degree of accuracy with which the model is able to simulate prevailing conditions. Given the fact that neither the model nor the satellite retrieval will be perfect, the combination of the two is seen as more reliable and better able to describe prevailing icing conditions with higher accuracy, meaning reduced numbers of misses and false alarms.

The function diagram in (Annex I: Algorithm flow-chart) illustrates the DIA-SAT algorithm logic. The initial part of the analysis workflow is the same as for the baseline algorithm with the first guess diagnosis being derived from the icing forecast based on simulated atmospheric parameters out of the weather model (Tafferner, Hauf et al. 2003). Largely unchanged is also the loop that iterates across all ADWICE grid points that are associated with a valid SYNOP or METAR ground observation. This portion of the algorithm attempts to find conditions in the model output that are associated with one of the four defined icing scenarios and are consistent with the reported ground weather, mainly precipitation type (Leifeld 2004; 2007). Two of the four ADWICE icing scenarios (*Stratiform* and *Freezing*) are associated with specific features in the vertical profiles of temperature and humidity, for which a specific vertical profile analysis is performed wherever indicated by observations. For a detailed description of the icing scenarios see section 3.3.2.

A number of additional checks are performed for cases with no match between observed precipitation type and scenario-specific features in the model output. The model-based first guess is produced by the ADWICE icing forecast module that derives the same four icing scenarios from the model output. Wherever the diagnosis algorithm is unable to positively determine icing potential, the first guess icing scenario is used as long as it is not directly contradicted by ground observations. Additionally, the algorithm attempts to determine icing potential for observed and reported cloud cover where there is no icing in the first guess. Lastly, some information from the ground observation is used to remove icing below reported cloud base, except in cases of supercooled precipitation, as well as removing all icing where cloud cover is reported as 4/8 or less.

The new algorithm portions added for the purposes of satellite-augmented icing diagnosis further process that diagnosed icing data in accordance with the reduction and addition steps outlined at the beginning of this chapter. After definition of the icing scenarios, the icing intensity calculation is performed largely unchanged.

4.5   Validation of algorithm improvements

A validation case study was performed to quantify the impact of implemented algorithm extensions on the icing diagnosis performance. In this case, the ADWICE diagnosis algorithm with the included satellite data is compared to a population of PIREP observations and subsequent calculation of the relevant skill scores. These results are compared to an equivalent validation study previously performed on the original baseline algorithm.

Circumstances for the validation of aircraft in-flight icing using pilot reports are not ideal in Europe where the fragmented airspace structure and non-standardised PIREP collection and dissemination procedures result in insufficient numbers of icing PIREPs being available for scientific analysis. For this reason the ADWICE in-flight icing diagnosis/forecast validation campaign was performed over the United States where a combination of favourable conditions exists, such as regular and widespread occurrence of icing conditions across the whole spectrum of intensity and formation mechanisms coinciding with great air traffic density along the east coast corridor which results in reliably numerous and diverse pilot reports. While US ground and radar observations could not be assimilated into the COSMO-US model runs, leading to the assumption of reduced model accuracy, a comparison between the baseline and advanced ADWICE diagnosis algorithms is not unduly affected by this.

For the purposes of evaluating the ADWICE satellite-assisted icing diagnosis algorithm it is also advantageous that the US National Weather Service's GOES-East geostationary weather satellite can provide good coverage of the areas in question. The GOES-derived cloud property retrieval products provided by NCAR/NASA (Minnis et al. 2008) for the purposes of this investigation are also readily interchangeable with the METEOSAT products intended for operational use in ADWICE over Europe.

4.5.1 Validation method

Validating an aircraft in-flight icing diagnosis on a model grid with unsystematic and irregularly spaced point observations presents several challenges and requires some processing to generate data that can legitimately be compared. The method presented here is based on the validation methodology employed by NCAR/NOAA (Madine et al. 2008) and begins by condensing the gridded diagnosis data into a single point value corresponding to each point observation. For the purposes of calculating a range of typical validation skill scores using a contingency table, the diagnosis and observation data points must be converted from their respective reporting scales into dichotomous yes/no values by applying individual thresholds. The validation results must be viewed in the context of the choices made during this data processing, as each decision has an impact on the real-world meaning of the final result.

4.5.2 Validation data types

Gridded forecast to point value conversion

The validation process chosen here relies upon the contingency table paradigm. A prerequisite for using a contingency table is the existence of single value forecast/observation pairs. PIREPs may be treated as a collection of independent point observations, but the forecast model's gridded output requires an extra step of pre-processing to generate a single forecast value for each individual PIREP. The simplest way of achieving this is to choose the model forecast value from the grid point closest to the PIREP location. However, this does not take into account the spatial and temporal variability inherent in model based forecasts, since any gridded model forecast output will have some error or "noise" on the order of the grid resolution (Ahijevych et al. 2009). A moderately high resolution regional weather model such as the COSMO (7km grid point spacing) is generally seen as having a resolution finer than the characteristic scale length of most icing phenomena. It is therefore necessary to consider the forecast values from several grid points around the PIREP location to draw more accurate assessment of the models forecast for the vicinity of the observation. This process is called "neighbourhood sampling" and involves defining an area or volume around the observation location (Figure 4-4) which can then be condensed into a point forecast value for comparison with the point observation value (Ebert 2009).
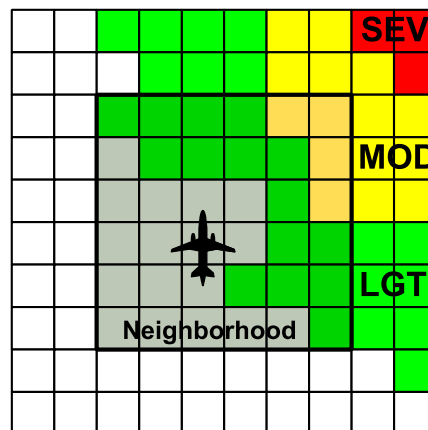

Figure 4-4: Neighbourhood selection on a model grid around PIREP, colours show icing severity.

Such a neighbourhood sampling has three main parameters affecting the derived forecast value that is ultimately taken as representative for this neighbourhood. The first two parameters control the horizontal and vertical extent of the neighbourhood respectively, while the third parameter represents the method of condensing the neighbourhood values into a point value. There are several different approaches that may be used for condensing a group of forecast grid values to a point value, such as calculating the average or median values with or without some kind of distance weighting. In order to maintain comparability of results with earlier studies that adopted the approach chosen in the NOAA/NCAR icing forecast Quality Assessment Reports (Chapman et al. 2004; Madine et al. 2008), the neighbourhood sampling in this study uses a horizontal extent of 42 km (6 x 6 grid boxes) and $+/-$ 1000ft vertical extent and then takes the maximum icing forecast value from the neighbourhood as representative for comparison with the observation. This has the effect of treating each neighbourhood containing any forecast icing as a positive forecast to be compared with the respective observation. The intent is to not penalize the model forecast for a "close miss". However, depending on the exact configuration of the neighbourhood there will also be a certain number of cases where a no-icing observation is reported close enough to forecast icing (just above cloud tops, just next to a sharply delineated frontal system) for the forecast to be treated as a "yes" even though the simulation put the observation location in the clear.

Dichotomisation

Once the neighbourhood sampling has been applied to the icing forecast products to derive a single point forecast to compare with the observation, one additional step must be performed before a contingency table can be created for the statistical analysis of forecast performance. Since the forecasts and observations report their values on individual and different scales (Figure 4-5 and Figure 4-6), a threshold must be applied to each to generate the yes/no information needed.

PIREP Icing Severity Scale								
0	1	2	3	4	5	6	7	8
None	Trace	Trace Light	Light	Light Moderate	Moderate	Moderate Severe	Severe	Heavy

Figure 4-5:   PIREP icing severity scale, dichotomisation threshold (>0.0).

Figure 4-6: ADWICE icing intensity scale (0.0-1.0), the three severity categories, and threshold for dichotomisation (>0.0).

The officially certified SIGMET/AIRMET only forecast icing areas that are expected to reach an intensity of at least *Moderate* or greater and so studies comparing model forecasts to AIRMET apply a dichotomisation threshold of "*Moderate* or Greater" to forecasts and observations. This study on the other hand intends to evaluate the diagnosis system's general ability to discriminate between icing and non-icing cases and therefore the dichotomisation threshold is set at "greater than zero" which classifies any observation of icing regardless of intensity as a "yes" and only observations of explicit absence of icing as a "no". The same threshold is applied on the diagnosis/forecast side to the point values derived by the neighbourhood sampling. In this particular case, with the neighbourhood sampling selecting the maximum value from the neighbourhood as representative, that means that a "yes" forecast is recorded for cases where the neighbourhood contains any non-zero values and a "no" forecast is recorded only for cases where the entire neighbourhood is zero.

The values of the dichotomisation thresholds are defining parameters of the subsequent statistical analysis and must therefore be taken into account when interpreting the results. After this process has been completed, all observations in the PIREP database have been assigned a diagnosis/forecast value and the process of filling the contingency table can begin.

4.5.3 Statistical measures

Skill Scores

There are several commonly used measures based upon the contingency table for verifying forecasts against observations and calculating a model forecast accuracy or "skill", such as true skill score (TSS), Brier skill score (BSS), or probability of detection (POD).

Contingency table

The four possible combinations between yes and no forecast and yes and no observations can be put in relation to each other in the context of a contingency table with two rows and two columns as in Figure 4-7. Cases where forecast and observation both have a "yes" value (yes/yes) are called a "Hit", meaning that the forecast correctly predicted an occurrence of the phenomenon in question. Cases where the forecast contains a yes value that did not materialise in the observation (yes/no) are called a "False Alarm". Cases where both forecast and observation have a "no" value (no/no) are called a "Correct Rejection" and denote cases where the forecast correctly predicted an observed non-occurrence of the phenomenon. Cases where the observation recorded an occurrence which was not predicted by the forecast (no/yes) are called a "Miss". Each cell in the table is filled with the count of data points that exhibit that particular combination of forecast and observation values.

		Observation	
		YES	NO
Forecast	YES	Hit	False Alarm
	NO	Miss	Correct Rejection

Figure 4-7:   Contingency table; Correct forecasts (green), errors (red)

Now, the skill scores may be calculated from combinations of two or more of the contingency table values. Often it is necessary to consider several skill scores to gain a full understanding of the nuances in the forecast accuracy distribution.

Probability of detection

Aircraft operating outside of icing conditions is the assumed default state and generally goes unreported, while explicit no-icing PIREPs are rare and most often highly correlated with positive icing PIREPs in space and time, frequently located within reasonable margins of spatial/temporal error for the icing diagnosis. This imposes a major constraint upon the statistics that may be validly calculated with this dataset, namely the requirement to consider positive and negative observations as two completely separate datasets (Brown and Young 2000). This in turn precludes the use of skill scores that require values

from both columns in the contingency table such as the False Alarm Ratio. There is an unfortunate conflict of abbreviations between False Alarm Ratio and False Alarm Rate, both of which are variously referred to by the term FAR which leads to frequent confusion (Barnes et al. 2009). The False Alarm Ratio is not used in this study due to the reasons mentioned above, so any instance of FAR refers exclusively to the False Alarm Rate.

H	FA
M	CR
PODyes = H/(H+M)	PODno = CR/(CR+FA)
Hit Rate = PODyes	False Alarm Rate = 1−PODno

Figure 4-8:   Per-column POD. Correct forecasts (green), errors (red).

Because of the limitations on verification statistics forecast evaluations using PIREPs mainly employ the skill score called Probability of Detection (POD) which is calculated for positive and negative observations separately. The POD for positive observations (PODyes or Hit Rate) is the fraction of correctly forecast events ("hits") out of all positive observations. The negative side also has a "rate" and a POD but here they are not equivalent. For negative observations one commonly refers to the False Alarm Rate (FAR), and the PODno. The (FAR) is the fraction of False Alarms out of the total number of negative observations whereas the PODno is the fraction of Correct Rejections out of the total number of negative observations (see Figure 4-8). This can be expressed as FAR $= (1 - \text{PODno})$.

When using POD to describe model forecast accuracy, it is necessary to consider PODyes and PODno in context. A trivial example to illustrate this point would be a forecast that predicts icing for all points of the dataset. Such a forecast would obviously score a perfect Hit Rate/PODyes of 1.0 (100%). But the corresponding PODno would be zero, making the FAR also 100%. This is plainly a useless forecast. A useful forecast maximises the Hit Rate while maintaining an acceptable False Alarm Rate.

ROC curve

When determining the optimal forecast dichotomisation threshold for best discrimination of a particular observation threshold, it is common to iterate along the forecast threshold scale calculating PODyes/PODno pairs for each step. These pairs can then be plotted on a graph called the "Receiver Operating Characteristic" (ROC) curve to quickly and visually express forecast accuracy. The ROC curve was developed in the early days of radar (signal detection theory), and serves as a tool to quantify the signal-to-noise ratio of electromagnetic transceivers. When applied to the evaluation of dichotomised forecast/observation pairs, it is presented as a plot of Hit Rate against False Alarm Rate (equivalent to PODyes vs. 1−PODno). The curve is plotted beginning at 0/0, through all the points in ROC space corresponding to the POD value pairs, and terminates at the 1/1 point. Points along the diagonal correspond to value pairs where Hit Rate equals False Alarm Rate, which represents the same skill as a random forecast. Points above the diagonal equate to forecast better than random while points below the diagonal represent forecasts worse than random.

Area under curve

A skill score derived from the ROC curve is the so-called "Area Under Curve" (AUC), which represents one way of further condensing the information expressed by a PODyes/PODno pair. As the name indicates, this is the area under the ROC curve (see Figure 4-9) and may be interpreted as a measure of the forecast's ability to discriminate between "yes" and "no" observations. The AUC of the diagonal, which represents a random equivalent forecast, is 0.5. Therefore, any AUC values above 0.5 represent a better than random forecast whereas AUC values below 0.5 is worse than random.
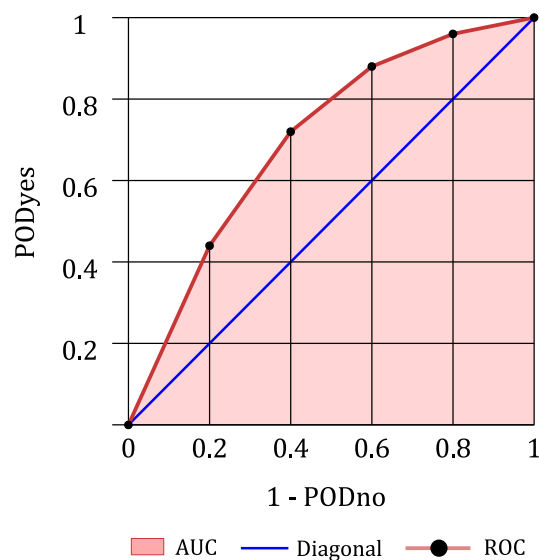

Figure 4-9:   ROC curve illustrating *area under curve* (AUC).

Confidence interval

A confidence interval is used to describe the reliability of a calculated probability value. The reliability of a contingency table skill score is determined by three major factors: the value of the score, or more precisely its deviation from a mean value of 0.5, the size of the sample used to calculate the value, and the variability within that sample.

Since the contingency table contains categorical values, a binomial proportion confidence interval is required. The central limit theorem permits the approximation of a binomial distribution with a normal distribution, and the choice of 95% for the confidence interval causes several parameters of the equation to closely approximate neat values (Madine et al. 2008). The final formula to calculate the 95% confidence interval therefore assumes the following form (4-1), where P is the calculated probability or skill score and n is the sample size:

$$95\% \ C.I. = P \pm \sqrt{\frac{P * (1 - P)}{n}} \tag{4-1}$$

Volume efficiency

The biased and non-systematic PIREP data makes it difficult to determine a reliable true False Alarm Rate for the diagnosis since most instances of aircraft flying in no-icing areas incorrectly associated with a warning (i.e. a false alarm experience for the aircrew in question) are not reported and therefore are not reflected in the data. The volume efficiency VolEff (4-3) is an alternative measure of diagnosis skill for cases with unreliable FAR (Brown et al. 1997). The Hit Rate (PODyes) is a reliable statistic when determined from a robust sample size, and the volume percentage is determined arithmetically, making VolEff more reliable than a False Alarm Rate derived from biased no-icing PIREPs.

$$Vol\% = 100 * \frac{Vol_{ice}}{Vol_{tot}} \tag{4-2}$$

$$Vol_{eff} = \frac{100 * POD_{yes}}{Vol\%} \tag{4-3}$$

VolEff is a metric used to quantify the relationship between PODyes and the icing volume from an icing forecast or diagnosis. The amount of icing a forecast or diagnosis produces is expressed as the volume percentage (Vol%) which is the ratio of the volume covered by icing to the total volume of the 3D model grid (4-2). The volume efficiency is the ratio of PODyes in percentage form to the volume percentage of icing (4-3). As the term "efficiency" implies, the dimensionless parameter VolEff is a measure of the amount

of icing volume the model has "invested" to achieve its PODyes. As has been shown earlier it is trivially easy to achieve a high PODyes by outputting more icing volume to cover more positive observations (higher Hit Rate). However, this comes at the cost of a higher true False Alarm Rate and an increase in icing Vol% disproportionate to the gain in PODyes. Since VolEff is dimensionless, an absolute value only carries meaning in context and a direct translation of VolEff to true False Alarm Rate is not reasonable. A reasonable assumption of significant inverse correlation between the two makes material improvements in VolEff apply analogously to the true False Alarm Rate. Higher volume efficiency implies real skill on the part of the forecast or diagnosis to reduce output icing volume in areas less likely to see positive icing observations, while adding icing volume in areas that do see positive icing observations and thereby maintaining a favourable PODyes. VolEff is therefore a useful metric in situations where a reliable PODyes may be calculated from a large number of positive observations but a low number of negative observations make the calculated PODno unreliable.

4.5.4 Validation input data

Input data for this investigation include a large number of icing related PIREPs and satellite cloud property products provided by NCAR as well as NWP model data from COSMO model runs from Deutscher Wetterdienst (DWD). However, ground observations and precipitation radar data, usually part of any ADWICE diagnosis, were not available and so this part of the investigation can only show the changes that satellite data inclusion can achieve over a purely model-based baseline diagnosis. The difference between a model-based diagnosis and a model/observation diagnosis is restricted to the areas of influence around the observation stations which represent a relatively small percentage of the overall model domain. The lack of ground observation data for this part of the evaluation therefore represents a noteworthy but non-critical constraint.

US PIREPS

As presented in detail in [section 3.1.1](#), pilot reports (PIREPs) play a key role among the readily available weather information sources, specifically for the validation of aircraft in-flight icing conditions. Although they are not ideal data sources from a scientific perspective, in the sense that they are not systematic and are associated with several subjectivities and uncertainties, PIREPs do deliver information about in situ observation of icing conditions that cannot readily be attained through remote sensing. Icing PIREPs were collected during the 2009-10 winter icing season over the United States, which included several severe winter storms along the East Coast corridor in February 2010.
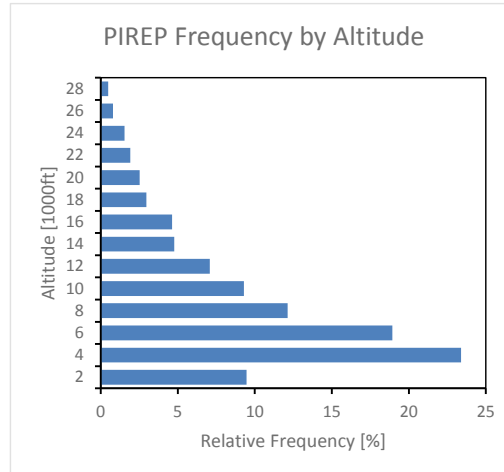
Figure 4-10: Icing PIREP vertical distribution for the US, 2009/2010.

Figure 4-10 shows the vertical distribution of PIREPs during the observation period. It shows a clear maximum in the lower altitude range but contains a significant number of reports at high altitudes also. This reinforces the fact that while icing is a predominantly mid-to-low altitude phenomenon, it regularly occurs at high altitudes where it may be less expected.

Figure 4-11 shows hourly PIREP counts across the observation period. The PIREP intensity category signified by colour shows a large proportion of PIREPs for light icing. Also important to note is the relatively low number of no-icing PIREPs, as these are used to calculate PODno. Lower numbers of no-icing PIREPs also result in a higher uncertainty for the calculated PODno values. The clearly visible diurnal cycle of PIREP counts is more directly attributable to the distribution of flights throughout the daytime hours in the US than to a variation in the weather patterns. Note that local times in the United States are 5 to 8 hours behind the values on the time axis of the graph, given in UTC.
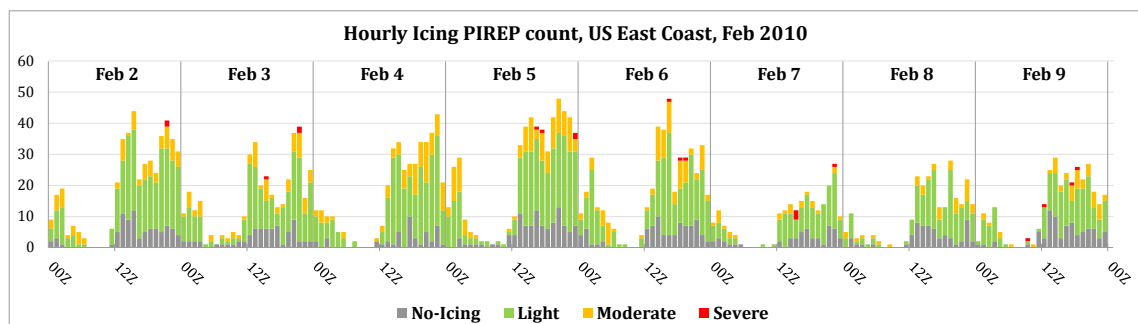
Figure 4-11: Hourly PIREP counts across the observation period. Winter storm activity from Feb. 2-6 is reflected in greater number of daily icing reports, while the later days see milder weather activity.

ADWICE data

COSMO-US model runs were performed for the same February 2010 time period over the Eastern CONUS, capturing the life cycle of several winter storms as well as calm spells. These available model data allow the subsequent preparation of ADWICE model-based icing diagnoses using the baseline algorithm (DIA) as well as three configurations of the advanced DIA-SAT algorithm. In addition to assessing the total improvement achieved by the extended DIA-SAT algorithm, the validation shall also separately quantify the impact on icing diagnosis accuracy of the lower icing intensity threshold as well as satellite data. Two variants of the DIA-SAT algorithm were created, applying only the lower icing intensity threshold or the satellite data respectively, and included in the final comparison.

**Satellite data**

Satellite products derived from the GOES-East geostationary weather satellite over the Eastern United States during the validation period were archived, for use in the satellite-augmented ADWICE diagnosis algorithm. The GOES-E satellite's instruments are not identical to the SEVIRI imaging spectrometer on the METEOSAT satellite covering Europe, and the US satellite products are produced by NASA using different algorithms from the ones produced by EUMETSAT for Europe. Therefore, the satellite products used in the US validation are somewhat different from the ones eventually used in the operational product. However, according to (Minnis et al. 2004b) the NASA cloud property retrieval algorithm VISST delivered satisfactory results for icing-relevant dense liquid and ice clouds when tested on METEOSAT. This supports the assumption that the basic cloud property products derived from either system are sufficiently interchangeable in practice to be used in a validation study such as this one.

4.6   Example case

The operation of the algorithm and its impact on the final diagnosis output is demonstrated using a representative case from the validation data set over the United States. This case illustrates the main modes in which the satellite algorithm removes icing volume from and adds icing volume to the model-based icing diagnosis to produce the final diagnosis output. A brief introduction of the overall weather situation in the region is followed by a graphical presentation of the icing diagnosis product and icing pilot reports for that time along with a discussion of how the satellite algorithm has contributed to the final output. Diagnosis skill is determined according to the method introduced in 4.5.1 and this quantitative analysis is used to assess the improvements that the satellite algorithm was able to bring to the icing diagnosis.
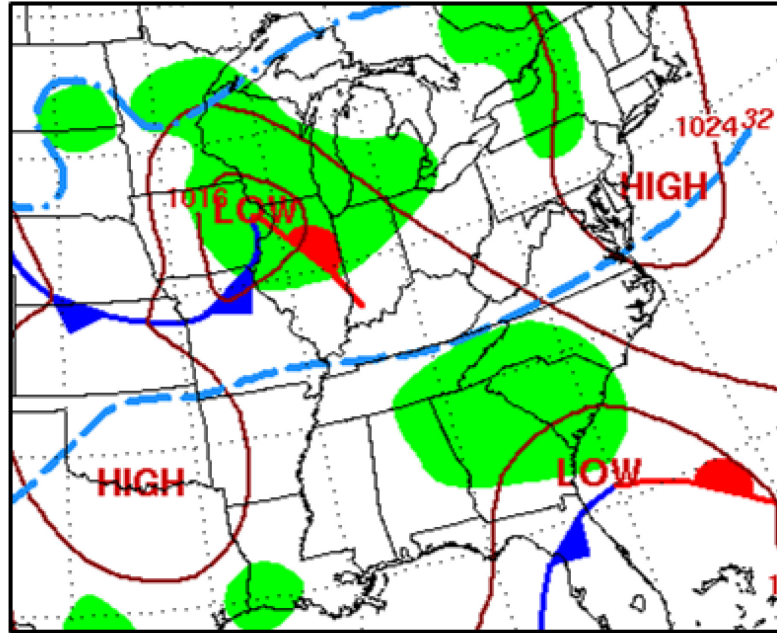
Figure 4-12: Surface Weather Map February 2, 2010 at 12:00 UTC (NCEP 2010).

The validation time period of Feb. 2 through February 9, 2010 saw several winter weather systems move through the Eastern United States, bringing with them a range of icing conditions typical for this time of year. For demonstration purposes, the weather situation on February 2 at 15:00 UTC was chosen because it is sufficiently representative of winter weather found in the region and a useful number of positive as well as negative icing PIREPs were reported around that time.

The general surface weather situation as presented in Figure 4-12 shows two low pressure systems present in the area, one off the Georgia coast and one on the Illinois/Wisconsin border south-west of the Great Lakes. This second surface low is associated with a short wavelength upper trough in the 500 hPa streamlines (not shown here), and exhibits a rotating frontal system with well-defined warm sector. It was moving towards the Great Lakes region from the West, bringing with it significant precipitation which reached the ground as mostly snow but contained increased potential for super-cooled liquid water at altitude.

The surface low diagnosed off the south-east coast constitutes a wave in an existing frontal system stretching from the Gulf of Mexico across northern Florida out over the Atlantic. This weak surface low was only in the beginning stages of cyclogenesis and not yet well organised. However, the frontal system is associated with intensive sub-tropical convection and resulting thunderstorms forming in the air mass over Florida.

Large-scale ascent, centred on South Carolina, resulted in non-convective medium altitude cloud cover with occasionally considerable precipitation. The medium cloud cover stretched all along the East Coast down through Florida, while the significant non-convective precipitation was centred on the Appalachian mountain range in the border area between the Carolinas, Georgia, and Tennessee. Forecasters expected local conditions near ground level to support pockets of freezing rain.

The western Plains as well as the northern half of the East coast were characterised by high pressure influence and subsidence, resulting in little cloud cover and low icing risk.

The northern surface low south-west of the Great Lakes is associated with a significant cluster of icing PIREPs of varying intensity, including several *No Icing* PIREPs. The high spatial correlation between the PIREP distribution and the winter storm precipitation area associated with that surface low is remarkable and indicative of the high icing potential contained within that air mass. A smaller but nonetheless noteworthy cluster of PIREPs reporting *Severe* icing encounters is located directly above the main ridge of the Appalachian mountain range in the border area between Virginia and North Carolina and Tennessee. Icing conditions in this location were most likely boosted by orographic lifting of the airflow across the mountains accelerating condensation and cloud droplet growth through coalescence.
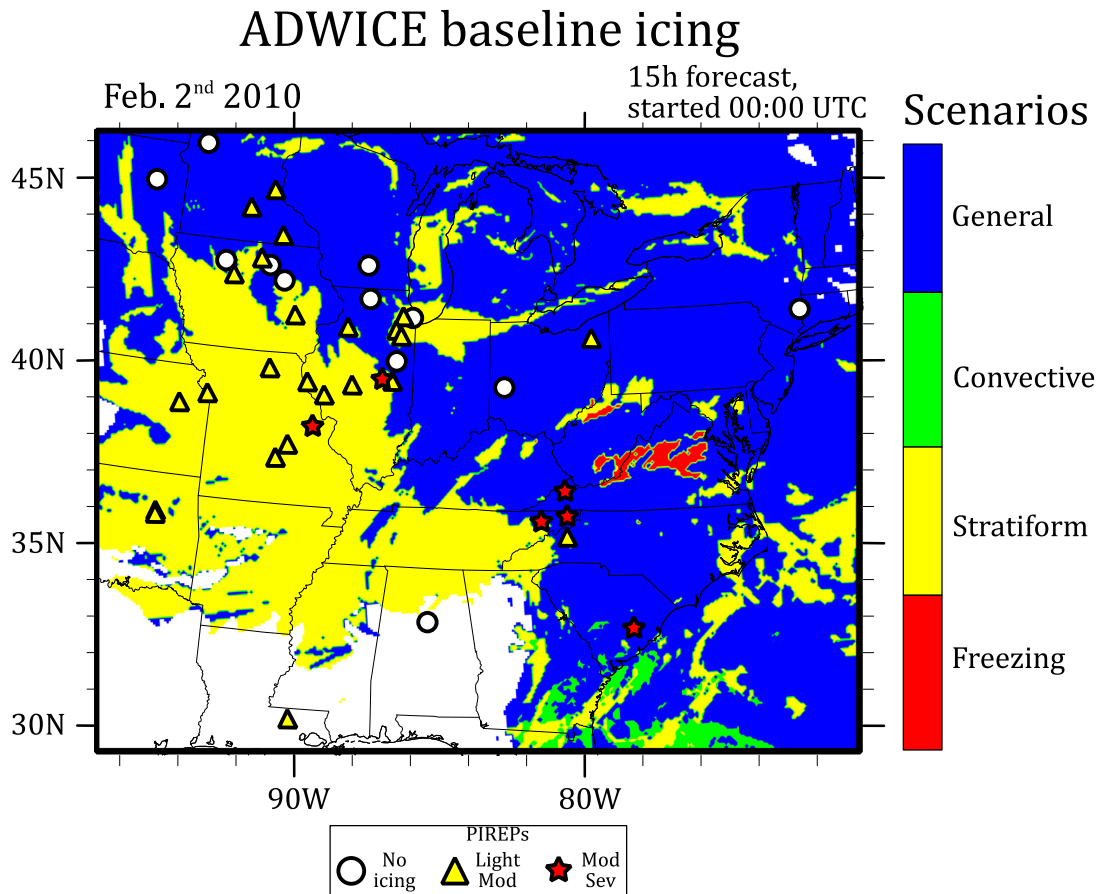
Figure 4-13: ADWICE baseline icing scenario coverage with icing PIREPs, example case Feb 2 2010, 1500UTC.

The ADWICE baseline model-based icing diagnosis in [Figure 4-13](#) correctly identified the mainly convective character of conditions over Florida and off the south-east coast, as well as identifying the potential for freezing rain conditions near the surface along the leeward side of the Appalachian mountain range, albeit somewhat further north than in fact observed. The algorithm also identified a sizeable area of icing potential due to stratiform conditions (supercooled drizzle), covering most of Tennessee and Missouri plus parts of surrounding states in the West. Most of the remaining model area, apart from the deep South with its above freezing temperatures, was diagnosed with icing conditions corresponding to the icing scenario *General* defined by a variable humidity/temperature criterion. Some parts of the area assigned icing scenario *General* were in fact partly or completely cloud free due to the subsidence associated with high pressure influence. This illustrates the tendency of the ADWICE baseline algorithm to overestimate icing conditions, particularly in weakly organised low pressure gradient conditions.

While this icing diagnosis is able to capture a very high percentage of the icing pilot reports, the no-icing PIREPs are mostly associated with positive icing diagnosis also, negating the high Hit Rate with a correspondingly high False Alarm Rate. In addition,

the total volume of model gridpoints assigned with icing conditions is improbably high, which results in an unexceptional ratio of Hit Rate to total icing volume which is expressed as the volume efficiency.

The satellite algorithm's ability to reduce icing volume by cloud mask and cloud top height correction has the potential to considerably improve the definition of icing free areas in the final diagnosis product, leading to a lower incidence of reported and unreported false alarms. The satellite algorithm's icing detection function adds icing volume where the model-based diagnosis underestimated cloud top height and helps in highlighting areas of increased icing potential that should be protected from other icing volume reduction efforts within the icing diagnosis algorithm.

Change in sat-augmented diagnosis over baseline
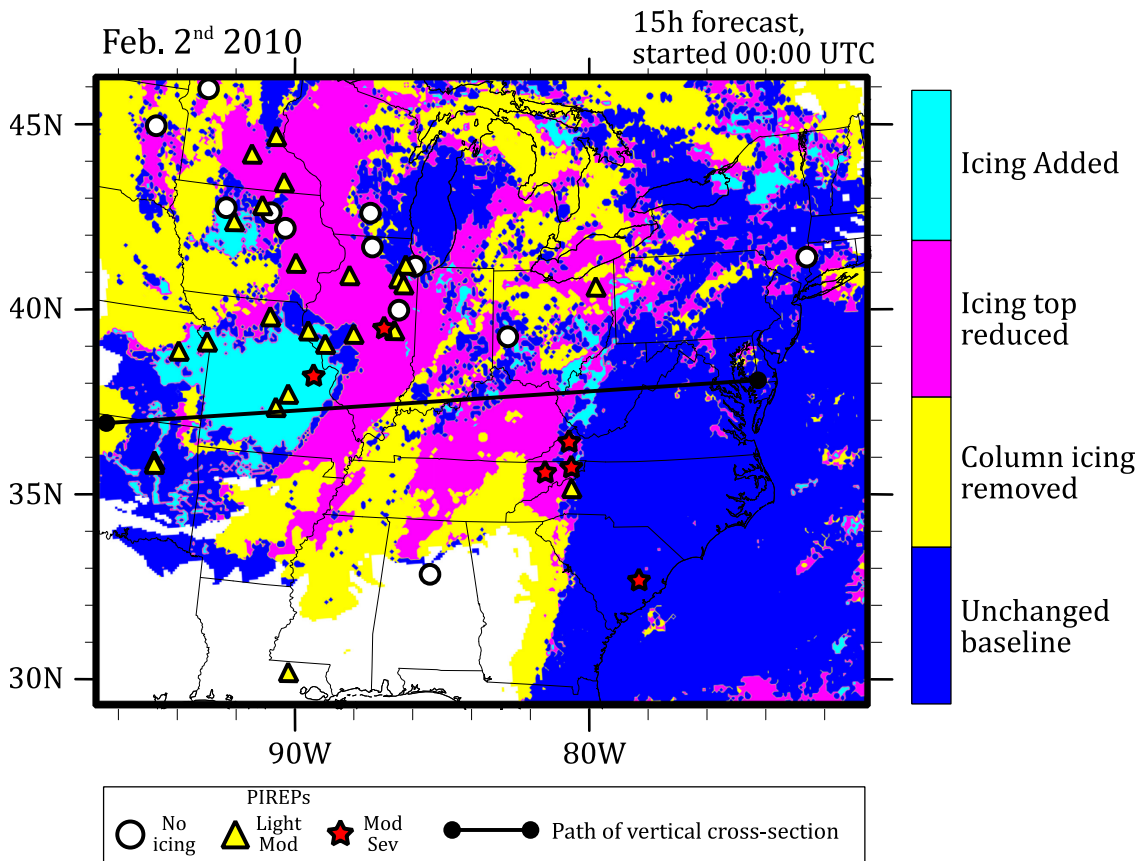
Figure 4-14: ADWICE validation map plot of sat-augented changes to ADWICE output over baseline, see **Figure 4-15** for cross-section.

The graphical presentation in [Figure 4-14](#) shows a map of the ADWICE satellite augmented icing diagnosis for the demonstration case. Areas modified by the reduction or addition functions of the satellite-based algorithm are highlighted. PIREPs are plotted on the map as point symbols, differentiated into the three categories of "*No Icing*"(circle), "less than *Moderate*" LTM (triangle), and "*Moderate* or greater" MOG (star).

The map view indicates that large portions of the central and northern model area are affected by the reduction function of the satellite algorithm, either through removal of icing from the entire column using the cloud mask or through the reduction of the vertical extent of diagnosed icing to conform to the satellite-derived cloud top height. There is a sizeable area over the state of Missouri in the west of the map, marked in cyan, where the satellite based icing detection function was able to add icing volume above the model-based icing. There are a number of icing PIREPs available for this region that clearly illustrate the improved vertical coverage of icing conditions after application of the satellite based icing detection algorithm.

Change in sat-augmented diagnosis over baseline
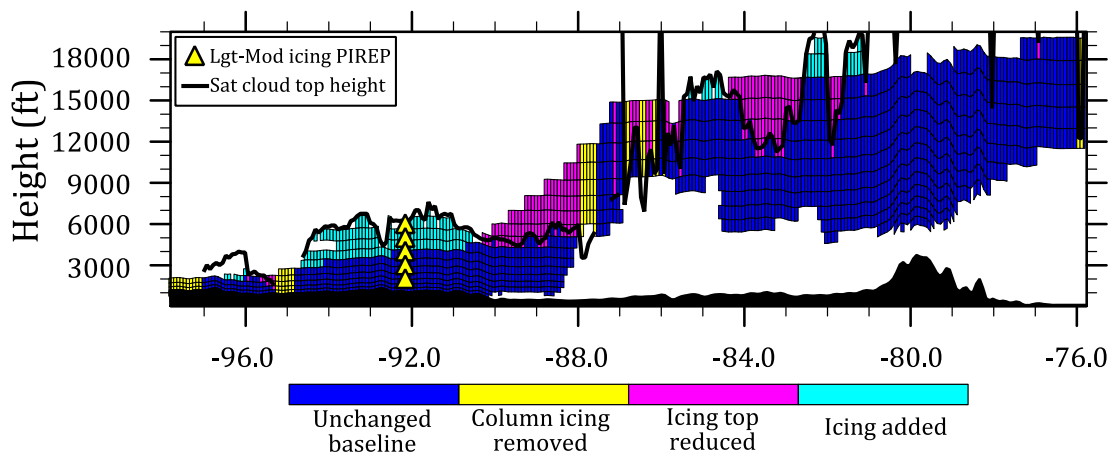
Figure 4-15: ADWICE validation cross-section plot of sat-augmented changes in icing diagnosis, along black line on the map in **Figure 4-14**, PIREP series covering height range.

The plot in Figure 4-15 shows a vertical cross-section through the centre of the map area which highlights the differences in vertical distribution of icing conditions associated with the surface low in the West and the mid-altitude precipitation over the East coast. PIREPs that refer to a vertical extent of greater than 2000ft are split up into individual data points, representative of 2000ft layers, to better resolve the vertical structure of reported icing and to allow a more granular assessment of the accuracy of the diagnosis's icing vertical coverage in cases of partial overlap. The plot intersects one icing PIREP with considerable vertical extent of reported icing in the vicinity of the Western surface low, and several more can be seen nearby on the map plot. Whereas the vertical extent of the PIREP icing extended significantly above the upper boundary of the baseline icing diagnosis (blue/yellow), the satellite augmented icing diagnosis (blue/yellow/cyan) much more closely matches the vertical extent of reported icing conditions.

This example illustrates the ability of the satellite algorithm to constructively add icing volume to the icing diagnosis to better capture reported icing conditions, while at the same time the reduction algorithm based on satellite cloud mask and satellite cloud top

height are able to significantly constrain the output icing volume (yellow and magenta grid boxes) to better define areas actually free of icing.

Table 4-1 contains the observation/diagnosis contingency tables for the example case on February 2, 2010, 1500 UTC for the ADWICE baseline diagnosis product and for the satellite-augmented final diagnosis product. Thirteen out of the 42 unique positive icing PIREPs reported icing over a large altitude range and these were therefore subdivided into 2000ft intervals, resulting in an increase in the total number of positive icing data points to 71. Negative icing PIREPs were not subdivided in this case and therefore the number of unique no-icing observations stands at 12, as reflected in the table.

Table 4-1:   Contingency tables for the example case on Feb 2, 2010, 1500 UTC.

	ADWICE baseline		Satellite-Augmented	
	Icing PIREP	No-Icing PIREP	Icing PIREP	No-Icing PIREP
Icing diagnosed	62	9	68	8
No-Icing diagnosed	9	3	3	4

The diagnosis skill scores in Table 4-2 were calculated from the contingency tables according to the method described in section 4.5.1. The approximately 10% improvement in Hit Rate is mainly attributable to the constructive addition of icing volume in areas where the baseline algorithm underestimated the cloud top height of icing conditions, as shown in Figure 4-15. The approximately 11% reduction in False Alarm Rate would also constitute an improvement but in the context of this case example's small sample size of negative observations, the error in the computed False Alarm Rate is larger than the arithmetic difference. As a consequence, the Area under Curve (AUC) value also carries greater error in this case than with a larger sample size. The real improvement achieved by the satellite-augmented diagnosis over the baseline lies in achieving this excellent Hit Rate while at the same time reducing overall icing volume by 30%. The resulting approx. 56.5% increase in Volume Efficiency demonstrates a considerable improvement in the diagnosis algorithm's ability to distribute icing volume in areas with increased actual icing potential and to more accurately leave out areas of little or no icing potential.

Table 4-2:   Icing diagnosis skill scores for the baseline ADWICE diagnosis and for the satellite-augmented final diagnosis product. Volume percentage based on a total volume of 99.483 x106km^3.

	ADWICE baseline	**Satellite augmented**	
Hit Rate/ *PODyes*	0.873	0.958	**+9.68%**
False Alarm Rate/ *(1−PODno)*	0.750	0.667	**(−11.11%)**
Area under ROC curve/ *AUC*	0.562	0.646	**+14.94%**
Icing volume (106km^3)	13.698	9.604	**−29.89%**
Volume Percentage (%)	13.769	9.654	**−29.89%**
Volume Efficiency	6.342	9.921	**+56.43%**

This example case illustrates the powerful potential for satellite augmentation in icing diagnosis to materially improve the tendency for over-diagnosis/forecasting existing in the purely model-based icing diagnosis algorithm and at the same time to significantly contribute to the identification of areas with icing conditions. While this example case chosen for visual clarity and PIREP availability lies at the upper end of the scale in terms of gains, the averages across the entire observation period presented in the following section nonetheless reflect solid double-digit improvements in most categories.

4.7   Validation results

Icing PIREPs collected during the validation period are associated with the closest hourly diagnosis time and neighbourhood matched to the diagnosis output for the generation of the contingency table, as outlined in above. Skill scores used for this evaluation are PODyes, PODno and the AUC derived from them, plus the percentage of total model volume that is covered by icing (Vol%) and the icing volume efficiency VolEff derived as the ratio of PODyes to Vol%. These skill scores are presented separately for the baseline diagnosis algorithm and the satellite-augmented advanced diagnosis algorithm.

Table 4-3:　　Skill comparison between baseline and satellite-augmented diagnosis configurations, overall values from Feb 2-Feb 9, 2010.

		ADWICE baseline	Satellite augmented	
Near PIREPs	*PODyes*	0.879	0.898	within error
	PODno	0.229	0.215	within error
	AUC	0.554	0.556	within error
Overall	*Vol%*	17.6%	14.4%	**-17.7%**
	VolEff	5.11	6.51	**±27.4%**

Validation scores in Table 4-3 are un-stratified totals across the entire model domain from February 2 to February 9, 2010. Qualitatively, these overall results reflect the example case presented in the previous section, although the magnitude of changes is reduced. Nonetheless, the application of satellite products produces a reduction of greater than 17% in average icing volume percentage across the validation period while maintaining an excellent Hit Rate (PODyes) against positive icing PIREPs. The arithmetic differences in PODyes, PODno, and the derived AUC are small enough for the 95% confidence intervals in the respective comparison to largely overlap (PODyes: ~8%; PODno: ~125%) and are therefore insignificant. The lack of a net effect of the satellite products on PIREP-based skill scores implies that any addition or reduction of icing volume in the vicinity of PIREPs is applied to positive and negative icing PIREPs in equal proportion. This is an example of the recurring challenge in discriminating closely clustered positive and negative icing PIREPs with any useful skill.

The results were also stratified by time to resolve trends or temporal variations. Since flight activity in the validation region greatly decreases approximately between local midnight and 6 AM, PIREPs were aggregated into six hour blocks spanning the entire validation period. This largely confines issues with low sample size to the 12-6AM block, leaving three blocks for each day with a reasonable number of PIREPs each.

Skill scores, ADWICE baseline
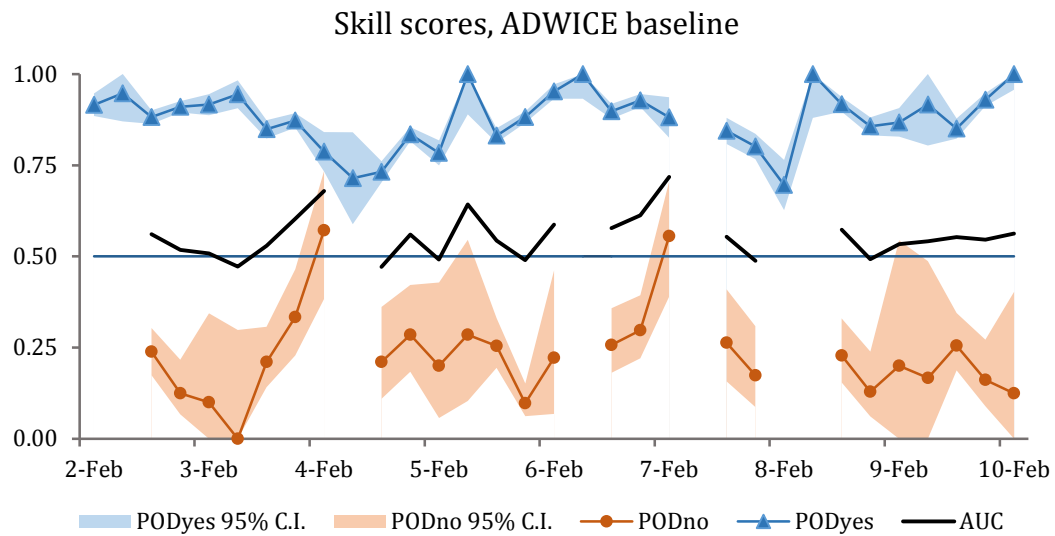
Figure 4-16: Validation time series of PODyes, PODno of the ADWICE baseline product with 95% confidence and AUC. Gaps indicate insufficient data due to lulls in flight activity between local midnight and morning.

Figure 4-16 shows the timeline of PIREP-derived skill scores for the ADWICE baseline product. A gap in the time series signifies a case of insufficient data for the calculation of that value, which occurs regularly during local night-time. 95% confidence intervals are included for PODyes and PODno to illustrate the greater uncertainty in calculated PODno values due to the much smaller number of negative icing PIREPs.

No clear trend appears in the skill scores across the validation period, apart from a certain reflection of the diurnal cycle in the size of the confidence intervals. On two days (Feb 3 and Feb 7) the PODno value spikes sharply upwards during the course of the day before midnight, returning to average values the following morning. An analysis of the weather situation and PIREP distribution did not reveal a clear pattern connecting the increased skill to any particular circumstance. It appears therefore that this is an artefact of a transient peak in the underlying COSMO weather model's skill in simulating atmospheric conditions that allowed ADWICE to better identify icing-free region.

As with the overall averages, the timeline of skill scores for the satellite-augmented product shows some variation from the baseline in positive as well as negative direction, but few of the differences are statistically significant and the full set of parameters is therefore not shown. Instead, a time series of the percentage difference over the baseline in PODyes for the satellite augmented diagnosis is used to illustrate the influence of satellite augmentation on the most robust and reliable of the PIREP derived skill scores (Figure 4-17).
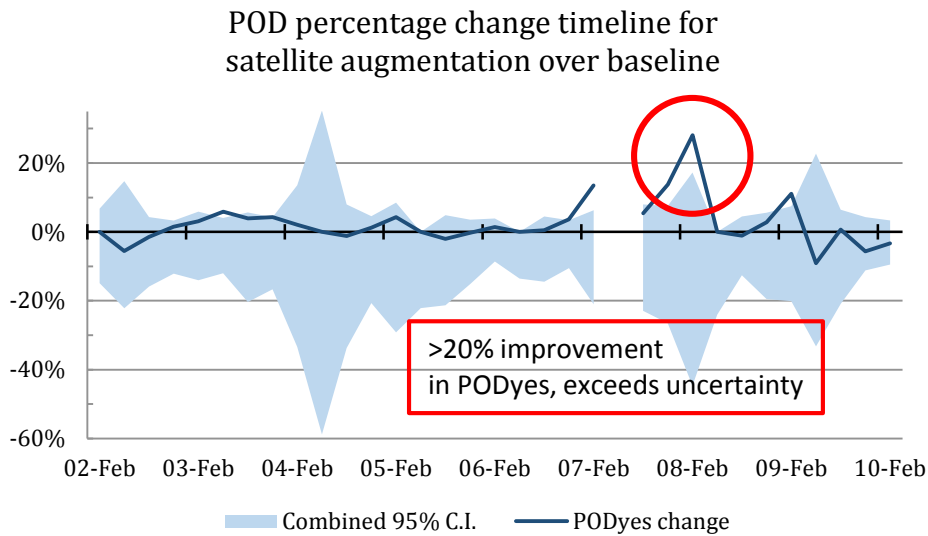
Figure 4-17: Validation time series of POD change in sat-augmentation over baseline, shaded area signifies overlapping 95% C.I.

There is little significant variation outside the error margins in the initial two thirds of the time series, showing modest and mostly random gains and losses in the proportion of correctly captured icing PIREPs used to calculate PODyes. However, the last third of the time series beginning Feb 7 shows variations well outside the error margins and therefore significant. While fluctuations are stronger, with at least one sizeable excursion into the negative, the significant variations outside the margin of error are in the positive, particularly so Feb 7 to Feb 8. This strong gain in PODyes indicates successful capture of a significant number of additional positive icing PIREPs through the addition of extra icing volume from the satellite diagnosis. PODno is not available for that time due to insufficient negative icing PIREPs, preventing the calculation of an AUC value. While the satellite algorithm was definitely able to identify an area associated with positive icing PIREPs that had been missed by the baseline algorithm, the number of PIREPs involved in that particular time step is small and so this particular anomaly has little effect on the overall difference in PODyes between the baseline and satellite algorithm.

Another clear signal of the satellite augmentation's impact is visible in the time series of the difference in icing volume percentage and volume efficiency between the baseline and satellite-augmented diagnosis Figure 4-18.

Volume percentage change timeline for
satellite augmentation over baseline
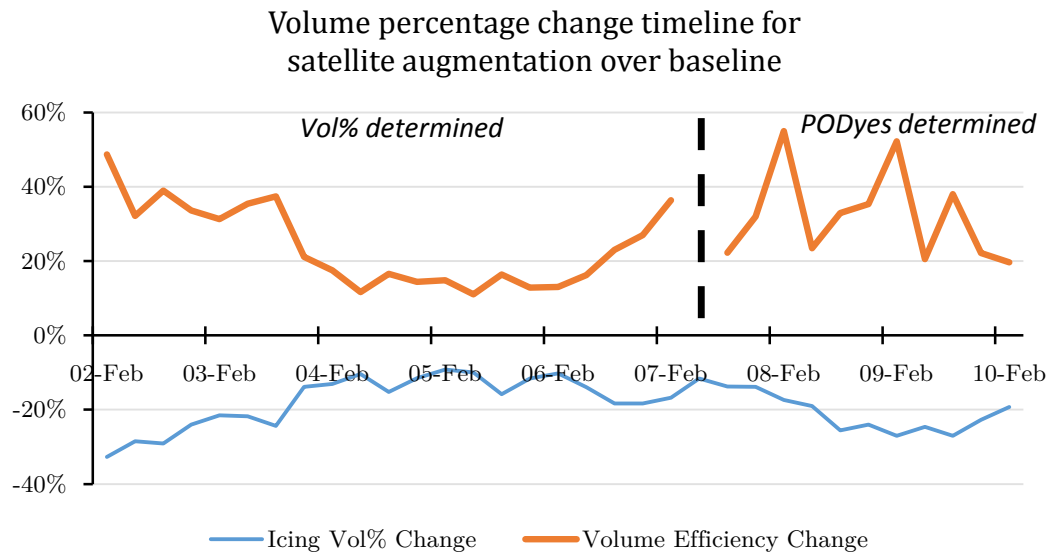
Figure 4-18: Validation time series of Vol%, VolEff change in sat-augmentation over baseline.

In contrast to the POD time series, the time series of difference in icing volume follows a much clearer evolution throughout the validation period. The reduction in volume percentage achieved through the application of satellite products is greatest at the beginning of the period and then gradually decreases in magnitude towards the middle of the period followed by another increase towards the end. Analysis of the weather developing during the validation period shows a clear inverse correlation with the proportion of the satellite field of view obscured by opaque ice crystal clouds. The presented time series are consistent with increased cirrus cloud cover reducing the overall area available for the application of satellite data and therefore reducing the potential magnitude in reduction of icing volume. Areas covered by opaque ice clouds are labelled as "indeterminate" by the satellite algorithm and retain the default values from the baseline algorithm.

The time series of the volume efficiency reflects characteristics of both its input parameters PODyes and Vol%. The first two thirds of the volume efficiency time series show a fairly straightforward inverse correlation with the time series for the change in Vol%, as is to be expected in a situation where PODyes remains stable. The last third of the volume efficiency time series beginning Feb 7 shows strong influence by the previously discussed variability in PODyes over the baseline. The sharp gains in PODyes in Figure 4-17 and a reduction in icing volume that has again increased in magnitude from its mid-week low combine to create the visible sharp volume efficiency maxima. This again demonstrates the dual character of the value added by satellite-augmentation in terms of adding and removing icing volume simultaneously where needed.

4.8   Discussion

The satellite based icing product is able to reduce the overall icing volume percentage by between 10% and 30+% while simultaneously adding icing volume in the vicinity of PIREP clusters, as indicated by significant maxima in the time series of PODyes gain over the baseline. An increase in icing volume in the vicinity of icing PIREPs combined with an overall reduction in icing volume indicates a positive correlation between the satellite-based icing detection product and icing PIREP clusters and thereby demonstrates skill on the part of the satellite product in discriminating icing areas. The reduction in overall Vol% is not only limited by the amount of excess icing produced by the baseline diagnosis but also by visibility issues for the satellite sensor as the satellite-based product is only able to definitively exclude icing under adequate observation conditions (see 4.3).

Ideally, an icing diagnosis system should be able to consistently achieve a high Hit Rate with regards to icing PIREPs while producing minimal unnecessary and incorrect icing volume elsewhere. The final DIA-SAT configuration in column two of Table 4-3 combines cloud masking and cloud top height correction with the satellite based icing detection product. It is able to achieve a reduction in diagnosed icing volume percentage by 17.7% while at the same time maintaining PODyes and PODno over the baseline ADWICE DIA. The resulting approx. 27.5% increase in volume efficiency is a considerable step change over the baseline system and demonstrates the potential of satellite based icing products in contributing to the increase of icing warning accuracy while at the same time reducing inappropriate over diagnosis.

There is value in and of itself in a reduction of icing volume while maintaining a sufficiently high Hit Rate for observations, since many participants in air traffic are required to avoid icing conditions entirely and must therefore rely on accurate forecasts and diagnoses of icing free areas for flight planning purposes. At the same time a reduction in overall icing volume also reduces the number of false alarm events which are massively underreported and therefore not adequately reflected in the False Alarm Rate. The reduction in false alarm experiences for aircrew builds trust in the icing diagnosis and increases the likelihood of future use, thereby achieving one step towards the goal of increasing flight safety.

5.   Summary and conclusions

This study was able to demonstrate the utility of integrating satellite cloud property products into an icing diagnosis algorithm. The main benefits that satellite data can deliver are the reliable identification of a large fraction of the total cloud free area and a characterisation of meteorological conditions at the cloud top which are helpful in assessing the probability of the presence of icing conditions in the upper region of that cloud. The value provided to icing diagnosis by ground-based observation remains wherever detailed precipitation type observations are recorded by human observers. The increasingly widespread automation of weather observation stations, and consequent loss of some detail in precipitation type observations, raises concerns because of the possibility that ground-based observations may contribute less to icing diagnosis in the future. Satellite data with their near uniform coverage of continental-scale model domains at high horizontal resolution are uniquely suited to augment model-derived icing diagnosis and can provide direct observation data which allows for the reduction of excessive icing volume output as well as improving the detection of icing conditions near the cloud top.

The first iteration of the DIA-SAT next generation satellite-augmented ADWICE icing diagnosis algorithm presented here has not only achieved the initial goal of reducing the amount of over-diagnosis compared to the previous version but has also proven its value in positively identifying areas of increased icing potential. This second capability will become more and more powerful in future as additional data sources and optimisations are integrated.

It is the ability to achieve competitive validation accuracy against icing PIREPs while at the same time substantially reducing diagnosed icing volume that is the most immediate and visible advance of DIA-SAT over the previous generation algorithm.

The satellite-augmented icing diagnosis algorithm DIA-SAT developed for this study implements a system-of-systems approach by integrating satellite cloud top property products provided by EUMETSAT's Nowcasting Satellite Application Facility (NWC-SAF) and a regional numerical weather prediction model (COSMO-EU) from Deutscher Wetterdienst with the improved ADWICE aircraft icing diagnosis algorithm developed at Leibniz University Hanover. The system-of-systems approach uses building blocks or individual modules that provide data or functionality but may be operated and developed by separate entities which each apply their specific expertise and manpower when and where necessary and available. The final product of the DIA-SAT algorithm automatically gains any improvements implemented in one of the constituent systems, since the exchange of data is based on atmospheric parameters and physical units and is

less reliant on hardwired tuning parameters than a comparable algorithm based upon the ingestion of raw measurement data. This allows for a more efficient use of limited development and maintenance manpower enabling the relatively straightforward integration of additional data sources through an inherently modular architecture.

The reference implementation of the DIA-SAT algorithm retains many elements of the previous generation ADWICE DIA algorithm, mostly relating to the diagnosis of icing conditions based upon ground observations. In addition to updated software architecture, DIA-SAT contains two significant changes over ADWICE DIA affecting the output. One is the introduction of a configurable lower icing intensity threshold which removes icing from grid points initially diagnosed with icing conditions if the subsequently determined icing intensity at that grid point does not exceed a certain threshold value. This opens up further opportunities to reduce the over forecasting by the model-based first guess diagnosis. The second major addition is of course the integration of satellite cloud products into the icing diagnosis. The satellite data provides valuable direct observation information about cloud cover, cloud top height, and icing potential at the cloud top. These products enable the algorithm to define areas with no icing risk (cloud free, above cloud top) as well as defining other areas with increased icing risk (super-cooled liquid water at cloud top). While there are many situations where satellite cloud products can provide no additional information either way, such as in the case of high ice cloud coverage, there is nonetheless a demonstrated and considerable net benefit to be gained.

Since the model-based first guess diagnosis has a strong tendency towards over forecasting, the satellite-based detection of icing conditions does not generally add significant icing volume. However, with the possible future introduction of a lower icing intensity threshold which removes extremely light icing from the diagnosis, the satellite based icing detection can serve to protect positively identified areas of high icing potential from any reduction based on model output fields.

5.1   Opportunities for further improvement

While the first iteration of the DIA-SAT satellite-augmented icing diagnosis algorithm presented here has already delivered significant improvements, there are possibilities for further improvement in several categories. These range from the integration of additional data sources to measures aimed at improving the underlying model forecasts, and include opportunities for further optimising the ADWICE algorithm.

5.1.1 Aircraft measurements and PIREPs

Increasingly automated and digitised measurement of atmospheric parameters is being routinely performed on commercial aircraft for on-board purposes. Some of this data is already available through the AMDAR data-link system. From the perspective of aircraft icing research there is a strong case to be made for integrating the data from icing sensors already on many aircraft in this downlink stream, to make icing data collection more reliable and systematic. This would also make data collection independent from pilot workload and attention as well as eliminating the human factor reporting biases. Location and time information is also much improved, provided this data is not withheld by operators for legal accountability reasons.

5.1.2 Application of satellite data

The extended DIA-SAT algorithm already represents an advance in the implementation of satellite cloud products within the ADWICE system, although it has deliberately been implemented in a conservative way with regard to flight safety considerations. There is therefore potential for future optimisation of the satellite-based icing algorithm. Specifically, the over-forecasting in the vicinity of PIREPs may be improved further by a fine tuning of reduction and addition, potentially in a context-aware adaptive mode, to achieve a balance that more accurately discriminates areas of icing potential and simultaneously capturing a higher percentage of no-icing PIREPs.

Due to lack of ready availability, the pre-operational implementation of the presented ADWICE satellite augmented algorithm over Europe currently also lacks some of the advanced cloud top products, mainly liquid water path (LWP), used during the presented validation study over the US.

5.1.3 ADWICE icing intensity estimation

ADWICE internally calculates icing intensity on a scale from 0 to 1 for every grid point diagnosed with an icing scenario. This icing intensity calculation is a fuzzy-logic based scheme using membership functions to arrive at an intensity value as a weighted contribution of several input factors such as degree of saturation, layer depth of icing conditions, and liquid water content (LWC). While LWC is a key variable in real-world icing intensity, the availability of LWC data for use in ADWICE is currently inadequate.

ADWICE uses the COSMO model's cloud liquid water content (QC) as well as an estimation of LWC from model water vapour via the parcel method. The use of LWC values calculated via the parcel method as a contributor to icing intensity estimation for all icing scenarios is questionable since the assumption inherent in the parcel method (assume

water vapour saturation, lift air parcel one model layer, condensate=LWC) is only remotely applicable in convective situations and produces implausible amounts and distribution of liquid water content across the model domain.

Since no positive and useful correlation could be established between icing PIREPs and LWC estimated via the parcel method, this parameter does not appear to be a useful contributor to the determination of icing conditions. It is therefore recommended to pursue the removal of this parameter from the icing intensity estimation at the next review of that portion of the algorithm. Indeed, the removal of this data field may actually improve the estimation of icing intensity since it is currently acting as a noisy signal perturbing the contribution of the other factors in the icing intensity algorithm.

An improved accuracy in the icing intensity estimation would also materially contribute to the successful implementation of an icing intensity lower threshold that can be used to remove volume with extremely low intensity icing from the diagnosis with reasonable confidence that no actual significant icing with associated PIREPs is located there. Thereby, overall icing volume can be further reduced without disproportionately penalising the diagnosis skill scores against icing PIREPs.

5.1.4 Icing intensity lower threshold

In the validation against pilot icing reports over the United States, an experimental application of a lower icing intensity threshold (set at 0.1 the scale from 0 to 1) was able to reduce the overall icing volume by 40-50% while maintaining an excellent hit rate with respect to the PIREPs since the satellite based icing detection algorithm was used to protect any areas from this reduction with icing potential not obscured from the satellite. This resulted in up to a >70% improvement in the important parameter of volume efficiency! Also, a lower icing intensity threshold applied to a reasonably accurate icing intensity field is able to significantly reduce over-diagnosis even in cases where the satellite's field of view is obscured.

5.1.5 Model liquid water

Parallel to this research and development project focused on satellite data, efforts are underway to improve the utilisation of existing COSMO model parameters in ADWICE as well as to provide feedback to the model development community about experiences with model behaviour, particularly the cloud microphysics package that determines the water mass distribution across hydrometeor classes and therefore the phase conditions within the simulated clouds. Of particular interest are more realistic simulations of amounts and distribution of atmospheric liquid water as well as any advances in accounting for ice nuclei in simulating the cloud glaciation process.

Annex I: Algorithm flow-chart

ADWICE DIA-SAT
satellite-augmented icing diagnosis

cont'd

OBS: shower, Tstorm, Cb — YES → Convective icing in model first-guess — YES → Within convective layers — NO → Above convection

Within convective layers — YES → CONVECTIVE icing ("confirmed")

Above convection — YES → GENERAL icing ("confirmed", "changed")

Convective icing in model first-guess — NO → Max conv. depth ± 3 GPs, Δz≤200m → Zero convective depth? — YES → convective base = cloud base / convective tops = cloud base + 3000m

Zero convective depth? — NO

Within convection, AND −40°C ≤ T ≤ 0°C — NO → Above convection, −20°C ≤ T ≤ 0°C — YES → RH ≥ 80% — NO → NO icing

Within convection, AND −40°C ≤ T ≤ 0°C — YES → CONVECTIVE icing ("changed", "set")

RH ≥ 80% — YES → GENERAL icing ("confirmed", "changed", "set")

End of loop over surface OBS

Loop over remaining unprocessed grid-points

First guess: STRATIFORM → OBS: Rain, snow, shower, Tstorm, radar echo >19dBz — ANY → GENERAL icing ("changed")

OBS: Rain, snow, shower, Tstorm, radar echo >19dBz — NONE → STRATIFORM icing ("confirmed")

First guess: FREEZING — At ground level → OBS: Drizzle, rain, snow, shower, Tstorm — ANY → NO icing at ground level

NO (rain, drizzle, ice pellets) – OR – NO radar echo — EITHER → GENERAL icing ("changed")

Remaining First guess → GENERAL ("confirmed") → CONVECTIVE ("confirmed") → STRATIFORM ("confirmed") → FREEZING ("confirmed")

cont.

cont'd

ADWICE DIA-SAT
satellite-augmented icing diagnosis

Loop over grid-points with cloud cover OBS

OBS: cld cover >4/8 & low/med clouds —YES→ Icing already diagnosed above —NO→ RH ≥80% above cloud base —YES→ $-20°C ≤ T ≤ 0°C$ above cloud base -YES→ **GENERAL icing ("set")**

For all grid-points with valid satellite observations

SAT cloudy pixel —YES→ Cloud phase = liquid –YES→ Cloud Top Temperature $-20°C ≤ CTT ≤ 0°C$ -YES→ ≤ 1000m under cloud top, no prev. diagnosis, $T<0°C$ ·YES→ **GENERAL icing ("set")**

Loop over all grid-points

Valid cloud cover OBS —YES→ OBS: cld cover ≤4/8 - OR - NO low/med cld —YES→ **NO icing in whole column**

—NO→ SAT non-cloudy pixel —YES→ **NO icing in whole column**

For all grid-points with valid satellite observations

SAT cloudy pixel —YES→ Existing icing diagnosis higher than SAT cloud top height —YES→ **NO icing above cloud top**

Loop over grid-points with cloud base OBS

No freezing precip —YES→ Existing icing diagnosis below OBS cloud base —YES→ **NO icing below cloud base**

Icing Severity calculation

END

Bibliography

AHIJEVYCH, D., E. GILLELAND, B. G. BROWN, and E. E. EBERT, 2009: Application of Spatial Verification Methods to Idealized and NWP-Gridded Precipitation Forecasts, *Weather and Forecasting*, **24**, pp. 1485-1497.

BARNES, L. R., D. M. SCHULTZ, E. C. GRUNTFEST, M. H. HAYDEN, and C. BENIGHT, 2009: CORRIGENDUM: False Alarm Rate or False Alarm Ratio? *Weather and Forecasting*, **24**, pp. 1452-1454.

BERNSTEIN, B., 1996: A new technique for identifying locations where supercooled large droplets are likely to exist: The stovepipe algorithm. *Preprints, AMS 15th Conference on Weather Analysis and Forecasting*, pp. 5-8.

BERNSTEIN, B., T. A. OMERON, F. MCDONOUGH, and M. POLITOVICH, 1997: The relationship between aircraft icing and synoptic-scale weather conditions. *Weather and Forecasting*, **12**, pp. 742-762. http://dx.doi.org/10.1175/1520-0434(1997)012<0742:TRBAIA>2.0.CO;2.

BERNSTEIN, B., T. RATVASKY, D. MILLER, and F. MCDONOUGH, 2000: Freezing Rain as an In-Flight Icing Hazard, *AMS 8th Conference on Aviation, Range and Aerospace Meteorology*, http://www.smartcockpit.com/docs/Freezing_Rain_as_an_In-Flight_Icing_Hazard.pdf.

BERNSTEIN, B., F. MCDONOUGH, M. POLITOVICH, B. G. BROWN, T. P. RATVASKY, D. R. MILLER, C. WOLFF, and G. CUNNING, 2005: Current icing potential: Algorithm description and comparison with aircraft observations. *Journal of Applied Meteorology*, **44**, pp. 969-986. http://dx.doi.org/10.1175/JAM2246.1.

BERNSTEIN, B., C. WOLFF, and P. MINNIS, 2006: Practical Application of NASA-Langley Advanced Satellite Products to In-flight Icing Nowcasts, *44th (AIAA) Aerospace Sciences Meeting and Exhibit.*

BERNSTEIN, B., C. WOLFF, and F. MCDONOUGH, 2007: An Inferred Climatology of Icing Conditions Aloft, Including Supercooled Large Drops. Part I: Canada and the Continental United States, *Journal of Applied Meteorology and Climatology*, **46**, pp. 1857-1878.

BERNSTEIN, B., and C. LEBOT, 2009: An Inferred Climatology of Icing Conditions Aloft, Including Supercooled Large Drops. Part II: Europe, Asia, and the Globe. *Journal of Applied Meteorology and Climatology*, **48**, pp. 1503-1526, http://dx.doi.org/10.1175/2009JAMC2073.1.

BORYS, R. D., **D. H. LOWENTHAL**, and **D. L. MITCHELL**, 2000: The relationships among cloud microphysics, chemistry, and precipitation rate in cold mountain clouds. *Atmospheric Environment*, **34**, pp. 2593-2602, http://www.sciencedirect.com/science/article/pii/S1352231099004926.

BRAGG, M., 1996: Aircraft aerodynamic effects due to large droplet ice accretions. *34th AIAA Aerospace Sciences Meeting, Reno* http://www.ae.illinois.edu/sis/papers/AIAA960932.PDF.

BROWN, B. G., **G. THOMPSON**, **R. T. BRUINTJES**, **R. BULLOCK**, and **T. L. KANE**, 1997: Intercomparison of in-flight icing algorithms. Part II: Statistical verification results. *Weather and Forecasting*, **12**, pp. 890-914.

BROWN, B., and **G. S. YOUNG**, 2000: Verification of icing and turbulence forecasts: Why some verification statistics can't be computed using PIREP. *AMS 9th Conference on Aviation, Range, and Aerospace Meteorology.*

CAA, 2000: Aircraft Icing Handbook. Civil Aviation Authority.

CHAPMAN, M., **B. G. BROWN**, **T. L. FOWLER**, **A. HOLMES**, and **J. L. MAHONEY**, 2004: *Quality Assessment Report: 20-km Current Icing Potential (CIP20)*. Quality Assessment, Product Development Team, Aviation Weather Research Program, NCAR, http://www.rap.ucar.edu/research/verification/FAA_reports/I8.pdf.

COBER, S. G., and **G. A. ISAAC**, 2012: Characterization of Aircraft Icing Environments with Supercooled Large Drops for Application to Commercial Aircraft Certification. *Journal of Applied Meteorology and Climatology*, **51**, pp. 265-284.

COOPER, W. A., **W. R. SAND**, **D. VEAL**, and **M. POLITOVICH**, 1984: Effects of icing on performance of a research airplane. *Journal of Aircraft*, **21**, pp. 708-715.

DOMS, G., and **U. SCHÄTTLER**, 2002: A Description of the Nonhydrostatic Regional Model LM. Consortium for Small-Scale Modelling (COSMO).

DONOVAN, M. F., **E. WILLIAMS**, **C. KESSINGER**, **G. BLACKBURN**, **P. H. HERZEGH**, **R. L. BANKERT**, **S. MILLER**, and **F. R. MOSHER**, 2008: The Identification and Verification of Hazardous Convective Cells over Oceans Using Visible and Infrared Satellite Observations. *Journal of Applied Meteorology and Climatology*, **47**, pp. 164-184.

EBERT, E. E., 2009: Neighborhood Verification: A Strategy for Rewarding Close Forecasts. *Weather and Forecasting*, **24**, pp. 1498-1510.

ELLROD, G. P., and **A. A. BAILEY**, 2007: Assessment of Aircraft Icing Potential and Maximum Icing Altitude from Geostationary Meteorological Satellite Data, *Weather and Forecasting*, **22**, pp. 160-174.

FAA, Federal Aviation Administration, 1997: FAA Inflight Aircraft Icing Plan, US Department of Transport.

FAA, 2012: Title 14 Code of Federal Regulations Ch. I., Part 25, Appendix C.

Finstad, K. J., **E. P. Lozowski**, and **L. Makkonen**, 1988: On the Median Volume Diameter Approximation for Droplet Collision Efficiency. *Journal of the Atmospheric Sciences*, **45**, pp. 4008-4012.

Haggerty, J. and Coauthors, 2005: Integration of advanced satellite cloud products into an icing nowcasting system. *WWRP Symposium on Nowcasting and Very Short Range Forecasting*, pp. 5-9
http://www.meteo.fr/cic/wsn05/DVD/resumes/courts/res_174.rtf.

Hauf, T., S. Rosczyk, and J. Tendel, 2007: The Provision of In-Flight Icing Information in the Cockpit The FLYSAFE concept. *SAE Conference on Aircraft and Engine Icing 2007, Sevilla*, SAE International.

Herbort, F., 2005: Die Bestimmung des Flüssigwassergehalts im Vereisungswarnsystem Adwice - Problemanalyse und Verbesserungsmöglichkeiten, *Institut für Meteorologie und Klimatologie*, Leibniz Universität Hannover.

Heymsfield, A., 2003, *Encyclopedia of Physical Science and Technology.* E. Meyers and R. Meyers, Eds., Academic Press, New York, pp. 15-31
http://www.sciencedirect.com/science/article/pii/B0122274105001083.

ICAO, 2007: Annex 3 to the Convention on International Civil Aviation: Meteorological Service for International Air Navigation. *ICAO International Standards and Recommended Practices.*
http://www.icao.int/publications/Documents/7300_9ed.pdf.

Jeck, R., 1998: A workable, aircraft-specific icing severity scheme. *36th AIAA Aerospace Sciences Meeting, Reno.*

Jeck, R., 2002: *Icing Design Envelopes (14 CFR Parts 25 and 29, Appendix C) Converted to a Distance-Based Format.* U.S. Department of Transportation Federal Aviation Administration, Office of Aviation Research Washington, DC 20591,
http://oai.dtic.mil/oai/oai?verb=getRecord&metadataPrefix=html&identifier=ADA401921.

Jeck, R., 2003: Converting Appendix C to Other Variables, *SAE Technical Paper*,
http://papers.sae.org/2003-01-2153.

Kraus, D., 2013: *Daniel's XL Toolbox* [Software], Würzburg, Germany,
http://xltoolbox.sourceforge.net.

LeBot, C., 2004: SIGMA : System of Icing Geographic identification in Meteorology for Aviation. *AMS 11th Conference on Aviation, Range, and Aerospace Meteorology*, https://ams.confex.com/ams/11aram22sls/techprogram/paper_81704.htm.

Leifeld, C., 2004: Weiterentwicklung des Nowcastingsystems ADWICE zur Erkennung vereisungsgefährdeter Lufträume. *Institut für Meteorologie und Klimatologie*, Leibniz Universität Hannover, http://www.muk.uni-hannover.de/download/free/pdf-diss/Dissertation_Leifeld.pdf.

Leifeld, C., 2007: ADWICE – Ein System zur Diagnose und Vorhersage von vereisungsgefährdeten Lufträumen. *Interner Bericht*, Deutscher Wetterdienst.

Madine, S., S. A. Lack, S. A. Early, M. Chapman, J. K. Henderson, J. E. Hart, and J. L. Mahoney, 2008: *Quality Assessment Report: Forecast Icing Product (FIP)*. Quality Assessment Research Team NOAA/ESRL/GSD.

Marshall, J. S., and W. M. Palmer, 1948: The distribution of raindrops with size. *Journal of Meteorology*, **5**, pp. 165-166.

McDonough, F., B. Bernstein, and M. Politovich, 2003: *The Forecast Icing Product (FIP)*. Federal Aviation Administration (FAA).

Mecikalski, J. R. and Coauthors, 2007: Aviation Applications for Satellite-Based Observations of Cloud Properties, Convection Initiation, In-Flight Icing, Turbulence, and Volcanic Ash., *Bulletin of the American Meteorological Society*, **88**, pp. 1589-1607.

Minnis, P. and Coauthors, 2004a: A real-time satellite based icing detection system. *Proceedings 14th Intl. Conf. Clouds and Precipitation*, http://www-pm.larc.nasa.gov/icing/pub/conf/Minnis.ICCP.467.pdf.

Minnis, P., L. Nguyen, and D. F. Young, 2004b: Comparison of cloud properties from Meteosat-8 and surface observations. *Proceedings MSG RAO*. http://www-pm.larc.nasa.gov/msg/pub/conference/Minnis.ext.RAO.04.pdf.

Minnis, P., W. Smith, L. Nguyen, F. Chang, D. A. Spangenberg, R. Palikonda, and C. Yost, 2008: Detection of Aircraft Icing Conditions Using an Enhanced Cloud Retrieval Method Applied to Geostationary Satellite Data. *AMS 13th Conference on Aviation, Range, and Aerospace Meteorology*.

Murray, J., P. Schaffner, P. Minnis, and L. Nguyen, 2004: Tropospheric Airborne Meteorological Data Reporting(TAMDAR) Icing Sensor Performance During the 2003 Alliance Icing Research Study(AIRS II). *AMS 11th Conference on Aviation, Range, and Aerospace Meteorology*.

--, 2012: *The NCAR Command Language NCL* (Version 6.1) [Software]. UCAR/NCAR/CISL/VETS, Boulder, Colorado http://dx.doi.org/10.5065/D6WD3XH5.

NCEP, 2010: *Daily Weather Maps.* National Centers for Environmental Prediction (NCEP), Hydrometeorological Prediction Center, http://www.hpc.ncep.noaa.gov/dailywxmap/index_20100202.html.

NTSB, 1996: *Aircraft accident report. In-flight icing encounter and loss of control, Simmons Airlines, d.b.a. American Eagle flight 4184, Avions de Transport Regional (ATR) Model 72-212, N401MA, Roselawn, IN, October 31 1994.* United States National Transportation Safety Board, http://www.ntsb.gov/.

NWC-SAF, 2012: *Algorithm Theoretical Basis Document for "Cloud Products"* http://www.nwcsaf.org/scidocs/document-ation/saf-nwc-cdop-mfl-sci-atbd-01_v3.2.pdf.

POLITOVICH, M., 1989: Aircraft icing caused by large supercooled droplets. *Journal of Applied Meteorology*, **28**, pp. 856-868.

POLITOVICH, M., 1996: Response of a research aircraft to icing and evaluation of severity indices. *Journal of Aircraft*, **33**, pp. 291-297.

PRUPPACHER, H. R., and **J. D. KLETT**, 1997: *Microphysics of Clouds and Precipitation.* Springer Netherlands.

RASMUSSEN, R. M., **I. GERESDI**, **G. THOMPSON**, **K. MANNING**, and **E. KARPLUS**, 2002: Freezing Drizzle Formation in Stably Stratified Layer Clouds: The Role of Radiative Cooling of Cloud Droplets, Cloud Condensation Nuclei, and Ice Initiation. *Journal of the Atmospheric Sciences*, **59**, pp. 837-860.

REYNOLDS, D. W., **D. A. CLARK**, **F. W. WILSON**, and **L. COOK**, 2012: Forecast-Based Decision Support for San Francisco International Airport: A NextGen Prototype System That Improves Operations during Summer Stratus Season. *Bulletin of the American Meteorological Society*, **93**, pp. 1503-1518.

ROGERS, R., and **M. YAO**, 1989: *A Short Course in Cloud Physics.* 3rd ed. Pergamon Press, New York.

ROLOFF, K., 2012: *Untersuchung zur Eignung wolkenmikrophysikalischer Parameter des numerischen Wettervorhersagemodells COSMO-EU zur Vereisungsprognose in ADWICE.* Leibniz Universität Hannover.

ROSENFELD, D., and **W. L. WOODLEY**, 2000: Deep convective clouds with sustained supercooled liquid water down to -37.5°C. *Nature*, **405**, pp. 440-442.

SCHULZ, J., and **U. SCHÄTTLER**, 2011: *Kurze Beschreibung des Lokal-Modells Europa COSMO-EU (LME) und seiner Datenbanken auf dem Datenserver des DWD.* Deutscher Wetterdienst.

SMITH, W., P. MINNIS, B. BERNSTEIN, F. MCDONOUGH, and M. M. KHAIYER, 2003: Comparison of Super-Cooled Liquid Water Cloud Properties Derived from Satellite and Aircraft Measurements. *FAA In-flight IcingGround De-icing International Conference.*

SMITH, W., P. MINNIS, C. FLEEGER, D. A. SPANGENBERG, R. PALIKONDA, and L. NGUYEN, 2012: Determining the Flight Icing Threat to Aircraft with Single-Layer Cloud Parameters Derived from Operational Satellite Data. *Journal of Applied Meteorology and Climatology*, **51**, pp. 1794-1810.

TAFFERNER, A., T. HAUF, C. LEIFELD, T. HAFNER, H. LEYKAUF, and U. VOIGT, 2003: ADWICE: Advanced Diagnosis and Warning System for Aircraft Icing Environments. *Weather and Forecasting*, **18**, pp. 184-203.

TAFFERNER, A., C. FORSTER, M. HAGEN, and T. HAUF, 2010: Improved thunderstorm weather information for pilots through ground and satellite based observing systems. *AMS 14th Conference on Aviation, Range, and Aerospace Meteorology, Atlanta* https://ams.confex.com/ams/pdfpapers/161186.pdf.

TENDEL, J., and C. WOLFF, 2011: Verification of ADWICE In-Flight Icing Forecasts: Performance vs PIREPS Compared to FIP. *SAE Conference on Aircraft and Engine Icing 2011, Chicago*, SAE International http://www.sae.org/technical/papers/2011-38-0068.

THOMPSON, G., R. T. BRUINTJES, B. G. BROWN, and F. HAGE, 1997: Intercomparison of in-flight icing algorithms. Part I: WISP94 real-time icing prediction and evaluation program. *Weather and Forecasting*, **12**, pp. 878-889.

TIEDTKE, M., 1989: A Comprehensive Mass Flux Scheme for Cumulus Parameterization in Large-Scale Models. *Monthly Weather Review*, **117**, pp. 1779-1800.

Curriculum Vitae

Personal

Full Name: Jakob Robin Tendel

Born: April 8 1979 in Berlin(West)

School Education

1985 – 1989   Finow Grundschule Berlin

1989 – 1991   John F. Kennedy Grundschule Berlin

1991 – 1998   John F. Kennedy Schule Berlin

June 1998   Abitur

University Education

1999 – 2002   Undergraduate studies in meteorology, Freie Universität Berlin

2002   Intermediate degree (*Vordiplom*) in meteorology

2002 – 2007   Graduate studies in meteorology, Freie Universität Berlin

2007   Degree (*Diplom*) in meteorology, academic title "Dipl.-Met." Thesis: "*Radiative transfer simulations in the thermal infra-red*"

2010 – 2013   Postgraduate studies in meteorology, Leibniz Universität Hannover

2013   Doctorate in meteorology, academic title "Dr. rer. nat." Thesis: "*Warning of in-flight icing risk through fusion of satellite products, ground observations and model forecasts*" (*this document*)